A Study on Four-dimensional Space Interaction by Principal Vanishing Points Operation

主消点操作による4次元空間インタラクションに関する研究

July 2017

Department of Pure and Applied Physics
Graduate School of Advanced Science and Engineering
Waseda University

Takanobu MIWA

Contents

List of Figures

List of Tables

Chapter 1

Introduction

Imagine a day when humans can form mental representations of higher-dimensional space and objects. These higher-dimensional spatial representations may enable us to gain unique insights into scientific and cultural advancements. To augment human spatial cognition from three to four dimensions, we have developed an interactive 4-D visualization system for acquiring an understanding of 4-D space and objects. Furthermore, we have examined whether humans are capable of formulating 4-D spatial representations through perceptual experiences in 4-D space with 4-D objects. In this dissertation, the research work is focused on 4-D space interactions and 4-D spatial cognition. In Chapter 1, the background and objectives of this research are introduced. In addition, the organization of the dissertation is described at the end of this chapter.

1.1 Background and Objectives

Mental representations of space and objects are strongly related to human cognitive processing, which includes thinking, learning, and problem solving. For instance, the ability to understand shapes, sizes, orientation, and spatial relations, to use mental maps to orient oneself in a mazelike environment, and to imagine different perspectives of an object, is rooted in these mental representations. Furthermore, spatial representations are important in nearly all areas of science, technology, engineering, and mathematics, because spatial thinking is widely employed as a tool for learning and development. For example, students of these disciplines might draw figures and diagrams to help grasp the relationships between variables when solving a problem or proving a theorem. Thus, for many psychologists, cognitive scientists, and educators, it is of both theoretical and practical importance to study the cognitive structure and development of human spatial representations.

As we live in a world with three dimensions and interact with 3-D objects, we have evolved a vision system and spatial cognition that is adapted to 3-D space and objects. For many researchers, this naturally makes mental representations of 3-D space and objects the primary area of interest [1, 2, 3, 4, 5, 6, 7, 8, 9, 10, 11, 12, 13, 14]. However, it is reasonable to consider whether the dimensional limitations of the physical world necessarily restrict human spatial representations to three dimensions. In other words, the question of whether humans can acquire mental representations of higher-dimensional space and objects without relying on mathematical representations remains an open question. As science and technology cannot make advances without an understanding of complex higher-dimensional data, and because higher-dimensional spatial representations enable us to gain direct insights into such data, this fundamental question merits greater attention.

On the other hand, mathematicians, thinkers, and artists realized long ago that there is nothing wrong with imaging space and objects of more than three dimensions. In particular, 4-D space and objects have been studied in various fields. Beginning with the pioneering work of Abbott [15], the idea of representing 4-D space and objects has been a subject of fascination in the field of mathematics, art, and computer science. For instance, in the field of geometry, the geometric elements of various 4-D solids have been described mathematically [16, 17]. As a 3-D solid is constructed from surfaces corresponding to a 2-D plane, a 4-D solid is constructed from cells corresponding to a 3-D solid. In the domain of art, cubists, surrealists, and other modern artists have adopted the concept of depicting 4-D space in art to advance their work. For example, in the artwork "Nu Descendant un Escalier No. 2" drawn by Marcel Ducamp, slices of 4-D space-time are rendered on a canvas in order to express the motion of a nude [18]. In the art work "Corpus Hypercubus" drawn by Salvatore Dali, Christ is painted together with a 3-D cross drawn as the expansion plan of a hypercube [19]. In the science fiction film "Interstellar" directed by Christopher Nolan, the Tesseract scene, in one of the final scenes of the movie, is inspired by the mathematical concept of a 4-D hypercube [20]. This scene presents time as a physical dimension. In the area of compute graphics, the process of 4-D solid formation by folding a 3-D solid in 4-D space is illustrated based on an analogy with origami [21].

Although various studies have been performed on 4-D space and objects, it is still not easy for humans to understand these in an intuitive manner. In other words, it remains an open question whether it is possible for humans to acquire mental representations or intuitive understandings of 4-D space and objects. To answer this question, one possible approach comes from the theory of empiricism. Empiricist philosophers consider all human knowledge to be primarily derived from sensory experience. According to this view, our mental representations of 3-D space are formed from perceptual experiences of and interactions with 3-D objects. Assuming this to be true, if we can accumulate experience of higher-dimensional space in an environment that provides interactions with higher-dimensional objects, we will acquire mental representations of higher-dimensional space and objects. Hence, the major aim of our research is to construct an interactive environment where people can gain experience and understanding of 4-D space and objects, and to test the validity of this hypothesis.

To achieve this end, we have been developing an interactive 4-D display system allowing people to observe various 3-D perspective drawings of a 4-D object displayed on a 3-D screen [22, 23, 24, 25, 26]. This system mimics human behavior in 3-D space, where people observe 3-D objects or their surrounding environment. To understand the shape of a 3-D object, humans move around the object to observe it from various directions in 3-D space. Similarly, to understand the surrounding environment, we look around and move in the environment. By analogy, we consider that, if we can move in 4-D space and observe 4-D objects from various positions, directions, and distances, we should be able to acquire an intuitive understanding of 4-D space and objects. Based on this idea, in the interactive system, we display various 3-D perspective drawings of 4-D objects from an arbitrary 4-D eye-point and viewing direction. The 4-D eye-point can be interactively controlled, to move along a 4-D spherical surface that surrounds a 4-D object. For this interaction, we focused on using the principal vanishing points displayed on the 3-D space as an interface for 4-D eye-point control. The principal vanishing points are represented by projecting points at infinity in the directions of the 4-D principal coordinate axes. Our previous research has shown that the principal vanishing points act as landmarks when people move in 4-D space, because they are associated with the spatial relationship between the 4-D eye-point, 4-D viewing direction, and 4-D world-coordinate system. Thus, it is expected that we can easily achieve intuitive 4-D interactions if we utilize the principal vanishing points as an interface for 4-D eye-point control.

In the first half of this dissertation, we propose a novel algorithm that determines the 4-D eye-point and 4-D viewing direction from the 3-D positions of the principal vanishing points. Using the proposed algorithm, we construct a new interactive 4-D visualization system that enables us to control the movement of the 4-D eye-point and changes in the 4-D viewing direction in 4-D space using simple pick-and-move operations on the principal vanishing points in 3-D space [24, 25, 26]. The developed system consists of a personal computer, a head-mounted display with a built-in 6-DoF sensor, a motion sensor, and a five-button wireless mouse. It works as an immersive virtual reality system. To evaluate the effectiveness of our interactive system based on principal vanishing points, we compared the usability of our system with that of two conventional interaction methods: a classic keyboard-based system, which handles parameter changes regarding the 4-D eye-point movement, and our previous system, which utilizes a flight-controller pad associated with human actions in 3-D space. The results suggest that our interactive system has superior usability in terms of 4-D eye-point control for observing various 3-D perspective drawings of 4-D data [24]. Thus, the proposed method improves the intuitiveness of the observation of 4-D data, and can provides users with experience or knowledge of 4-D space.

Additionally, we propose an interactive control of the 4-D viewing direction based on our 4-D eye-point control technique. The system enables a user to intuitively change the 4-D viewing direction to look around a 4-D scene at an arbitrary position in 4-D space. Moreover, we applied this to a framework of interactions allowing a user to execute a fly-through of 4-D space. Consequently, the proposed system enables us not only to observe a single 4-D object, but also to explore any 4-D scene consisting of multiple 4-D objects. The system enlarges the range of 4-D data that can be observed, and will be helpful for understanding spatial relationships in 4-D space [25].

In the latter half of this dissertation, we examine the hypothesis that humans can acquire 4-D spatial representations from perceptual experiences with 4-D objects, by testing participants' spatial abilities in 4-D space. In the field of psychology, some recent studies have demonstrated the validity of this hypothesis experimentally [27, 28, 29, 30, 31, 32]. These studies examine human 4-D spatial abilities by measuring judgments of simple 4-D tasks and provide important evidence that humans are capable of acquiring 4-D spatial representations. Hence, our current research interest continues to more complex 4-D judgments, such as spatial orientation, perspective taking, and spatial transformations. Our experimental design differs from those of previous studies in the flexibility of the 4-D visualization and the 4-D interaction. In the experiment, we provide participants with extensive training of 4-D space and objects through the interactive 4-D visualization system. We then use two different spatial recognition tasks to measure the participants' 4-D spatial visualization ability. The abilities required for the tasks involve mental representations of the spatial relations between an individual and objects in 4-D space. The participants demonstrate the ability to perform perspective taking, navigation, and mental spatial transformation tasks in 4-D space. Thus, the results provide empirical evidence that humans are able to learn 4-D spatial representations through perceptual experiences [33, 34].

1.2 Organization of the Dissertation

This dissertation is organized as follows:

In Chapter 2, we propose a novel algorithm for 4-D space interaction, which determines the 4-D eye-point and 4-D viewing direction from the 3-D positions of the principal vanishing points based on the geometric relationship between the 4-D eye-point, 4-D viewing direction, and 4-D world-coordinate system. This algorithm makes the operations on the positions of the principal vanishing points in 3-D space correspond to the movements of the 4-D eye-point bounded on a 4-D spherical surface that surrounds an object being observed. Because the principal vanishing points act as the landmarks when a user moves in 4-D space, we can smoothly move in 4-D space and intuitively observe 4-D data from various positions, directions and distances, without becoming disoriented in 4-D space.

In Chapter 3, we construct an interactive 4-D visualization system using the proposed algorithm. The proposed system consists of commercially available products: a personal computer, a head-mounted display with a built in 6-DoF sensor, a motion sensor, and a five-button wireless mouse. The system works as an immersive virtual reality system. In this system, we can consistently control the 4-D eye-point while handling the principal vanishing points in 3-D space with simple pick-and-move operations, and observe various 3-D perspective drawings of a 4-D object. We present the experimental results that demonstrate the effectiveness of our proposed system. The experiments include subjective and objective evaluation experiments that compare the usability of our system with that of two conventional interaction methods. In addition, the effect of the change in the 4-D viewing field on the usability of the proposed system is investigated.

In Chapter 4, we propose a novel 4-D interaction technique that allows us to have free-look actions in 4-D space, with simple pick-and-move operations on the principal vanishing points. This technique is implemented by extending the 4-D eye-point control algorithm presented in Chapter 2 to the control of the 4-D observed point, and enables us to freely look around a 4-D scene at arbitrary 4-D positions. Furthermore, a fly-through of 4-D space is achieved with a combination of the 4-D viewing direction control and the simultaneous movement of the 4-D eye-point and 4-D observed point along the 4-D visual axis. Consequently, we can smoothly explore and observe any 4-D scene consisting of multiple 4-D objects or intricate spatial constructions such as a 4-D maze. To evaluate the effectiveness of the proposed system, we perform a user test in which the participants control the 4-D viewing direction to spot a target object that randomly appears in 4-D space.

In Chapter 5, to examine whether humans are capable of learning 4-D spatial representations through perceptual experience in 4-D space with 4-D objects, we perform experiments with the use of the proposed interactive system. The experiments include two experiments. In the first experiment, we assess the participants' ability relating to perspective taking and navigational skills in 4-D space. Then, in the second experiment, we assess the participants' ability relating to mental spatial transformations in 4-D space.

Finally, the conclusions and future prospects are given in Chapter 6.

A list of the references cited in this study, an appendix, and a list of the author's publications are attached at the end of the dissertation.

Chapter 2

4-D Eye-point Control by Principal Vanishing Point Operations

In Chapter 2, we propose a novel 4-D interaction technique that employs the principal vanishing points in 3-D space as an interface to control the movement of the 4-D eye-point. Because the principal vanishing points are geometrically related to the 4-D visual axis, they act as landmarks when we move in 4-D space. Using the proposed interaction technique, we can smoothly move in an arbitrary direction in 4-D space, and consistently observe a 4-D object from various 4-D positions, directions, and distances in a natural and intuitive fashion.

2.1 Literature Review of 4-D Space Visualization and 4-D Space Interaction

In this section, we review the relevant literature on 4-D visualization and 4-D interaction. We summarize methods from the fields of computer graphics and virtual reality for visualizing and interacting with 4-D objects.

There are a number of approaches to visualizing multi-dimensional data via dimensionally reduction techniques. A principal components analysis, a multi-dimensional scaling and a parallel coordinate plot [35] are typical methods. These methods are useful to analyze multi-dimensional statistical data. However, in these approach, it is difficult to overview higher-dimensional geometric data without degenerating any dimensions.

Conventional 4-D visualization techniques take one of two major approaches. The first projects a 4-D object into 3-D space, just as 2-D projections of 3-D objects are formed on the retina [36, 37, 38, 39, 40, 41]. The second approach slices a 4-D object with a hyperplane in 4-D space, just as we cut a 3-D object with a 2-D plane [41, 42, 43, 44]. Additionally, in order to enrich quality of 4-D graphics, some studies were made on applying 3-D computer graphics techniques such as a lighting model and GPU computing to shading and lighting techniques in 4-D visualization [45, 46, 47]. In this paper, we focus on the first approach. This has the advantage that it maintains various original 4-D geometric features, not only the structural continuity and spatial relations, but also parallelism and orthogonality. This advantage helps people determine the overall shape of a 4-D object and geometric features such as its size, position, and orientation. In previous studies, a 4-D eye-point is either fixed or undergoes limited changes. Here, we construct a visualization algorithm that enables 4-D objects to be observed from an arbitrary position and direction in 4-D space.

There have been some efforts to develop 4-D interaction techniques. In these systems, the operation of common input devices such as a mouse, keyboard, or touch-screen [48, 49, 50] was associated with geometric operations on a 4-D object. Another approach associates human body motion with geometric operations on 4-D objects [51]. These systems enable the user to observe the rotation of a 4-D object in 3-D space. However, because the interface in these studies was designed in 3-D space, the association between the user's operation in 3-D space and the geometric operation in 4-D space is determined by art rather than nature. Therefore, we have developed a new interface that enables the user to control a 4-D eye-point and a 4-D viewing direction in a natural fashion using the geometric processing of 4-D space.

In our previous work, we constructed a 4-D visualization algorithm via 5-D homogeneous processing. This algorithm enables 3-D perspective drawings of any 4-D data to be visualized in 3-D space from an arbitrary 4-D eye-point, viewing direction, and viewing field [22, 23]. Moreover, we constructed an interactive 4-D space display system that translates human actions in 3-D space to the movement and direction of a 4-D eye-point bounded on a 4-D spherical surface [22]. We associated human actions in 3-D space with an intuitive interface, in this case, a flight-controller pad. With this system, users can observe 4-D data such as 4-D solids, 3-D time-series data, and 4-D mathematical data in an arbitrary 4-D viewing field while intuitively moving in 4-D space [22, 52, 53]. In addition, we generalized 4-D geometric element definitions and interference via 5-D homogeneous processing [54].

Through these studies, we have found that people utilize principal vanishing points as landmarks to understand their position and orientation as they move in 4-D space. Inspired by this discovery, we developed a novel algorithm that determines the 4-D eye-point and 4-D viewing direction from the 3-D positions of the principal vanishing points. Using this algorithm, we constructed a new interactive 4-D visualization system that employs the principal vanishing points as an interface to control the movement of a 4-D eye-point and changes in the 4-D viewing direction [24, 25, 26].

2.2 Basic Concept of the 4-D Eye-point Control

To understand the shape of a 3-D object, humans move around the object to observe it from various directions in 3-D space. Similarly, to understand the surrounding environment, we look around and move in the environment. By analogy, we consider that, if we can move in 4-D space and observe 4-D objects from various positions, directions, and distances, we should be able to acquire an intuitive understanding of 4-D space and objects. Based on this idea, in the interactive system, we display various 3-D perspective drawings of 4-D objects from an arbitrary 4-D eye-point and viewing direction. The 4-D eye-point can be interactively controlled to move along a 4-D spherical surface that surrounds

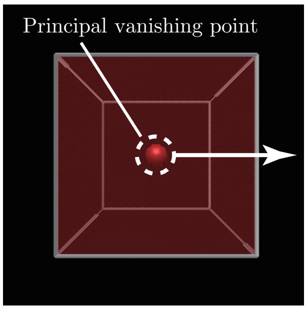

(a)

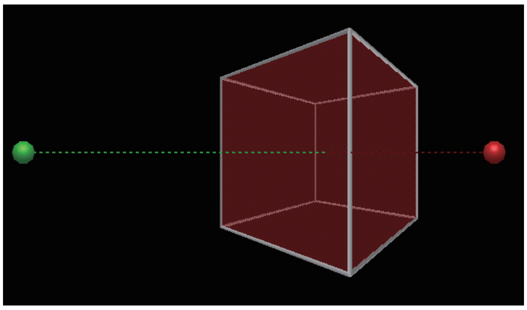

(b)

Figure 2.1. Observation of a cube in 3-D space, operating on the principal vanishing points. (a) 2-D perspective drawing of the cube and the principal vanishing point. (b) Principal vanishing point after eye-point movement in 3-D space.

the 4-D object. For this interaction, we focused on using the principal vanishing points as an interface for 4-D eye-point control.

Before considering the 4-D case, we begin with a study of the 3-D case. As stated by Foley et al. [55], in 3-D space, a perspective projection is a method of mapping 3-D points to a projection plane. The projection points are obtained as the intersections of straight projection rays with the projection plane. The straight projection rays, called projectors, are formed by connecting the center of projection, called the eye-point, and each of the 3-D points. The projection plane, called a 2-D screen, floats in front of the eye-point and is perpendicular to the viewing direction. The perspective projection shows distant objects as being smaller than near objects. This is similar to the human eye and camera lenses; therefore, the perspective projection produces a realistic representation of a 3-D object on the 2-D screen. To be more precise, when any parallel lines in 3-D space are not parallel to the 2-D screen, their perspective projections will converge towards a single "vanishing point" on the 2-D screen. In 3-D projective space, the parallel lines intersect at infinity. Hence, the vanishing point is the projection of the point at infinity associated with the parallel lines. If the parallel lines are parallel to one of the three principal coordinate axes, the vanishing point is specifically referred to as a "principal vanishing point." In the 3-D case, one, two, or three principal vanishing points will appear on the 2-D screen, corresponding to the number of principal coordinate axes that are not parallel to the 2-D screen.

Each principal vanishing point is determined by the geometric relationship among the eye-point, viewing direction, and principal coordinate system. Conversely, it is possible to estimate the eye-point and viewing direction in 3-D space from each position of the principal vanishing points on the 2-D screen [56]. This implies that it is possible to control the eye-point in 3-D space by manipulating the position of the principal vanishing points on the 2-D screen, as shown in Figure 2.1.

2.3 Algorithm for 4-D Eye-point Control

We now explain interactive 4-D eye-point control by operating on the principal vanishing points. We extend the setup explained above from 3-D space to 4-D space. That is, as shown in Figure 2.2, we consider controlling the 4-D eye-point to move along a 4-D spherical surface, centered on the origin of the 4-D world-coordinate system, by handling the principal vanishing points displayed in 3-D space.

2.3.1 Visualization Model and Principal Vanishing Points

Figure 2.3 shows the 4-D visualization model to observe a 4-D data from an arbitrary eye-point, viewing direction and distance in 4-D space. A 3-D perspective drawing of a 4-D object is obtained by converting data defined in the 4-D world-coordinate system $x_w y_w z_w w_w$ to data in the 3-D screen-coordinate system $x_s y_s z_s w_s$ [22, 23]. The 4-D viewing direction is defined as the direction from the 4-D eye-point $p_f(x_{p_f}, y_{p_f}, z_{p_f}, w_{p_f})$ to the 4-D observed point $p_a(x_{p_a}, y_{p_a}, z_{p_a}, w_{p_a})$ in the 4-D world-coordinate system, and coincides with the negative direction of the w_e-axis of the 4-D eye-coordinate system $x_e y_e z_e w_e$

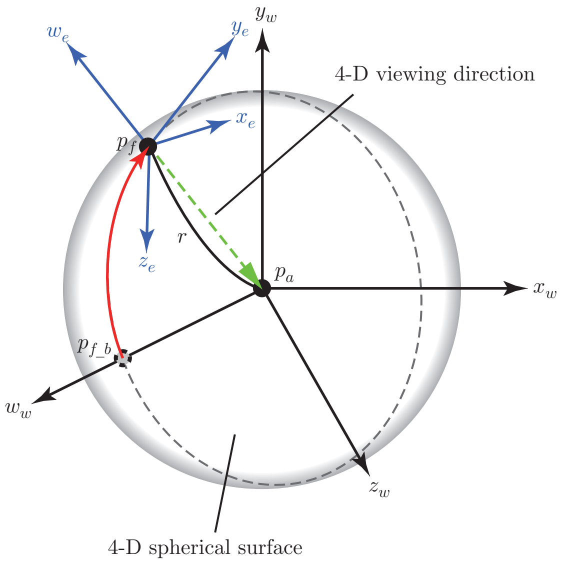

Figure 2.2. Movement of the 4-D eye-point along the 4-D spherical surface.

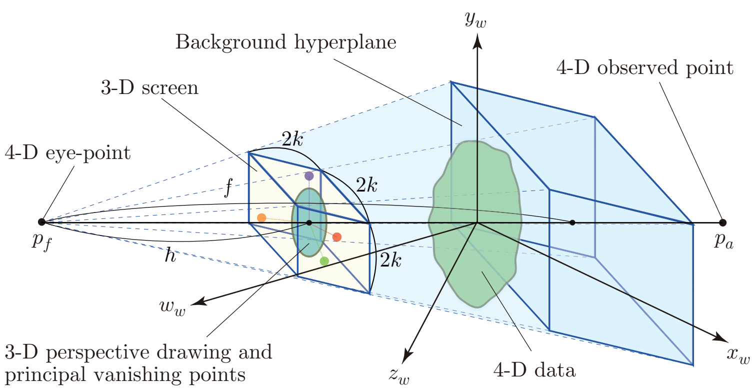

Figure 2.3. Visualization model of 4-D space and objects.

in which the origin lies at the 4-D eye-point. The center of the 3-D screen and that of the background hyperplane are located at distances h and $f(> h)$, respectively, from the 4-D eye-point on the 4-D visual axis. The dimension of the 3-D screen is $2k \times 2k \times 2k$ in the $x_s y_s z_s$-space of the 3-D screen-coordinate system. In contrast to visualization models in conventional studies, only 4-D objects that are inside the 4-D viewing field (defined as a truncated pyramid formed by the 4-D eye-point, 3-D screen and background hyperplane) are visualized on the 3-D screen. The visualization algorithm includes a view field transformation, perspective transformation, and clipping operation in 4-D space using 5-D homogeneous processing. This framework can visualize any 4-D data, including points at infinity, onto 3-D space from an arbitrary 4-D eye-point and viewing direction.

The transformation from the data defined in the 4-D world-coordinate system $x_w y_w z_w w_w$ to data in the 3-D screen-coordinate system $x_s y_s z_s w_w$ is represented by the transformation from the homogeneous coordinates V_w including the points at infinity in 4-D space to the homogeneous coordinates V_s as follows:

$$\begin{aligned} \boldsymbol{V}_s =& [X_s \quad Y_s \quad Z_s \quad W_s \quad v_s] \\ =& [X_w \quad Y_w \quad Z_w \quad W_w \quad v_w] \boldsymbol{T}_v(p_f, p_a) \boldsymbol{T}_p(k, h, f), \end{aligned} \tag{2.1}$$

where the transformation matrices $\boldsymbol{T}_v$ and $\boldsymbol{T}_p$ are the 4-D view field transformation matrix and the 4-D perspective transformation matrix, respectively. The 4-D view field transformation matrix $\boldsymbol{T}_v$ is derived from the 4-D eye-point $p_f(x_{p_f}, y_{p_f}, z_{p_f}, w_{p_f})$ and the 4-D observed point $p_a(x_{p_a}, y_{p_a}, z_{p_a}, w_{p_a})$ as follows:

$$\begin{aligned} &\boldsymbol{T}_v(p_f, p_a) \\ &= \boldsymbol{T}_t(-x_{p_f}, -y_{p_f}, -z_{p_f}, -w_{p_f}) \boldsymbol{T}_{xy}(\sin\alpha, \cos\alpha) \\ &\quad \boldsymbol{T}_{yz}(\sin\beta, \cos\beta) \boldsymbol{T}_{xz}(\sin\gamma, \cos\gamma), \end{aligned} \tag{2.2}$$

where

$$\left.\begin{aligned} \cos\alpha &= \tfrac{w_{p_f} - w_{p_a}}{\sqrt{(z_{p_f}-z_{p_a})^2 + (w_{p_f}-w_{p_a})^2}} \\ \sin\alpha &= \tfrac{z_{p_f} - z_{p_a}}{\sqrt{(z_{p_f}-z_{p_a})^2 + (w_{p_f}-w_{p_a})^2}} \\ \cos\beta &= \tfrac{\sqrt{(z_{p_f}-z_{p_a})^2 + (w_{p_f}-w_{p_a})^2}}{\sqrt{(x_{p_f}-x_{p_a})^2 + (z_{p_f}-z_{p_a})^2 + (w_{p_f}-w_{p_a})^2}} \\ \sin\beta &= \tfrac{x_{p_a} - x_{p_f}}{\sqrt{(x_{p_f}-x_{p_a})^2 + (z_{p_f}-z_{p_a})^2 + (w_{p_f}-w_{p_a})^2}} \\ \cos\gamma &= \tfrac{\sqrt{(x_{p_f}-x_{p_a})^2 + (z_{p_f}-z_{p_a})^2 + (w_{p_f}-w_{p_a})^2}}{\sqrt{(x_{p_f}-x_{p_a})^2 + (y_{p_f}-y_{p_a})^2 + (z_{p_f}-z_{p_a})^2 + (w_{p_f}-w_{p_a})^2}} \\ \sin\gamma &= \tfrac{y_{p_a} - y_{p_f}}{\sqrt{(x_{p_f}-x_{p_a})^2 + (y_{p_f}-y_{p_a})^2 + (z_{p_f}-z_{p_a})^2 + (w_{p_f}-w_{p_a})^2}} \end{aligned}\right\},$$

The transformation matrix $\boldsymbol{T}_t$ is the 4-D translation matrix, and the transformation matrices $\boldsymbol{T}_{xy}$, $\boldsymbol{T}_{yz}$, and $\boldsymbol{T}_{xz}$ are the 4-D rotation matrices around the xy-, yz-, and xz-planes, respectively. Therefore, the 3-D screen coordinates v_s are obtained from Equation (2.1) as follows:

$$\begin{aligned} v_s =& (x_s, y_s, z_s, w_s) \\ =& \left(\frac{X_s}{v_s}, \frac{Y_s}{v_s}, \frac{Z_s}{v_s}, \frac{W_s}{v_s} \right). \end{aligned} \tag{2.3}$$

This algorithm enables one to observe various types of 4-D data to be observed from an arbitrary 4-D viewing direction for an arbitrary 4-D eye-point. Moreover, by changing the parameters k, h, and f of the 4-D perspective transformation matrix $\boldsymbol{T}_p$, we can visualize 4-D data not only with various 4-D viewing fields, but also with various 4-D projection methods such as a perspective projection, parallel projection, or slice operation.

Now, we consider the principal vanishing points in 3-D space. The points at infinity in the x_w-, y_w-, z_w- and w_w-directions are represented as $V_{x_w}\overline{(1,0,0,0,0)}$, $V_{y_w}\overline{(0,1,0,0,0)}$, $V_{z_w}\overline{(0,0,1,0,0)}$, and $V_{w_w}\overline{(0,0,0,1,0)}$, respectively. Substituting these points into Equation (2.1), we can obtain the principal vanishing points vp_x, vp_y, vp_z, and vp_w on the 3-D screen from Equation (2.3) as follows:

$$\begin{aligned}
vp_x &= (x_{vp_x}, y_{vp_x}, z_{vp_x}) \\
&= \left(\frac{h}{k} \frac{1}{\tan\beta\cos\gamma}, -\frac{h}{k}\tan\gamma, 0 \right), \\
vp_y &= (x_{vp_y}, y_{vp_y}, z_{vp_y}) \\
&= \left(0, \frac{h}{k} \frac{1}{\tan\gamma}, 0 \right), \\
vp_z &= (x_{vp_z}, y_{vp_z}, z_{vp_z}) \\
&= \left(-\frac{h}{k} \frac{\tan\beta}{\cos\gamma}, -\frac{h}{k}\tan\gamma, -\frac{h}{k} \frac{1}{\tan\alpha\cos\beta\cos\gamma} \right), \\
vp_w &= (x_{vp_w}, y_{vp_w}, z_{vp_w}) \\
&= \left(-\frac{h}{k} \frac{\tan\beta}{\cos\gamma}, -\frac{h}{k}\tan\gamma, \frac{h}{k} \frac{\tan\alpha}{\cos\beta\cos\gamma} \right),
\end{aligned} \tag{2.4}$$

where α, β, and γ are the parameters of the 4-D viewing direction for the 4-D view field transformation.

2.3.2 Determination of the 4-D Eye-point from the Principal Vanishing Points

From Equation (2.4), the number of principal vanishing points and their 3-D positions are determined by the spatial relationships among the 4-D eye-point, 4-D viewing direction, and 4-D world-coordinate system. Moreover, the principal vanishing points always satisfy their geometric positional relationship in 3-D space. Accordingly, it is assumed that there is a converse relation of Equation (2.4) such that the 4-D eye-point can be derived from the positions of the principal vanishing points. Based on this assumption, we constructed an interaction algorithm that made position changes of the principal vanishing points in 3-D space correspond to movement of the 4-D eye-point in 4-D space [24].

Figure 2.4 shows an activity diagram of this algorithm. This algorithm is composed of two processing steps. As the user picks and moves one principal vanishing point in 3-D space, the first processing step estimates the other principal vanishing points from the principal vanishing point being operated on. The second processing step estimates the parameters α, β, and γ of the 4-D viewing direction in 4-D space using the principal vanishing points in 3-D space

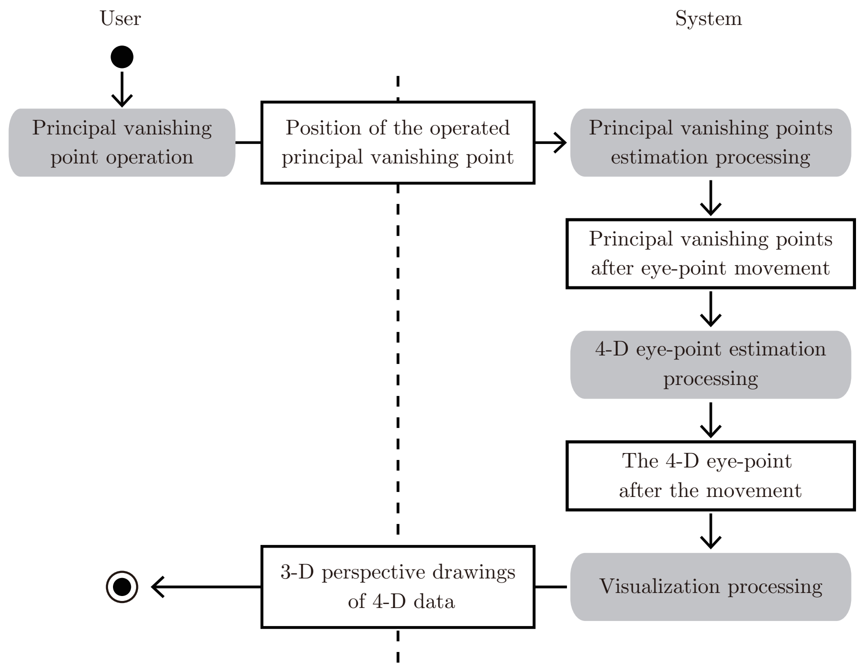

Figure 2.4. Activity diagram of the interaction algorithm.

to determine the 4-D eye-point. With this interaction algorithm, the user can intuitively control the 4-D eye-point by manipulating the position of the principal vanishing points in 3-D space while using them as landmarks to recognize his/her viewing position in 4-D space.

We now discuss the first processing step. When one principal vanishing point is picked and moved by a user in 3-D space, the other three principal vanishing points should be automatically allocated to the corresponding positions that satisfy their geometric positional relationship in 3-D space. For instance, suppose the principal vanishing points vp_{x_b}, vp_{y_b}, vp_{z_b}, and vp_{w_b} are displayed in 3-D space at a 4-D eye-point p_{f_b}. When the principal vanishing point vp_{w_b} moves to vp_w through user operations, Equation (2.4) allows us to estimate the other three vanishing points vp_x, vp_y, and vp_z using the position of the operated principal vanishing point vp_w as follows:

$$\begin{aligned}
vp_x =& (x_{vp_x}, y_{vp_x}, z_{vp_x}) \\
=& \left(-\frac{1}{x_{vp_w}}\left\{\left(\frac{h}{k}\right)^2 + {y_{vp_w}}^2\right\}, y_{vp_w}, 0\right), \\
vp_y =& (x_{vp_y}, y_{vp_y}, z_{vp_y}) \\
=& \left(0, -\frac{1}{y_{vp_w}}\left(\frac{h}{k}\right)^2, 0\right), \\
vp_z =& (x_{vp_z}, y_{vp_z}, z_{vp_z}) \\
=& \left(x_{vp_w}, y_{vp_w}, -\frac{1}{z_{vp_w}}\left\{\left(\frac{h}{k}\right)^2 + {x_{vp_w}}^2 + {y_{vp_w}}^2\right\}\right).
\end{aligned} \tag{2.5}$$

If another principal vanishing point is operated on, or if any principal vanishing points are displayed in 3-D space, the estimation of the principal vanishing points can be achieved in the same manner as in Equation (2.5). (see Appendix A for more details of the calculations.)

Next, we discuss the second processing step. For 4-D eye-point control, we consider movement of the 4-D eye-point p_f along a 4-D spherical surface with radius r. The 4-D spherical surface is centered at the origin of the 4-D world-coordinate system. The 4-D observed point p_a is fixed at the origin of the 4-D world-coordinate system. Parameters α, β, and γ of the 4-D viewing direction are derived from Equation (2.4) as follows:

$$\begin{aligned}\alpha &= \tan^{-1}\frac{z_{vp_w}}{\sqrt{-z_{vp_z}z_{vp_w}}},\\ \beta &= \tan^{-1}\frac{-x_{vp_w}}{\sqrt{-x_{vp_x}x_{vp_w}}},\\ \gamma &= \tan^{-1}\frac{-y_{vp_w}}{\sqrt{-y_{vp_y}y_{vp_w}}}.\end{aligned} \tag{2.6}$$

Substituting the coordinate values of the principal vanishing points, for example, the coordinate values of Equation (2.5), into Equation (2.6), we can determine the corresponding parameters α, β, and γ. Finally, the 4-D eye-point p_f is computed with the following equation:

$$\begin{aligned}p_f &= [x_{p_f} \;\; y_{p_f} \;\; z_{p_f} \;\; w_{p_f} \;\; 1]\\ &= [0 \;\; 0 \;\; 0 \;\; r \;\; 1]\boldsymbol{T}_{xz}^{-1}(\gamma)\boldsymbol{T}_{yz}^{-1}(\beta)\boldsymbol{T}_{xy}^{-1}(\alpha)\end{aligned} \tag{2.7}$$

where the transformation matrices $\boldsymbol{T}_{xz}$, $\boldsymbol{T}_{yz}$, and $\boldsymbol{T}_{xy}$ represent the 4-D rotation matrices around the xz-, yz-, and xy-planes, respectively.

2.3.3 Implementation of the Proposed Algorithm

Let us add a complementary explanation of the implementation of these algorithms. In the 4-D visualization algorithm, the 4-D view field transformation enables movements of the 4-D eye-point and changes in the 4-D viewing direction from the 4-D eye-point to the 4-D observed point [22, 23]. Thus, when we integrate the interaction algorithm into the visualization algorithm, we initially introduce the 4-D eye-point determined from the second processing step of the interaction algorithm and the 4-D observed point into the 4-D view field transformation. We then recalculate the movement of the 4-D eye-point and the change in the 4-D viewing direction from the 4-D eye-point to the 4-D observed point. However, part of this algorithmic procedure is modified when we implement the algorithms in the interactive system. In this case, we do not introduce the 4-D eye-point p_f and the 4-D observed point p_a into the 4-D view field transformation matrix $\boldsymbol{T}_v$ in Equation (2.2), but rather the 4-D eye-point and the parameters α, β, and γ in Equation (2.6) to Equation (2.2). That is, the 4-D view field transformation matrix $\boldsymbol{T}_v$ of Equation (2.2) is arranged and represented as follows:

$$\begin{aligned}&\boldsymbol{T}_v(p_f, \alpha, \beta, \gamma)\\ &= \boldsymbol{T}_t(-x_{p_f}, -y_{p_f}, -z_{p_f}, -w_{p_f})\boldsymbol{T}_{xy}(\alpha)\boldsymbol{T}_{yz}(\beta)\boldsymbol{T}_{xz}(\gamma).\end{aligned} \tag{2.8}$$

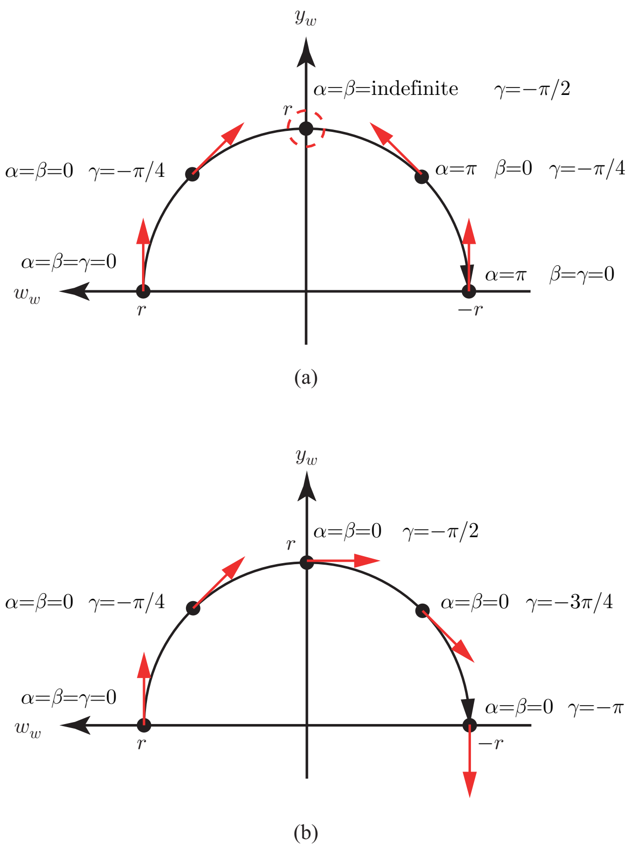

Figure 2.5. Difference in the pose of the 4-D eye-point caused by modification of the implementation. (a) Original visualization algorithm. (b) Our implementation.

Although this modified 4-D view field transformation may differ from the 4-D view field transformation of the original algorithm depending on the movement history of the 4-D eye-point, in our implementation, this modification has a positive effect on the style of the 4-D observation. In the rest part of this section, we explain the effect of this modification on the implementation with a concrete example to better clarify the 4-D interaction.

Suppose that the 4-D eye-point starts at the 4-D position $(0, 0, 0, r)$ on the w_w-axis and moves to $(0, 0, 0, -r)$ via a zenith of the 4-D spherical surface $(0, r, 0, 0)$ on the y_w-axis, where $r(> 0)$ represents the radius of the 4-D spherical surface. When the 4-D eye-point is in the 4-D half-space, which is defined as the 4-D region satisfying $0 \leq w_w$, the modification of the implementation does not affect the visualization and the interaction because the 4-D view field transformation matrix $\boldsymbol{T}_v$ of Equation (2.2) coincides with that of Equation (2.8). The effect of the modification becomes apparent once the 4-D eye-point arrives at the zenith and enters the other 4-D half-space, which is defined as the 4-D region satisfying $w_w < 0$. This is the pose of the moving 4-D eye-point.

Figure 2.5 shows the difference in the 4-D pose brought about by the modification of the implementation. For simplification, we only describe the $y_w w_w$-plane, which includes the movement path of the 4-D eye-point, and focus on five positions along the movement path. The pose of the 4-D eye-point at each position is expressed by the 4-D upper direction of the 4-D eye-point, represented by a red arrow. In addition, in the figure, we include the values α, β, and γ of the 4-D viewing direction for the corresponding method.

When we visualize 4-D space and objects according to the original method using the 4-D view field transformation matrix $\boldsymbol{T}_v$ of Equation (2.2), which is derived from the 4-D eye-point p_f of Equation (2.7) and the 4-D observed point p_a, the values α, β, and γ of the 4-D viewing direction are in the range $-\pi \leq \alpha \leq \pi$ and $-\pi/2 \leq \beta, \gamma \leq \pi/2$. In this case, the 4-D upper direction is indefinite at the zenith of the 4-D spherical surface and is reversed by 180° before and after the 4-D eye-point passes through the zenith, as shown in Figure 2.5(a). The continuity of 4-D observation is therefore lost, and the interaction becomes unnatural at the zenith.

In this way, if we implement the visualization algorithm without any modification, the pose of the 4-D eye-point is restricted, as the 4-D upper direction of the 4-D eye-point is always in the upward vertical direction in 4-D space. This restriction causes the pose of the 4-D eye-point to change at some positions on the 4-D spherical surface, regardless of the user's will. In this state, the continuity of 4-D observation is not ensured, and the interaction becomes unnatural at some points on the 4-D spherical surface.

To remove this irregularity, we determine the parameters α, β, and γ of the 4-D viewing direction of Equation (2.6) in the range $-\pi \leq \alpha, \beta, \gamma \leq \pi$, depending on the movement history of the 4-D eye-point, so that the pose of the 4-D eye-point is maintained before and after it passes through the zenith, as shown in Figure 2.5(b). Then, we do not generate the 4-D view field transformation matrix $\boldsymbol{T}_v$ of Equation (2.2), but that of Equation (2.8). As a result, our implementation enables the user to observe 4-D space and objects while he/she continuously moves the eye-point along the 4-D spherical surface in a natural style.

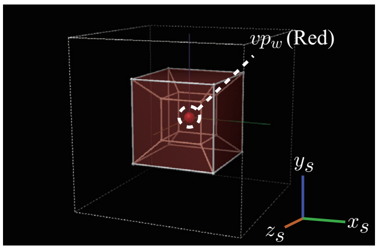

One-point 3-D perspective drawing
$p_f(0, 0, 0, 1.5)$, $p_a(0, 0, 0, 0)$

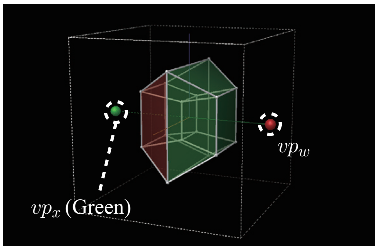

Two-point 3-D perspective drawing
$p_f(0, 1.1, 0, 1.1)$, $p_a(0, 0, 0, 0)$

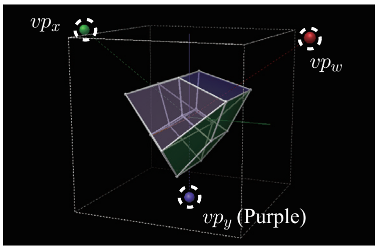

Three-point 3-D perspective drawing
$p_f(0.75, 1.1, 0, 0.75)$, $p_a(0, 0, 0, 0)$

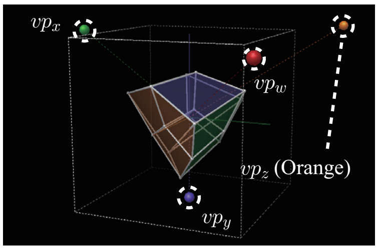

Four-point 3-D perspective drawing
$p_f(0.75, 1.1, 0.53, 0.53)$, $p_a(0, 0, 0, 0)$

Figure 2.6. Principal vanishing points and 3-D perspective drawing of a hypercube. The inside region surrounded by the white dashed wire-frame cube corresponds to the 3-D screen.

2.4 Observation of 4-D Solids with Principal Vanishing Point Operations

In this section, we present examples of 4-D space visualization with the proposed interaction algorithm. We demonstrate that the proposed method enables us to freely move in 4-D space and observe 4-D data from various 4-D eye-points.

2.4.1 Correspondence between 4-D Eye-point and Principal Vanishing Points

The pictures in Figure 2.6 show examples of principal vanishing points and the 3-D perspective drawing of a hypercube (see Appendix B for the definition of the hypercube). The principal vanishing points vp_x, vp_y, vp_z, and vp_w are represented by green, purple, orange, and red solid spheres, respectively. In this example, the coordinates of the hypercube vertices are normalized as the permutations of $(\pm 0.5, \pm 0.5, \pm 0.5, \pm 0.5)$. We assign a different color to each cell of the hypercube and place it at the origin of the 4-D world-coordinate system such that each of the eight cells is located in a different positive and negative position on each axis of the 4-D world-coordinate system, at a distance of 0.5 from the origin. To clearly visualize the edges inside the 3-D perspective drawing, the 3-D perspective drawings are rendered with semitransparent surfaces and a reticular stipple pattern. We visualize this from different 4-D eye-points, at a distance of 1.5 from the origin of the 4-D world-coordinate system. The 4-D observed point is fixed at the origin of the 4-D world-coordinate system. The parameters (k, h, f) of the 4-D viewing field are $(0.5, 0.5, 100)$, respectively.

In each image shown in Figure 2.6, the inside region surrounded by the white dashed wire-frame cube corresponds to the 3-D screen. The three axes rendered from the center of the 3-D screen correspond to the x_s-, y_s-, and z_s-axes of the 3-D screen coordinate system, respectively.

As shown in the figure, the number of principal vanishing points and their 3-D positions are determined by the spatial relationships between the 4-D eye-point, 4-D viewing direction, and 4-D world-coordinate system. For example, in the top-left image in Figure 2.6, one principal vanishing point vp_w is displayed on the 3-D screen. However, after the 4-D eye-point moves in 4-D space, as shown in the bottom-right image, the other three principal vanishing points vp_x, vp_y, and vp_z are also displayed in 3-D space. These 3-D perspective drawings are classified as one-point, two-point, three-point, and four-point 3-D perspective drawings in accordance with the number of principal vanishing points. Although our visualization algorithm visualizes only 4-D data inside the 4-D viewing field onto the 3-D screen, the principal vanishing points are displayed in the entire 3-D space around the 3-D screen, regardless of the 4-D clipping operation, because they are projections of points at infinity in 4-D space.

2.4.2 Movements of the 4-D Eye-point along the 4-D Spherical Surface

Figure 2.7 depicts image sequences of 3-D perspective drawings of the hypercube obtained through moving on the 4-D spherical surface with a radius of 1.5, centered at the origin of the 4-D world-coordinate system. The parameters (k, h, f) of the 4-D viewing field are $(0.5, 0.5, 100)$, respectively.

The images in Figure 2.7(a) show the 3-D perspective drawings of the hypercube obtained by the operations on the principal vanishing points vp_x and vp_w. When these principal vanishing points are moved in the x_s-direction in 3-D space, the 4-D eye-point moves around the 4-D spherical surface within the $x_w w_w$-plane.

In a similar fashion, the images in Figure 2.7(b) show the 3-D perspective drawings of the hypercube obtained by the operations on the principal vanishing points vp_y and vp_w. In this case, when these principal vanishing points are moved in the y_s-direction in 3-D space, the 4-D eye-point moves around the 4-D spherical surface within the $y_w w_w$-plane.

Furthermore, the images in Figure 2.7(c) show the results when we move the principal vanishing points vp_z and vp_w in the z_s-direction in 3-D space, to make the 4-D eye-point move around the 4-D spherical surface within the $z_w w_w$-plane.

In these 4-D eye-point movement, as shown in the images 1 and 5, 2 and 6, 3 and 7, and 4 and 8, in Figure 2.7, the same principal vanishing points are obtained in 3-D space at different 4-D eye-points. This signifies that two eye-points corresponding to each image pair are antipodal to each other on the 4-D spherical surface. The understanding of these relationships will help us navigate ourselves in 4-D space.

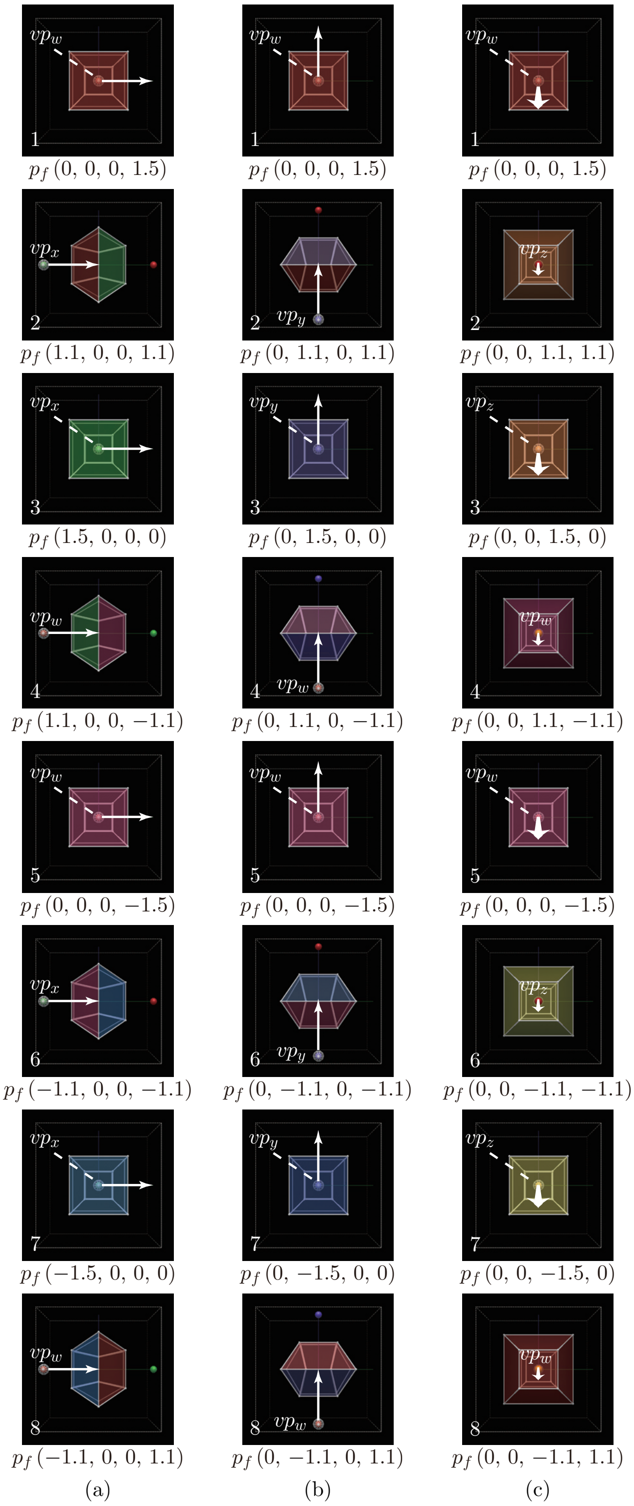

Figure 2.7. Basic example of the 4-D eye-point movements along the 4-D spherical surface. (a) Movement in $x_w w_w$-plane. (b) Movement in $y_w w_w$-plane. (c) Movement in $z_w w_w$-plane.

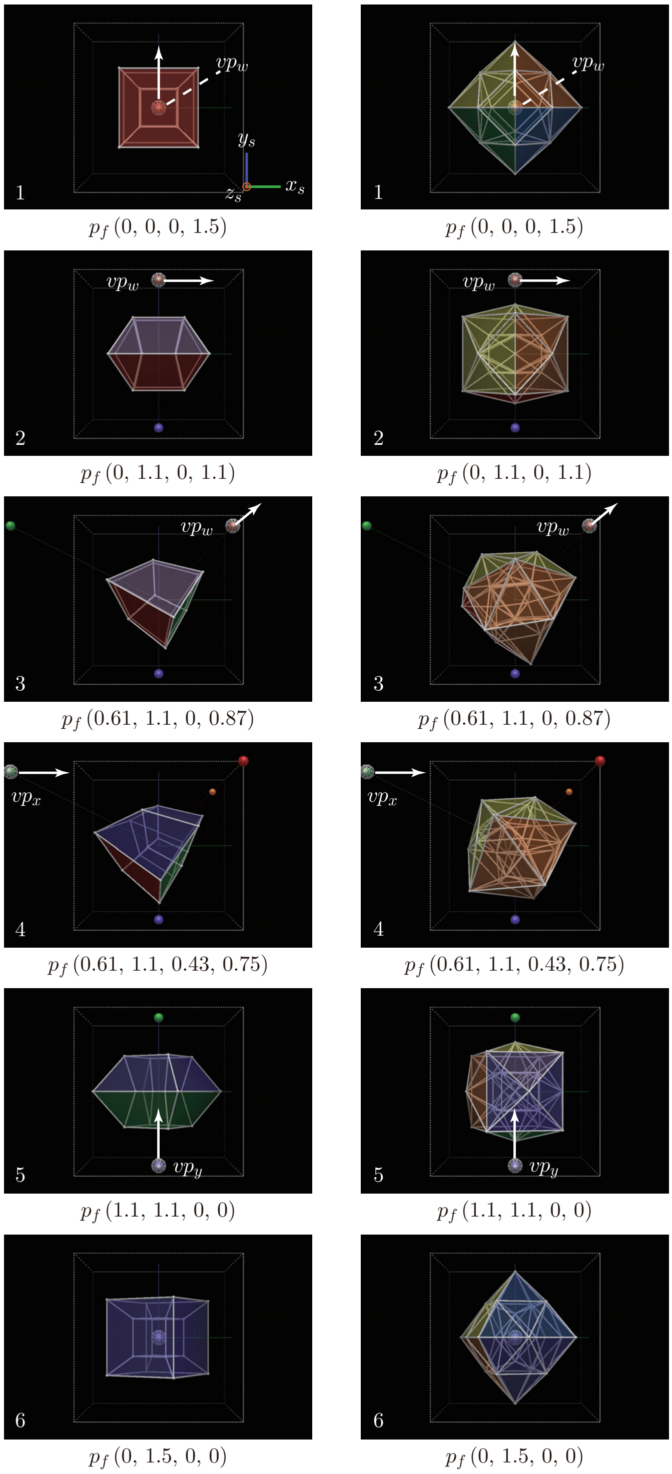

(a) (b)

Figure 2.8. Practical example of the observation of 4-D solids. (a) Hypercube. (b) 24-cell.

2.4.3 Observation of 4-D Solids from an Arbitrary 4-D Eye-Point

Figure 2.8 shows 4-D solids observed from different 4-D eye-points. The figure depicts image sequences of 3-D perspective drawings of the hypercube and a 24-cell (see Appendix B for the definition of the 24-cell) obtained by the movement of the 4-D eye-point controlled by the principal vanishing point operations. In this example, the coordinates of the vertices of the hypercube and the 24-cell are normalized such that their vertices are inscribed inside a 4-D spherical surface with a radius of 1.0. We assign a different color to each cell of the hypercube and 24-cell. To clearly visualize the edges inside the 3-D perspective drawing, the 3-D perspective drawings are rendered with semitransparent surfaces and a reticular stipple pattern. We place each 4-D solid at the origin of the 4-D world-coordinate system, and observe it while we move on the 4-D spherical surface with a radius of 1.5, centered at the origin of the 4-D world-coordinate system. The parameters (k, h, f) of the 4-D viewing field are $(0.5, 0.5, 100)$, respectively.

In this example, the 4-D eye-point is initially at $(0, 0, 0, 1.5)$, and only the principal vanishing point vp_w is displayed at the center of the 3-D screen (image 1 in Figure 2.8). Starting from this situation, the principal vanishing point vp_w is first moved in the y_s-direction in 3-D space. This results in the movement of the 4-D eye-point in the $y_w w_w$-plane on the 4-D spherical surface. Accordingly, the shape of the 3-D perspective drawing of the 4-D solid changes to the two-point perspective drawing (image 2 in Figure 2.8). Then, when the principal vanishing point vp_w is moved in the x_s-direction in 3-D space, the 4-D eye-point moves on the 4-D spherical surface in parallel to the $x_w w_w$-plane. Consequently, the three-point perspective drawing is visualized on the 3-D screen (image 3 in Figure 2.8). After this, when the principal vanishing point vp_w is moved in the z_s-direction in 3-D space, the 4-D eye-point moves on the 4-D spherical surface in parallel to the $z_w w_w$-plane. The 3-D perspective drawing changes to the four-point perspective drawing (image 4 in Figure 2.8). Following these eye-point movements, the principal vanishing point being operated on is changed from vp_w to vp_x, and this is moved in the x_s-direction in 3-D space. This operation results in the movement of the 4-D eye-point in parallel to the $x_w z_w w_w$-hyperplane. As a result, the 3-D perspective drawing changes to the two-point perspective drawing again (image 5 in Figure 2.8). Finally, the principal vanishing point vp_y is moved along the y_s-axis to make the 4-D eye-point move to the zenith of the 4-D spherical surface. When the 4-D eye-point arrives on the y_w-axis in 4-D space, the 3-D perspective drawing becomes the one-point perspective drawing (image 6 in Figure 2.8).

In this manner, by operating on the principal vanishing points in 3-D space, we can control the movement of the 4-D eye-point and observe 4-D data from arbitrary 4-D positions intuitively. Specifically, as described in images 2 through 5 in Figure 2.8, the proposed system allows us to move around and observe the 4-D data without changing the altitude (the y_w-coordinate of the 4-D eye-point) and distance of the 4-D eye-point. These types of movement are known as circle strafing actions, and are helpful for obtaining a complete picture of the object. However, such movement is not implemented in conventional 4-D visualization techniques. Thus, our interaction technique enhances the latitude and flexibility of the 4-D space observation.

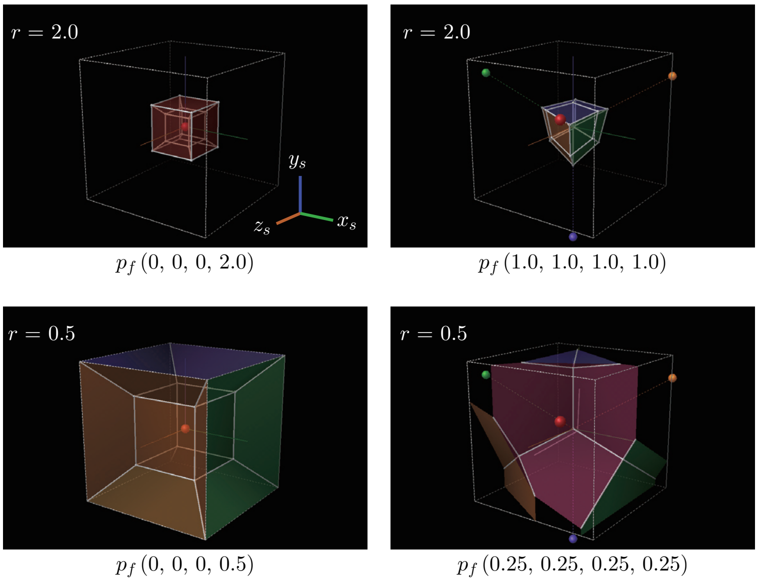

Figure 2.9. Observation of the hypercube with the different radius of the 4-D spherical surface.

2.4.4 Observation of 4-D Solids with Various 4-D Viewing Field

Our 4-D visualization algorithm can visualize 4-D data with various distances and viewing fields, respectively, by changing the radius r of the 4-D spherical surface and the parameters (k, h, f) of the 4-D perspective transformation [22, 23].

Figure 2.9 shows the hypercube observed from different distances in 4-D space. The parameters (k, h, f) for the 4-D perspective transformation are $(0.5, 0.5, 100)$, respectively. When the radius r of the 4-D spherical surface is increased and the 4-D eye-point moves away from the hypercube, the 3-D perspective drawing of the hypercube becomes smaller on the 3-D screen. Conversely, when the radius r is decreased and the 4-D eye-point approaches the hypercube, we can see the inside of the hypercube clipped by the 3-D screen. Even if the radius changes, the positions of the principal vanishing points do not change unless the 4-D eye-point changes in 4-D space.

Figure 2.10 shows the hypercube observed with different 4-D viewing fields. In our visualization algorithm, the viewing angle is determined by the ratio of the parameter k of the 3-D screen dimensions to the parameter h of the distance from the 4-D eye-point to the 3-D screen. When we observe the hypercube with a wide viewing field, the 3-D perspective drawing becomes smaller on the 3-D screen. Conversely, when we observe the hypercube with a telescopic viewing field, part of the hypercube protrudes from the 4-D viewing field and is clipped by the 3-D screen. Consequently, we can see the inside of the hypercube from the clipped part. Unlike when we change the radius of the 4-D spherical surface, the positions of the principal vanishing points differ according to the form of the 4-D viewing field. As the 4-D viewing field becomes telescopic, the distance from

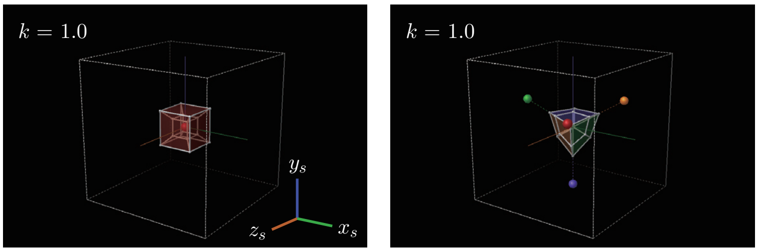

$p_f\,(0,\ 0,\ 0,\ 1.5)$ $p_f\,(0.75,\ 0.75,\ 0.75,\ 0.75)$

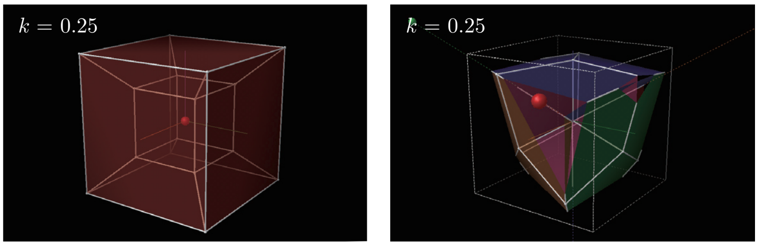

$p_f\,(0,\ 0,\ 0,\ 1.5)$ $p_f\,(0.75,\ 0.75,\ 0.75,\ 0.75)$

Figure 2.10. Observation of the hypercube with the change of the 4-D viewing field.

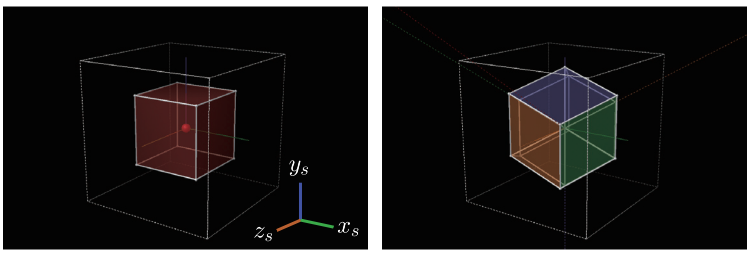

$p_f\,(0,\ 0,\ 0,\ 1000)$ $p_f\,(500,\ 500,\ 500,\ 500)$

k 0.5, h 500, f 2000 k 0.5, h 500, f 2000

Figure 2.11. Observation of the hypercube with the parallel projection.

the center of the 3-D screen to the principal vanishing point increases. Thus, the change of the 4-D viewing field may affect the usability of the principal vanishing point operations. This concern will be examined in Chapter 3.

Figure 2.11 shows the hypercube observed by parallel projection. This parallel projection is performed by significantly decreasing the ratio of the parameter k to the parameter h, and locating the 4-D eye-point extremely far from the 3-D screen. In the parallel projection, depth information of the 4-D data is lost from the 3-D perspective drawing. Instead, the parallelism and orthogonality of the 4-D data are emphasized. Because the principal vanishing points are substantially displayed at the points at infinity in 3-D space, the principal vanishing point operations are not realistic when we use the parallel projection.

2.5 Application of the 4-D Space Visualization

We can expect that the proposed interactive system can facilitate not only the handling of geometric information such as 4-D solids, but also the handling various 4-D data such as mathematical functions, statistical data, and analysis of physical phenomena. In addition, this kind of system might be used as a supporting tool for creative activities. In this section, as possible applications of the proposed system, we present some examples of 4-D statistical data visualization, 4-D phase space visualization, and 4-D animations.

2.5.1 Visualization of 4-D Statistical Data

Consider representing 4-D data that contains multiple items consisting of four variables. For such data, parallel coordinates [35] are a common way of visualizing and analyzing the relationships between variables. Figure 2.12(a) shows a representative sample for parallel coordinates. We visualize 4-D data with ten items consisting of four variables (X, Y, Z, W). Each polyline in the figure represents one item. In parallel coordinates, when lines between two parallel axes are parallel to each other, these two corresponding variables have a positive relationship. On the other hand, when lines cross each other and make a superposition of x-shapes, there is a negative relationship between the two variables. When some lines are parallel and others cross, this signifies that there is no relationship.

We now represent this 4-D data in our proposed system. We associate the variables X, Y, Z, and W of the 4-D data with the x_w-, y_w-, z_w-, and w_w-axis of the 4-D world-coordinate system, respectively. Then, we connect each pair of variable values of the 4-D data item with a line. Visualization results are obtained in which ten tetrahedrons are formed with various sizes to represent the 4-D data items, as shown in Figure 2.12(b). A relationship between the two variables is now represented by the mesh pattern appearing on a 4-D coordinate plane. For example, parallel lines appearing on the $y_w z_w$-plane suggest that there is a positive relationship between the variables Y and Z, and a mesh pattern appearing on the $x_w z_w$-plane indicates that there is a negative relationship between the variables X and Z. The uniformity of the mesh pattern indicates the strength of the relationship. For instance, because the mesh pattern on the $x_w w_w$-plane is biased toward the w_w-axis, we can infer out that the relationship between the variables X and W is weaker than that between the variables X and Y.

Although parallel coordinates have many advantages for data visualization and analysis, they cannot show all relationships in the given data, because each axis can have at most two neighboring axes. This introduces a limitation to parallel coordinates: it is necessary to find a good axis arrangement in order to obtain a better visualization. In contrast, using the proposed system, we can see all relationships at one time, or we can find them by exploring in 4-D space. We do not claim that our representation will replace parallel coordinate; however, we can expect that it will help to find a good preliminary axis arrangement when using parallel coordinates.

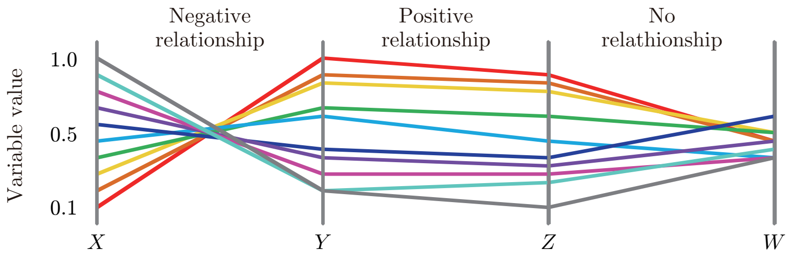

(a)

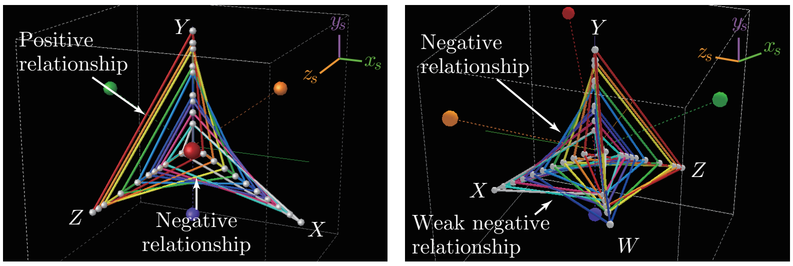

$p_f(514, 707, 400, 275)$

k 0.4 h 500 f 2000

(b)

Figure 2.12. Visualization of the correlation among four variables. (a) Representations by parallel coordinate plots. (b) Representations by the proposed system.

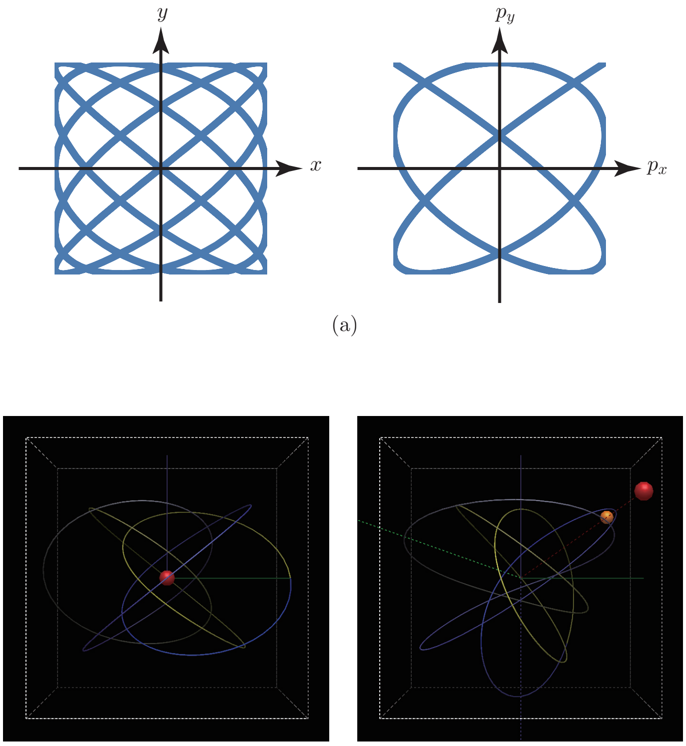

(a)

p_f (0, 0, 0, 2.0)
k 0.5, h 0.5, f 100.0

p_f (1.0, 1.0, 1.0, 1.0)
k 0.5, h 0.5, f 100.0

(b)

Figure 2.13. Trajectory of the 2-D harmonic oscillator represented in the 4-D phase space. (a) Possible position states and momentum states of the oscillator. (b) 3-D perspective drawings of the trajectory visualized by the proposed system.

2.5.2 Visualization of 4-D Phase Space

The movement of a point mass in 2-D space is represented by a trajectory in 4-D phase space, where two axes are defined as the two spatial dimensions x and y, and the other two are defined as the two momentum dimensions p_x and p_y. Although the higher-dimensional phase space can be visualized by a Poincaré map, the proposed system can visualize a 4-D phase space without any degeneration. For example, a 2-D harmonic oscillator can be visualized as a 3-D perspective drawing of a single trajectory defined in 4-D space, as shown in Figure 2.13, by associating the positions x and y with the x_w-and y_w-axis, respectively, and the momentums p_x and p_y with the z_w- and w_w-axis of the 4-D world-coordinate system, respectively. The movement of the point mass is visualized as a single closed trajectory in 4-D space. This signifies that the 2-D harmonic oscillator is periodic and isoenergetic. In addition, because the trajectory does not intersect itself, the mass point never takes the same state during an oscillation period. In this manner, the proposed system can visualize the position and momentum of the point mass at one time, and helps us understand the character of the movement. We will study the possibility of visualizing a phase space of chaotic motion or 3-D movement in future work.

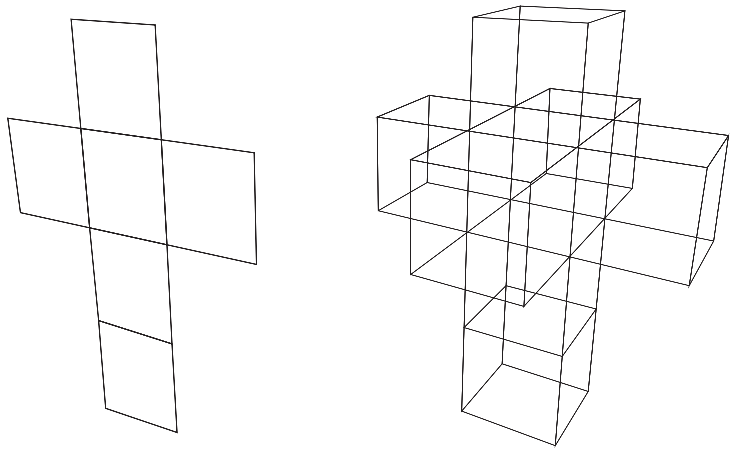

(a) (b)

Figure 2.14. Development plans of 3-D and 4-D solids. (a) Cube. (b) Hypercube.

2.5.3 Animation of Folding Processes of a 3-D Development of a 4-D Solid

As 3-D solids are produced by folding their 2-D development plan at their edges in 3-D space, 4-D solids are produced by folding their 3-D development plan at their surfaces in 4-D space. For instance, unfolding a cube into a 2-D plane results in a flat cross, as shown in Figure 2.14(a). Then, the cube is restored by folding the development plan at each edge shared by two squares at 90 degrees in 3-D space. Similarly, unfolding a hypercube into a 3-D hyperplane results in a 3-D cross, which consists of eight cubes, as shown in Figure 2.14(b). Then, the hypercube is restored by folding the development plan at each surface shared by two cubes at 90 degrees in 4-D space. Figure 2.15 depicts animation sequences of folding a 3-D development plan into a hypercube from different 4-D eye-points. In this example, the 3-D development plan of the hypercube is placed on the hyperplane of $w_w = -0.5$, and is restored as the center of the resulting hypercube arrives at the origin of the 4-D world-coordinate system. Although we have visualized this folding process from the fixed 4-D eye-point in the figure, we can,of course observe this sequence from various positions while we move in 4-D space, by operating on the principal vanishing points. In this manner, the proposed system enables us to interact not only with static 4-D data, but also with dynamic 4-D data. This signifies that the proposed system can be used not only as an interactive environment where we gain intuitive understandings of 4-D space and objects, but also as the interactive tool that supports creative activities such as 4-D origami [21] in the future.

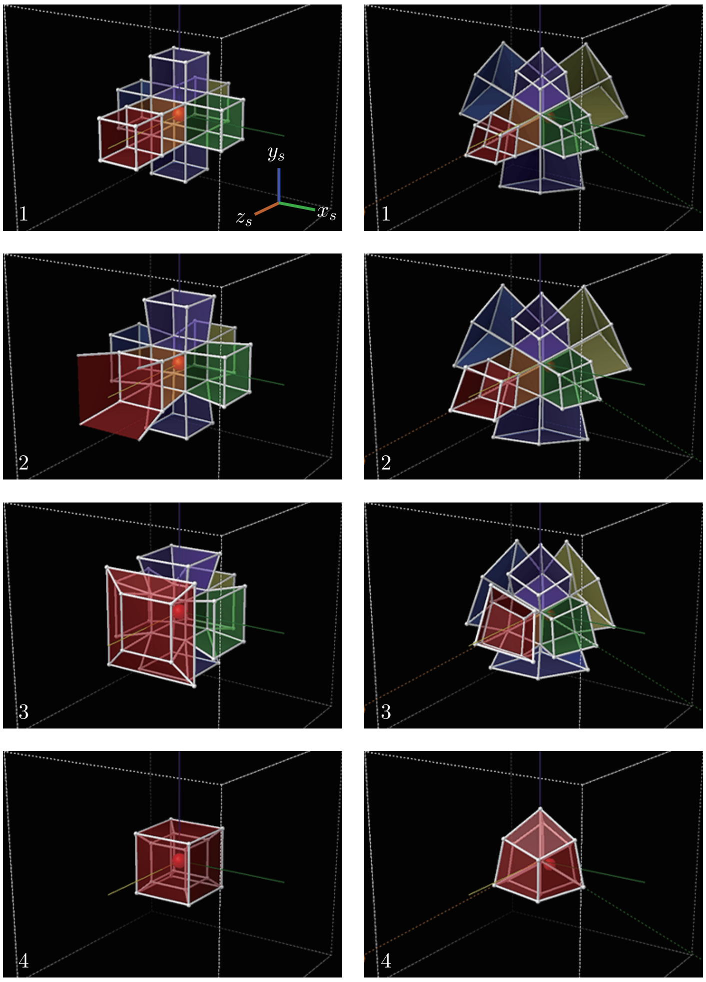

$p_f\,(0,\,0,\,0,\,2.4)$
k 0.5 h 0.5 f 100

$p_f\,(-1.2,\,-1.2,\,-1.2,\,1.2)$
k 0.5 h 0.5 f 100

Figure 2.15. Animation sequences of the hypercube restored from its 3-D development plan in 4-D space.

2.6 Summary

In Chapter 2, we have proposed a novel algorithm that determines the 4-D eye-point from the 3-D positions of the principal vanishing points. Using this algorithm, we can interactively control the 4-D eye-point to move along a 4-D spherical surface that surrounds a 4-D observation object, by handling the principal vanishing points displayed in 3-D space. In addition, we showed some possible applications of the proposed 4-D interaction technique, and suggested that our proposed interaction technique will be effective in various fields, not only in the observation of 4-D geometric objects, but also in representations of 4-D statistical data, visualizations of physics, and tools for creating 4-D animations.

Chapter 3

Evaluation of the Interactive 4-D Visualization System

In Chapter 3, we construct an interactive 4-D visualization system using the interaction algorithm described in Chapter 2. The proposed system consists of recent commercially available devices: a personal computer, a head-mounted display with built in 6-DoF sensor, a motion sensor, and a wireless mouse. Using the proposed system, we can smoothly move in 4-D space and observe any 4-D data with simple pick-and-move operations of the principal vanishing points. To evaluate the effectiveness of the interactive system, we perform user tests that compare the usability of our proposed system with that of two conventional interaction methods. Moreover, we investigate the effect of the change in the 4-D viewing field on the usability.

3.1 Construction of the Interactive System

Figure 3.1 shows a configuration of the interactive system. The system consists of commercially available products: a personal computer, a head-mounted display with a built in 6-DoF sensor, a motion sensor, and a five-button wireless mouse.

The 3-D virtual space seen through the head-mounted display coincides with the $x_s y_s z_s$-space in the 3-D screen-coordinate system $x_s y_s z_s w_s$. The movable region for two of the principal vanishing points, vp_x and vp_y, is restricted to the $x_s y_s$-plane and the y_s-axis, respectively, whereas the other principal vanishing points, vp_z and vp_w, can move freely in 3-D space. These restrictions mean that the 4-D upper direction of the 4-D eye-point is maintained in an upward or downward vertical direction in the 4-D world-coordinate system during the interaction. The 3-D virtual space has the same scale as real space, and the viewing position and viewing direction in 3-D virtual space are associated with the user's head position and orientation, respectively; likewise, the user can observe a 3-D perspective drawing from any direction as shown in Figure 3.2. The 3-D perspective drawing, principal vanishing points, and 3-D screen are

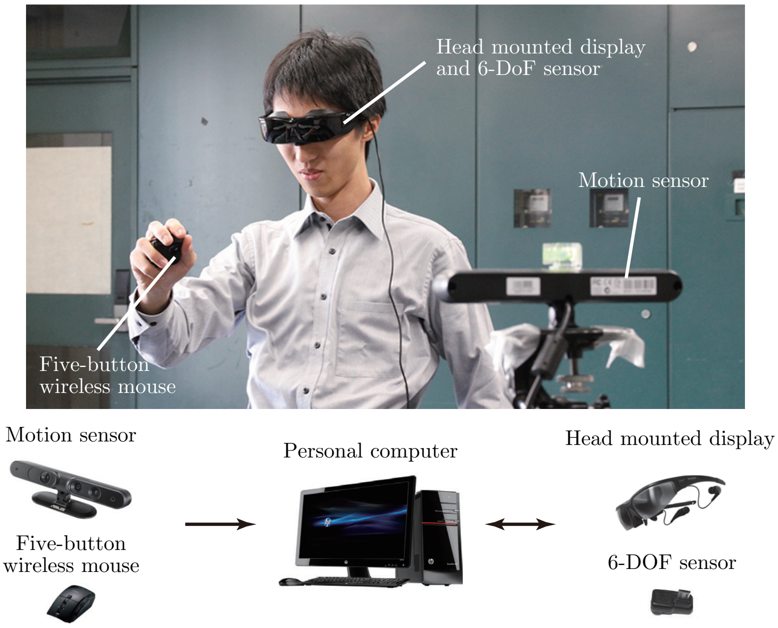

Figure 3.1. Configuration of the interactive system.

displayed in 3-D virtual space as a stereoscopic image.

The user observes various 3-D perspective drawings of the 4-D object while handling the principal vanishing points in 3-D space with simple pick-and-move operations using a 3-D cursor associated with their hand motion. In the system, the user can handle the principal vanishing points with two-step left button operations with the five-button wireless mouse. The first step is a click operation to pick one principal vanishing point, and the second step is a drag operation to move it in the 3-D virtual space. Figure 3.3 shows actual operations of the interactive system. When the moving 3-D cursor and a target principal vanishing point overlap with each other, the user can perform the principal vanishing point operations using the above-mentioned mouse button operation. Additionally, we associate click operations on each of the two side buttons of the wireless mouse with the forward and backward movements of the 4-D eye-point along the 4-D visual axis, respectively. This enables the user to change the distance from the 4-D eye-point to the 4-D observation object in 4-D space. Thus, the user can interactively observe various 3-D perspective drawings of 4-D data from different viewing positions, directions, and distances in 4-D space.

3.2 Experiment 1: Effectiveness of the Interactive System

To evaluate the effectiveness of our interactive system based on principal vanishing points, we compared its usability with that of two conventional interaction methods: a classic keyboard-based system, which handles parameter changes regarding the 4-D eye-point movement, and our previous system [22], which utilizes a flight-controller pad associated with human actions in 3-D space. We

(a)

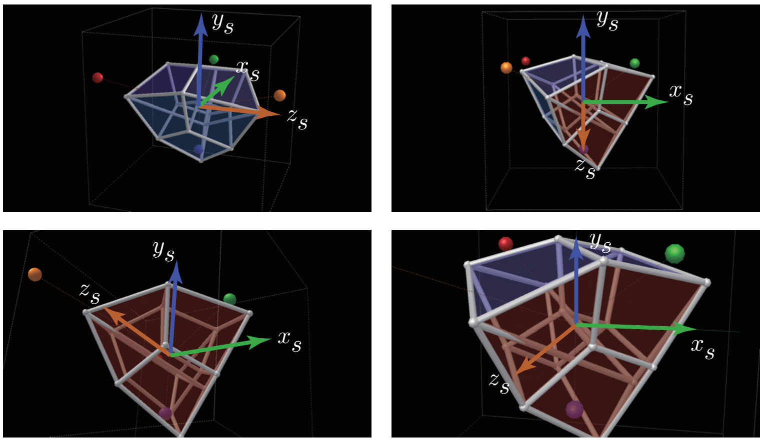

(b)

Figure 3.2. Observation of 3-D perspective drawings by the user's head motion tracking. (a) Images of a user. (b) User's view.

(a)

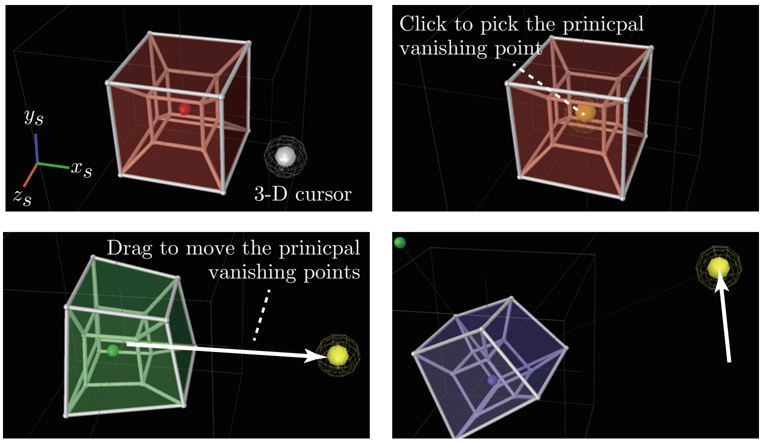

(b)

Figure 3.3. Pick-and-move operations of the principal vanishing points. (a) Images of a user. (b) User's view.

performed an objective evaluation of the operation time.

3.2.1 Method

We first introduce the participants, apparatus, and stimuli of the experiment.

Participants

Fourteen male participants and seven female participants were tested. They were students or graduate students, and their mean age was 22.3 years. None of the participants had knowledge or experience of 4-D space and objects, and they were unfamiliar with the design of the study. In addition, they had no experience in the 3-D virtual space displayed on the head mounted display.

We divided the participants into three random groups. Group A, consisting of four males and three females with a mean age of 22.1 years, used the principal vanishing points to control the 4-D eye-point. Group B, consisting of five males and two females with a mean age of 21.9 years, used the keyboard. Group C, consisting of five males and two females with a mean age of 22.9 years, used the flight-controller pad.

Apparatus

The proposed system, used by the participants of group A, consisted of a personal computer (Intel Core i7 3.90GHz, NVIDIA GeForce GTX 680, 8GB RAM) with Windows 8 (Microsoft) installed, a head mounted display with a built-in 6-DOF sensor (Wrap 1200VR, Vuzix), a motion sensor (Xtion PRO LIVE, ASUS), and a five-button wireless mouse (M-GE3DL, ELECOM). The system guaranteed a real-time performance (250 frames per second when displaying a hypercube, 30 frames per second when displaying a 600-cell), and we confirmed that the operating speed of the interactive system did not cause any trouble during the experiment. The horizontal field of view of the head mounted display was 35 degrees. The screen resolution of the head mounted display was 1280 $\times$ 720. The 3-D perspective drawing of 4-D data, principal vanishing points, and the 3-D screen were displayed as a side-by-side stereoscopic image on the head mounted display. The 3-D screen has a size of 300 mm $\times$ 300 mm $\times$ 300 mm, and was placed 1.5 m off the ground, according to the participants' request. Under this configuration, the participants used the head mounted display and wireless mouse to manage the experimental tasks performed in the interactive system.

The keyboard-based system, used by the participants of group B, employed a keyboard for the input device. Instead of controlling the principal vanishing points, in this system, the participants directly manipulated the parameter α, β, and γ regarding the 4-D viewing direction of Equation 2.6 in Chapter 2. We associated six keys on the numeric keypad with the increase and decrease of the parameter values. Each of the 7-8-9 and 1-2-3 keys were used to increase/decrease α, β, and γ, respectively. In addition, we associated the WASD keys on the character keypad with horizontal and vertical rotations of the 3-D screen in order to allow the participants to observe them from various directions in the 3-D virtual space. The 3-D perspective drawing and principal vanishing points are displayed on a 24-inch LCD monitor with depth cueing. The participants performed the experimental tasks with these keyboard operations in front of the monitor device.

The flight-controller pad system, used by the participants of group C, adopted a flight-controller pad (FLIGHT SIM YOKE, CH Product) as the input device. Two steering actions of the flight controller pad corresponded to rotations at a 4-D eye-point on the 4-D spherical surface. These actions allowed the participants to observe a 3-D perspective drawing of 4-D data from various directions in 3-D space. Moreover, the 4-D upper direction was changed by these steering actions. The right button on the handle corresponded to the movements of the 4-D eye-point in the 4-D upper direction along the 4-D spherical surface. This action enabled the participants to change the viewing position in 4-D space, and observe various 3-D perspective drawings of 4-D data. The participants combined these actions in front of the monitor device to handle the experimental tasks.

Stimuli

In the first part of the experiment, we used a hypercube as the object of observation. The coordinates of the hypercube vertices are normalized as the permutations of $(\pm 0.5, \pm 0.5, \pm 0.5, \pm 0.5)$, and was placed at the origin of the 4-D world-coordinate system such that each of the eight cells was located in a different positive or negative position on each axis of the 4-D world-coordinate system, at a distance of 0.5 from the origin. We assigned one of eight colors (red, pink, green, cyan, purple, blue, orange, or yellow) to each cell of the hypercube. In order to clearly visualize the edges inside the 3-D perspective drawing, the 3-D perspective drawings were rendered with a semitransparent surface with a reticular stipple pattern.

In the latter part of the experiment, we used a 24-cell as the object of observation. Although the 24-cell was normalized and was located at the origin of the 4-D world-coordinate system like the hypercube, it was colored in a different manner. We observed that the participants found it significantly difficult to memorize and distinguish 24 different colors, if we assigned a different color to each cell of the 24-cell. The purpose of the experiment was not to evaluate the participants' memory power, but to examine whether the proposed system had sufficient usability to smoothly control the 4-D eye-point. Accordingly, inspired by the structural coloration of morpho butterflies, we programmed the 24-cell to change its color according to the viewing angle in 4-D space. The 24-cell became one of the eight colors (red, pink, green, cyan, purple, blue, orange, or yellow) when the participants observed it from each positive or negative direction of the 4-D world-coordinate axes. When the participants were in the middle between the axes, the color of the 24-cell was determined as the blend of the four colors corresponding to the nearest four axes. For example, if the participants moved from the positive position on the w_w-axis to one on the x_w-axis, the appearance of the 24-cell gradually changed from red to green.

3.2.2 Procedure

The experiment started from a learning period. Each participant first received a brief lecture on some basic aspects of 4-D space and objects. Then, he/she

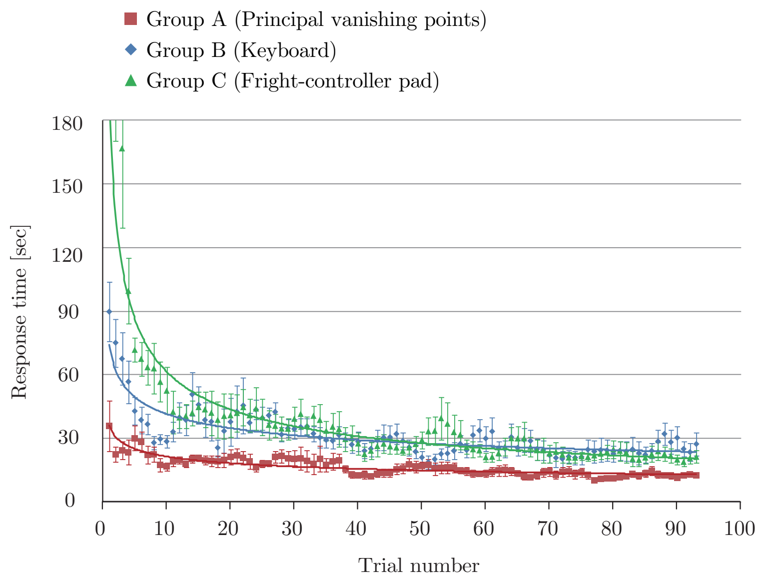

Figure 3.4. Response time to reach a goal point in 4-D space.

received an explanation regarding how to use the interactive system, and practiced using the system for ten minutes. In this practice period, the participants freely observed the hypercube.

Following the practice, the participants proceeded to the task period. The participants were told to move around the hypercube along the 4-D spherical surface with a radius of 1.5 from the start point to a goal point. In order to perform 32 trials, we created eight random start points on the 4-D spherical surface and assigned them to four goal points $(1.5, 0, 0, 0)$, $(0, 1.5, 0, 0)$, $(0, 0, 1.5, 0)$, and $(0, 0, 0, 1.5)$. In each trial, the goal point was given to the participants by informing and showing them the color and image of the 3-D perspective drawing obtained at the goal point. We presented the 32 trials in a random order, in order to avoid order effects. The participants started the trial when they received the starting signal. Then, they signaled their arrival when they reached the goal point. If the distance between the 4-D eye-point and participant's 4-D position was under a threshold value at that time, then the participant finished the trial, and was allowed to move to the next trial. If the distance was over the threshold, then they had to continue the trial until they came sufficiently close to the goal point. We recorded the response time and final distance between the 4-D eye-point and goal point. In the present study, the threshold was 0.4, which corresponded to an angular difference of 15 degrees between the 4-D viewing direction and the direction from the origin of the 4-D world-coordinate system to the goal point. We repeated the 32 trials three times with five minute intervals. After this, we changed the observation object from the hypercube to the 24-cell, and ran another 32 trials.

3.2.3 Results and Discussion

A total of 2688 trials were run with 21 participants. We regarded 2524 trials as valid results, because we failed to properly record the results in 64 trials, due to an unexpected error in the recording system. Sufficient data was collected from the participants to evaluate the usability of the proposed system.

Figure 3.4 shows the results of the first three repetitions of the 32 trials. In order to compare the response times from the three groups, we first applied a moving window average of size four to the raw data, to compensate for the noise in the time data. Then, we computed the average response times and standard errors for the seven participants in each group. Next, we plotted the average response times with the standard errors displayed as error bars. In addition, we added a power trend line to indicate the inclination of the learning effect. The response times of group A, who used the proposed system, were shorter than those of the other groups. The standard errors of group A were also smaller than those of the other groups. In order to investigate further, we conducted an unequal variance t-test on the last 32 trials with the null hypothesis—the proposition that the mean values of the response times for the proposed system and each of the conventional interfaces are the same. The p-values were $7.9 \times 10^{-9} < 0.01$ and $6.6 \times 10^{-7} < 0.01$ for groups B and C, respectively, and the difference between the mean response times was highly significant. Thus, we rejected the null hypothesis, and concluded that the mean response times for the proposed system and conventional systems are significantly different. This result indicated that the proposed system had a sufficient usability to observe 4-D data while intuitively controlling the 4-D eye-point in 4-D space.

We computed the mean response time over the last 32 trials, in which we used the 24-cell as the observation object, for each group. Again, we performed an unequal variance t-test on these trials in order to compare the proposed system with each of the conventional systems. The mean response time of group A was 17.7 seconds, that of group B was 39.9 seconds, and that of group C was 25.5 seconds. The p-values were $5.8 \times 10^{-7} < 0.01$ and $1.5 \times 10^{-4} < 0.01$ for groups B and C, respectively. This result indicated a significant difference between the proposed system and the conventional systems. Thus, it was indicated that the usability of the proposed system was independent of the appearance of the 4-D solid.

Because the participants operated the principal vanishing points using their hand in the air, it was expected that making a slight adjustment of the 4-D eye-point would be more difficult than for the conventional systems. In addition, it was thought that a 150 to 250 millisecond latency of the motion sensor and a 50 to 100 millisecond latency of the 6-DoF sensor might impair the accuracy of the principal vanishing point operation, because people begin to feel a latency at 50 milliseconds, and lose comfort at 150 milliseconds [57] in general when they use a virtual reality system. In order to investigate these concerns, we evaluated the accuracy of the 4-D eye-point control. We computed the average angular difference over the last 32 trials of the hypercube observation for each group, and then performed a paired t-test on these data in order to compare the proposed system with each of the conventional systems. The mean angular difference of group A was 6.5 degrees, which was larger than the 5.4 degrees of group B and 5.5 degrees of group C. The p-values were 0.004 and 0.003 for the groups B and C, respectively, indicating a significant difference between the proposed system and the conventional systems. However, when we compared the results of the 24-cell observation, the mean angular differences of groups A, B, and C were 5.6 degrees, 5.0 degrees, and 6.8 degrees, respectively. Moreover, the p-values were 0.03 and 0.05 for groups B and C, respectively, indicating that the accuracy of the proposed system was not significantly different from those of the conventional systems. In fact, the trend of the accuracy between the proposed system and the flight-controller pad system was reversed. Therefore, we can conclude that the accuracy of the 4-D eye-point control in the proposed system does not differ from those of the conventional systems. The participants were still able to control the 4-D eye-point accurately in the proposed system. Moreover, because the participants did not point out the latency problem during the experiment, we were able to surmise that the latency of the motion sensor and 6-DoF sensor in the current system did not significantly affect the usability during the experiment.

3.3 Experiment 2: Subjective Impression of the Interactive System

In order to examine the usability of the proposed system, we conducted an evaluation experiment in which we compared the proposed system with the two conventional systems according to a subjective evaluation of how it feels to operate the system. In this experiment, the participants performed 4-D observation tasks with the proposed system and the conventional systems, and they ranked them for each of the question items.

3.3.1 Method

We first introduce the participants, apparatus, and stimuli of the experiment.

Participants

The 20 participants involved in Experiment 1 were invited to join Experiment 2. Each participant was tested between one and two weeks after Experiment 1.

Apparatus

We again used the proposed system and the same two conventional systems utilized in Experiment 1.

Stimuli

The objects of observation were the hypercube and 24-cell used in Experiment 1.

3.3.2 Procedure

Each participant received an explanation of how to use the interactive systems. Then, the participants were told to freely observe the hypercube and 24-cell for

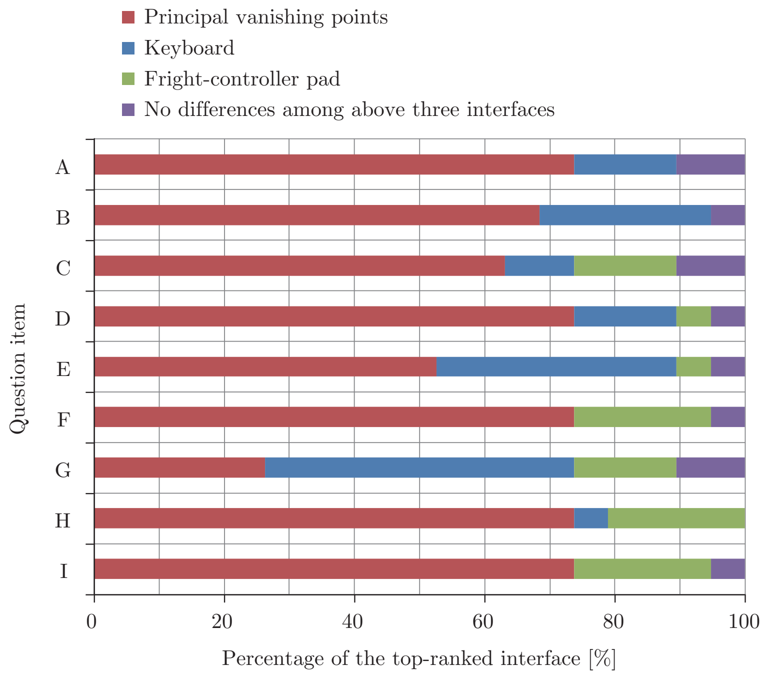

Figure 3.5. Subjective evaluation of the proposed system.

four minutes with each interactive system. In order to avoid ordering effects, we shuffled the usage order of the systems for each participant.

After the observation tasks, the participants ranked the three systems for each of the following questions. If the participants were not able to find a difference between the systems, then they were allowed to answer "No difference". In addition, we collected feedback comments from the participants.

A. Which system was easy to understand how to use?
B. Which system was easy to get accustomed to quickly?
C. Which system was easy to understand the movement of the 4-D eye-point?
D. Which system was able to control the 4-D eye-point as desired?
E. Which system was able to predict the change of a 3-D perspective drawing when operated?
F. Which system was able to control the 4-D eye-point without feeling uncomfortable when an observation object was changed?
G. Which system was able to control the 4-D eye-point to the desired position accurately?
H. Which system did you enjoy using?
I. Which system did you want to use again in the future?

3.3.3 Results and Discussion

Figure 3.5 shows the results of the experiment. We produced a band chart that shows the percentage of the system ranked at the top for each question item. Overall, most participants were satisfied with the usability of the proposed system. This suggested that the proposed system was accepted by the users. In particular, the proposed system received higher evaluations regarding the intuitiveness of the eye-point control in 4-D space. The participants gave many positive comments. For example, participants reported that the principal vanishing points were helpful for understanding the 4-D eye-point movements. They also reported that they felt that the 3-D perspective drawing just changed its shape in 3-D space with special transformation rules when they used the keyboard system. However, they felt that they directly interacted with the 4-D solids when using the proposed system. These positive results indicated that the principal vanishing points were suited to the interface for 4-D interaction.

We also received some negative comments from the participants. Some participants felt that the detailed operation of the principal vanishing points was difficult. When they used the keyboard operation or the flight-controller pad, the magnitude of input on the interface and amount of movement of the 4-D eye-point are in one-to-one correspondence, and the amounts were not affected by noises or latencies. On the other hand, the proposed system used the participants' hand motions, tracked by the motion sensor, to handle the principal vanishing points in 3-D space. Although this style was simple and intuitive, it was affected by sensor noise or unconscious blurring of the hand. This might have made the participants feel uncomfortable. However, this problem can be solved, and is not essential, because sensor resolution and accuracy are rapidly improving owing to recent technological advances in virtual reality devices.

3.4 Experiment 3: Effects of Change in the 4-D Viewing Field

As shown in Section 2.4.4, our 4-D visualization algorithm can visualize 4-D data with various 4-D viewing fields by changing the radius r of the 4-D spherical surface and the parameters (k, h, f) for the 4-D perspective transformation [22, 23]. In this section, we examine whether changes in the 4-D viewing field affect the usability of the proposed system, with a subjective evaluation.

3.4.1 Method

We first introduce the participants, apparatus, and stimuli of the experiment.

Participants

The seven participants involved in Experiments 1 and 2 were invited to join Experiment 3. Thus, the participants had sufficient usage experience of the proposed system.

Apparatus

We used the proposed system with the same configuration as Experiments 1 and 2. Thus, the participants operated the principal vanishing points in the 3-D virtual space displayed in the head mounted display with the wireless mouse held in the hand.

Table 3.1. Settings of the 4-D viewing field.

Setting name	r	k	h	f
Initial setting	1.5	0.5	0.5	100
Far distance	2.0	0.5	0.5	100
Close distance	0.5	0.5	0.5	100
Wide view	1.5	1.0	0.5	100
Telescopic view	1.5	0.25	0.5	100

Stimuli

The object of observation was the hypercube used in Experiments 1 and 2.

3.4.2 Procedure

In this experiment, the participants were told to observe the hypercube with various settings of the 4-D viewing field. Table 3.1 lists the settings. First, the participants observed the hypercube with the initial setting. Then, they tried the other four settings in order. The observation lasted for five minutes for each setting. After completing the observation tasks, the participants answered the following questionnaire to evaluate whether the usability of the system or ease of understanding 4-D space and objects changed.

A. Was it easy to operate the principal vanishing points in 3-D space?
B. Were you able to control the 4-D eye-point as desired?
C. Were you able to understand the movements of the 4-D eye-point?
D. Were you able to predict changes of the 3-D perspective drawing of the hypercube when you moved in 4-D space?

Each question item had a seven-point scale between “minus three” and “plus three”. A minus score meant that the usability of the proposed system deteriorated after the 4-D viewing field changed from the initial setting. Conversely, a plus score meant that the usability of the propose system improved after the 4-D viewing field changed from the initial setting.

3.4.3 Results and Discussion

Figure 3.6 shows the results of the experiment. We first computed the average score over the seven participants for each setting. Then, we produced a bar chart with the standard deviations displayed as error bars. The results indicated that the change of the view angle affected the usability of the proposed system. As shown in Figure 2.10, the principal vanishing points were displayed far away from the center of the 3-D screen when 4-D data was visualized with the telescopic viewing field. Because the participants’ reachable distance was limited in such cases, it was surmised that the principal vanishing point operation became difficult.

The results also indicated that it became difficult to predict changes of a 3-D perspective drawing caused by the 4-D eye-point movement when the 4-D

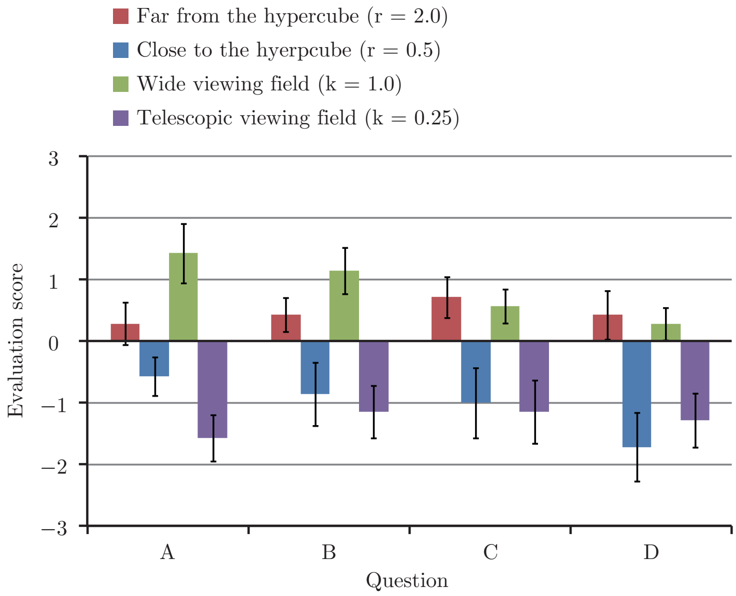

Figure 3.6. Effect on the usability from the change of the 4-D viewing field.

eye-point was close to the hypercube. This trend was also observed when the 4-D viewing field was telescopic. A common point to both settings was that the participants saw the inside of the hypercube clipped by the 4-D viewing pyramid. In such cases, as compared to observing the external appearance of the hypercube, the participants might find it difficult to understand the structure of the hypercube.

These results suggest that changing the 4-D viewing field can affect the usability of the principal vanishing point operations and understandability of the 4-D space and objects. However, these results did not instantly invalidate the effectiveness of the observation with various 4-D viewing fields. As described in Section 2.4.4, for example, when we change the 4-D viewing field from wide-angle to telescopic, it will become easier to visually understand the orthogonality and parallelism of a 4-D object. Moreover, according to a comment from the participants, the observation of the inside of the hypercube was interesting when considering the topology of a 4-D solid. Therefore, it is thought that changing the 4-D viewing field to suit a certain purpose will help people to gain understandings of the 4-D data structure.

3.5 Summary

In Chapter 3, we have examined the usability of the proposed system using objective and subjective evaluation experiments. We compared the proposed system with two conventional systems, and confirmed that the proposed system had sufficient usability for the observation of 4-D space and objects. Users were able to learn how to use the system within a short time, and they can control the 4-D eye-point intuitively, even if they had no prior knowledge or experience of 4-D space and objects. We also investigated the effects on usability of changes to the 4-D viewing field, and confirmed that the operation of principal vanishing points is limited when the 4-D viewing field is telescopic. However, such a viewing field is still useful to visually understand the orthogonality and parallelism of 4-D data. The observation with various 4-D viewing fields will be useful in gaining understandings of 4-D space and data.

Chapter 4

4-D Space Visualization Using Viewing Direction Control

In Chapter 4, we propose a novel 4-D space visualization technique that enables us to control the 4-D viewing direction with operations on the principal vanishing points. The proposed algorithm is implemented by extending the 4-D eye-point control algorithm introduced in Chapter 2. Moreover, we apply the proposed algorithm to the framework of a system that enables us to fly through 4-D space. Using the proposed system, we can look around and explore any 4-D solid scene constructed with multiple 4-D objects or an intricate spatial construction, such as a 4-D maze.

4.1 Basic Concept of 4-D Viewing Direction Control

To understand the surrounding environment, we look around and move in the environment. By analogy, if we can bring actions of this type into the 4-D space visualization system, we will be able to improve the degrees of freedom in the 4-D observation. In this chapter, to achieve this action in 4-D space, we construct a 4-D viewing direction control algorithm as an extension of the 4-D eye-point control algorithm presented in Chapter 2. This algorithm determines the 4-D observed point, which moves on a 4-D spherical surface centered on the 4-D eye-point, from the positions of the principal vanishing points in 3-D space. Furthermore, we combine this 4-D viewing direction control with the simultaneous movement of the 4-D eye-point and observed point in the 4-D viewing direction, in order to achieve 4-D fly-through actions in 4-D space. From this, the exploration of the entire 4-D space in a first person view can be achieved. Although conventional studies [21, 36, 37, 38, 39, 40, 41, 45, 46, 47, 49] have given weight to the observation of a single 4-D object, the proposed visualization method handles 4-D scenes consisting of multiple 4-D objects.

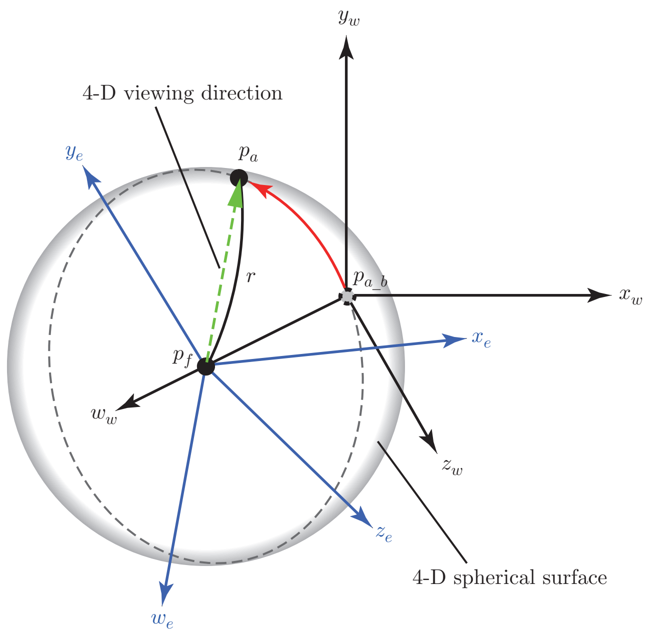

Figure 4.1. Model of the 4-D viewing direction control.

4.2 Algorithm for 4-D Viewing Direction Control

In this section, we describe an algorithm that determines the 4-D viewing direction from the principal vanishing points. Figure 4.1 shows the model of the 4-D viewing direction control. We consider controlling the movement of the 4-D observed point p_a along a 4-D spherical surface of radius r, centered at the 4-D eye-point p_f. To achieve this, we apply the 4-D eye-point control algorithm described in Chapter 2 to the 4-D observed point control. Unlike our previous 4-D visualization system [23], the proposed interaction algorithm enables us to look in all 4-D viewing directions from an arbitrary 4-D eye-point.

The proposed algorithm is composed of two processing steps, as well as the 4-D eye-point control algorithm. That is, the first step, which estimates the positions of the principal vanishing points in accordance with the user's operation, and the second step, which estimates the parameters for the 4-D viewing direction and computes the 4-D observed point.

When the user picks and moves one principal vanishing point in 3-D space, the first processing step allocates the other three principal vanishing points to the corresponding correct positions in 3-D space using Equation (2.5) from Section 2.3.2. Then, the second processing step computes the parameters for the 4-D viewing direction from Equation (2.6). The 4-D observed point p_{a_b} is represented by the transformed coordinates $(0, 0, 0, -r)$ in the 4-D eye-coordinate system $x_e y_e z_e w_e$, which is defined with the origin at the 4-D eye-point p_f, and with the w_e-axis in the direction from the 4-D observed point p_a to the 4-D eye-point p_f. Therefore, the 4-D observed point p_a in the 4-D world-coordinate system $x_w y_w z_w w_w$ can be computed with the following equation:

$$\begin{aligned} p_a =&[x_{p_a} \quad y_{p_a} \quad z_{p_a} \quad w_{p_a} \quad 1] \\ =&[0 \;\; 0 \;\; 0 \quad -r \quad 1]\boldsymbol{T}_{xz}^{-1}(\gamma)\boldsymbol{T}_{yz}^{-1}(\beta)\boldsymbol{T}_{xy}^{-1}(\alpha)\boldsymbol{T}_{t}^{-1}(-p_f), \end{aligned} \tag{4.1}$$

where the transformation matrix $\boldsymbol{T}_t$ represents the 4-D translation matrix, and transformation matrices $\boldsymbol{T}_{xz}$, $\boldsymbol{T}_{yz}$, and $\boldsymbol{T}_{xy}$ represent the 4-D rotation matrices around the xz-, yz-, and xy-planes, respectively.

When we implemented the interaction algorithm described above, we used the 4-D view field transformation matrix from Equation (2.8) in Section 2.3.3, instead of Equation (2.2) in Section 2.3.1. We determined the parameters α, β, and γ for the 4-D viewing direction in the range of $-\pi \leq \alpha, \beta, \gamma \leq \pi$, depending on the movement history of the 4-D observed point. As a result, the pose of the 4-D eye-point corresponding to the 4-D upper direction is maintained before and after the 4-D observed point passes through the zenith of the 4-D spherical surface.

4.3 Observation of 4-D Solid Scenes

In this section, we present examples of 4-D solid scenes from an arbitrary 4-D eye-point and 4-D viewing direction. We demonstrate that we can interactively move in 4-D space and look around various 4-D scenes.

4.3.1 Change of Viewing Direction in 4-D Space

Figure 4.2 illustrates the basic corresponding relationship between principal vanishing point operations in 3-D space and changes in the 4-D viewing direction. In this example, we place a hypercube at $(0, 0, 0, -1.5)$ in the 4-D world-coordinate system, and visualized it from the 4-D eye-point that lies at the origin of the 4-D world-coordinate system. The coordinates of the vertices of the hypercube are normalized such that the vertices are inscribed inside a 4-D spherical surface of radius 1. The parameters (k, h, f) of the 4-D viewing field are $(0.5, 0.5, 100)$, respectively. To clearly visualize edges inside the 3-D perspective drawings of the hypercube, the 3-D perspective drawing are rendered with a semitransparent surface and a reticular stipple pattern.

Initially, the 4-D observed point is at $(0, 0, 0, -1.5)$, and the 4-D viewing field coincides with the negative direction of the w_w-axis. Therefore, the principal vanishing point vp_w and 3-D perspective drawing of the hypercube are displayed at the origin of the $x_s y_s z_s$-space corresponding to the 3-D space and on the 3-D screen, respectively. The other three principal vanishing points vp_x, vp_y, and vp_z do not appear at that time. Then, when we move the principal vanishing point vp_w in the direction of the principal coordinate axes of 3-D space, which coincides with the x_s-, y_s-, and z_s-directions of the 3-D screen coordinate system, the 4-D viewing direction changes towards the directions of the w_w-, y_w-, and z_w-axes of the 4-D world-coordinate system, respectively. As a result, the 4-D viewing direction deviates from the current direction towards the hypercube. The hypercube gradually moves outside the 4-D viewing field, and is clipped out by the 4-D viewing pyramid. Although changes in the viewing direction can be divided into horizontal and vertical changes in 3-D space, there is another

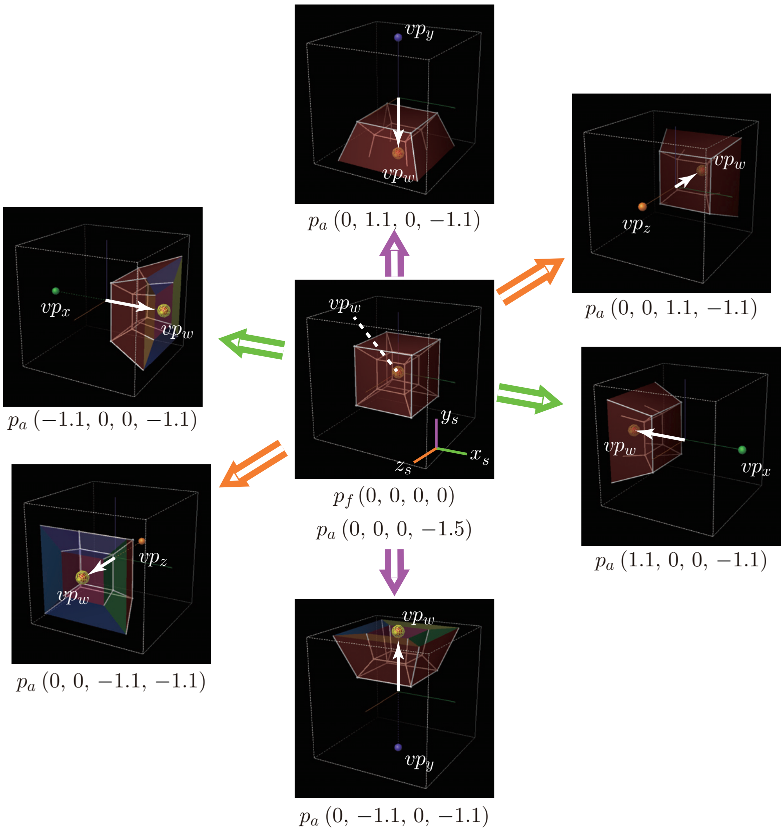

Figure 4.2. Correspondence relationship between the principal vanishing point operation in 3-D space and viewing direction change in 4-D space.

direction in 4-D space. Thus, the operations of the principal vanishing points vp_z and vp_w in the z_s-direction will be key to understanding 4-D space.

4.3.2 4-D Solids Observed from the Insides

By placing the 4-D eye-point inside a 4-D solid and changing the 4-D viewing direction inside it, we can visualize various inside views of the 4-D solid clipped by the 4-D viewing pyramid.

Figures 4.3 and 4.4 show examples. We visualize the insides of a 24-cell and a 120-cell (see Appendix B for the definitions of these 4-D solids) from two different 4-D eye-points with various 4-D viewing directions. In this visualization, the 4-D solids are placed at the origin of the 4-D world-coordinate system, and the coordinates of their vertices are normalized such that the vertices are inscribed into a 4-D sphere of radius 1.0. Each cell of each 4-D solid is assigned one of eight different colors. The parameters (k, h, f) for the 4-D viewing field are $(0.5, 0.5, 100)$, respectively.

From the visualization results shown in Figures 4.3 and 4.4, we can see that the 24-cell and 120-cell are constructed from octahedrons and dodecahedrons, respectively. Moreover, this type of visualization leads to an understanding of the fundamental properties of 4-D solids; each vertex, edge, and surface of a 4-D solid is shared by a fixed number of cells. For example, the visualization of the 120-cell clearly shows that a vertex, an edge, and a surface are shared by four, three, and two cells, respectively. In this manner, through this observation we can understand the geometric characteristics and structure of a 4-D solid.

4.3.3 Interaction with Multiple 4-D Objects

Unlike with the conventional 4-D visualization, the proposed system allows us to interact with a 4-D scene consisting of multiple 4-D objects by controlling the 4-D eye-point and viewing direction.

First, we demonstrate the observation of a simple 4-D scene. Figure 4.5(a) shows the configuration of the 4-D solid scene. A hypercube, 5-cell, and 16-cell are placed at $(0, 0, 0, 1.5)$, $(1.5, 0, 0, 0)$, and $(0, 1.5, 0, 0)$ in the 4-D world-coordinate system, respectively, to construct the 4-D solid scene (see Appendix B for the definitions of these 4-D solids). The coordinates of the vertices of each 4-D solid are normalized such that they are inscribed inside a 4-D spherical surface of radius 1.0. In this 4-D scene, we observe these 4-D solids from a 4-D eye-point at the origin of the 4-D world-coordinate system while we change the 4-D viewing direction. The parameters (k, h, f) of the 4-D viewing field are $(0.5, 0.5, 100)$, respectively.

Figure 4.5(b) depicts an image sequence of 3-D perspective drawings obtained by turning the 4-D viewing direction towards each 4-D solid in order. Initially, the 4-D observed point is at $(0, 0, 0, 1.5)$, and the 3-D perspective drawing of the hypercube is shown at the center of the 3-D screen (image 1 in Figure 4.5(b)). Then, we move the principal vanishing points vp_w and vp_x towards the x_s-direction. Consequently, the hypercube recedes, and the 5-cell comes into the 4-D viewing field (images 2 and 3 of Figure 4.5(b)). Finally, when we move the principal vanishing points vp_x and vp_y towards the y_s-direction, the 5-cell recedes, and the 16-cell comes into the 4-D viewing field (images 4 and 5 in Figure 4.5(b)).

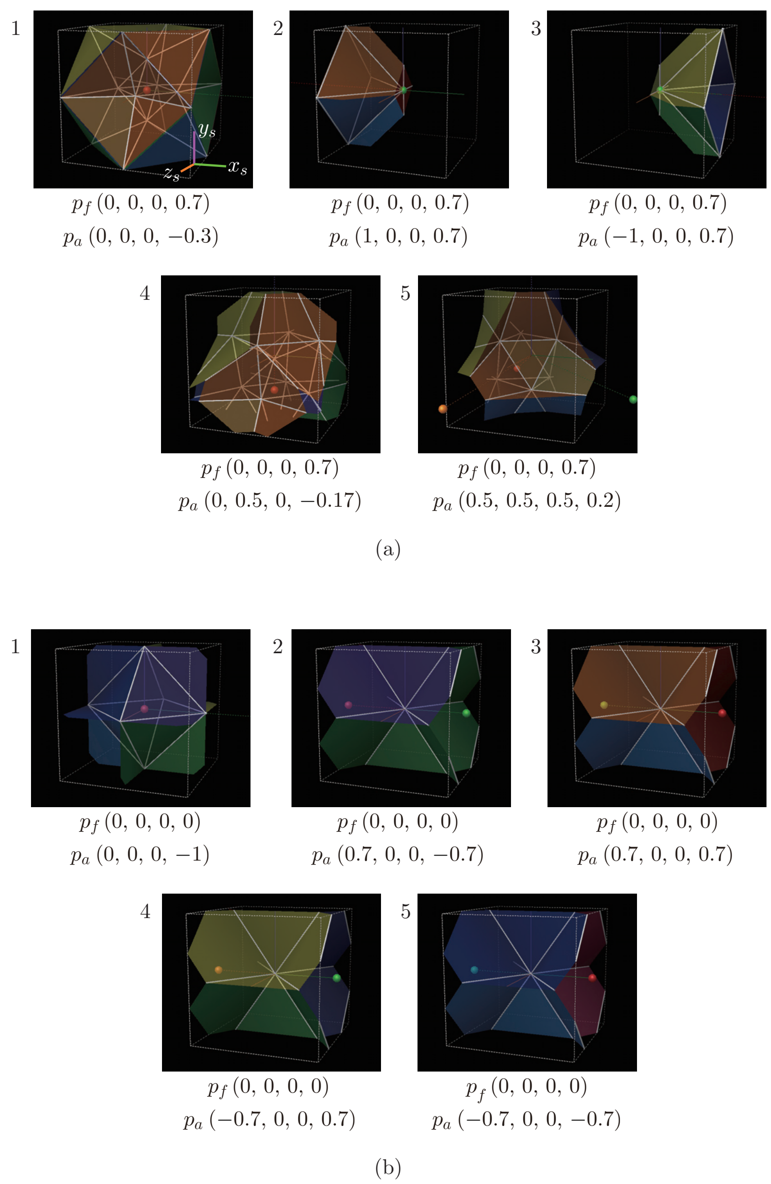

Figure 4.3. Visualization of the insides of a 24-cell. (a) The 4-D eye-point at the position $(0, 0, 0, 0.7)$. (b) The 4-D eye-point at the origin of the 4-D world-coordinate system.

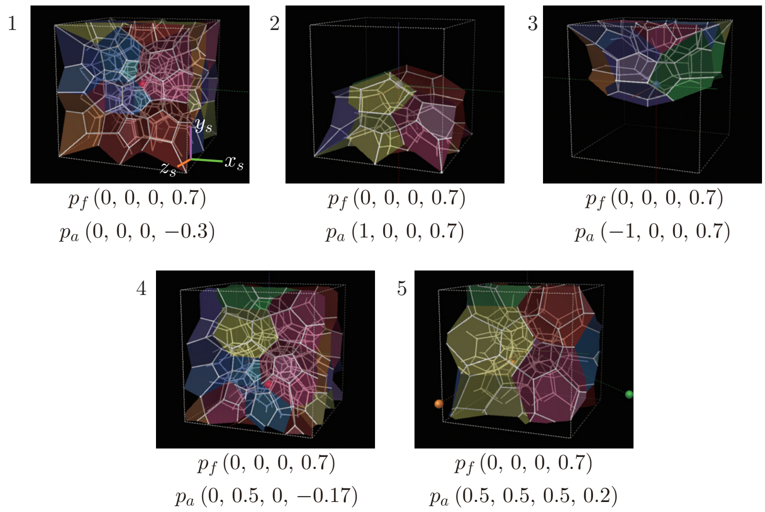

(a)

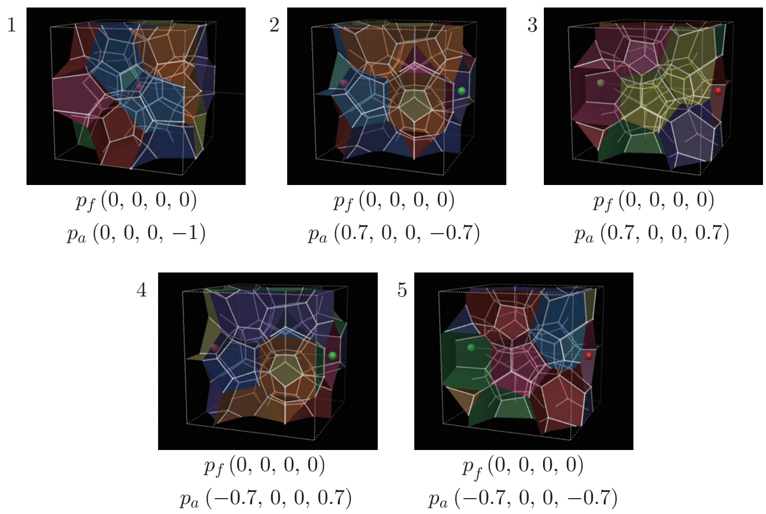

(b)

Figure 4.4. Visualization of the insides of a 120-cell. (a) The 4-D eye-point at position $(0, 0, 0, 0.7)$. (b) The 4-D eye-point at the origin of the 4-D world-coordinate system.

Next, let us demonstrate the exploration of a simple 4-D solid scene with 4-D fly-through actions. In our proposed system, we can freely fly through 4-D space by simultaneously moving both the 4-D eye-point and the 4-D observed point back and forth in the 4-D viewing direction. In this case, we can say that the principal vanishing points act as a steering handle to control the traveling direction.

Figure 4.6(a) shows the arrangement of a 4-D solid scene. This scene includes a hypercube and a 16-cell, which are allocated at the origin of and $(0, 0, 0, 3.5)$ in the 4-D world-coordinate system, respectively. Starting from the initial 4-D eye-point at $(0, 0, 0, 1.5)$ and the 4-D observed point $(0, 0, 0, 0.5)$ in the 4-D world-coordinate system. We fly through this 4-D scene along the path indicated by the blue line to observe the 4-D solids. In visualization processing, the 4-D viewing field parameters (k, h, f) were $(0.5, 0.5, 100)$, respectively.

Figure 4.6(b) presents an image sequence of the 3-D perspective drawings obtained along the 4-D fly-through path. In the initial projection, the 3-D perspective drawings of the hypercube and a 16-cell overlap with each other on the 3-D screen (image 1 in Figure 4.6(b)). This signifies that the 16-cell is occluded by the hypercube, or vice versa. However, because the current 4-D visualization algorithm does not incorporate occlusion culling processing, it is difficult to determine the depth relationship between the two 4-D solids from only image 1 in Figure 4.6(b). Thus, to observe the 4-D solids from different viewing positions, we change the 4-D viewing direction, and move away from the w_w-axis by performing the 4-D fly-through operations (images 2 through 5 of Figure 4.6(b)). At this stage, the 3-D perspective drawings of the two 4-D solids separate on the 3-D screen, and align in the direction connecting the center of the 3-D screen and the principal vanishing point vp_w. Therefore, we find that the two 4-D solids are physically separated in the w_w-direction. In this manner, the 4-D fly-through actions will help us understand the spatial relations and orientations among 4-D objects in 4-D space.

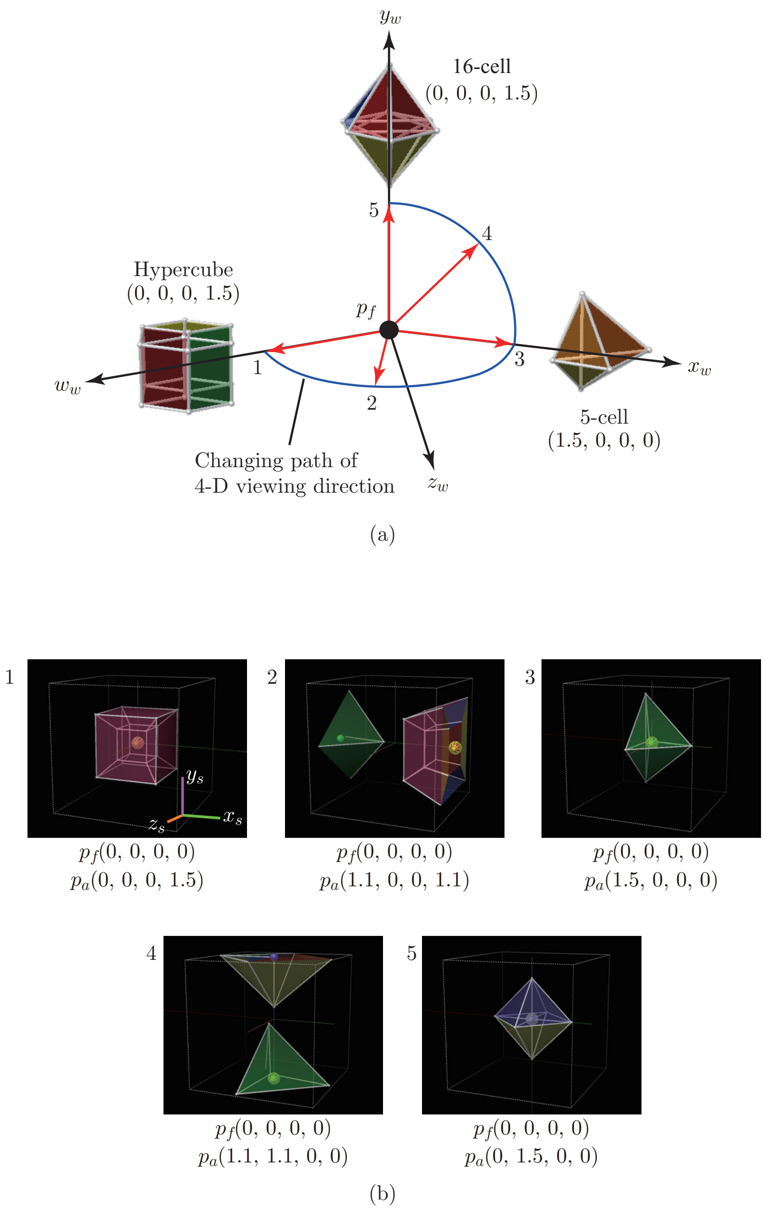

Figure 4.5. Visualization of the 4-D scene by 4-D viewing direction changes. (a) Layout of the 4-D solids and the changing path of the 4-D viewing direction. (b) Image sequence obtained by the 4-D viewing direction changes. The numbers of the pictures correspond to the numbers of the 4-D viewing direction in (a).

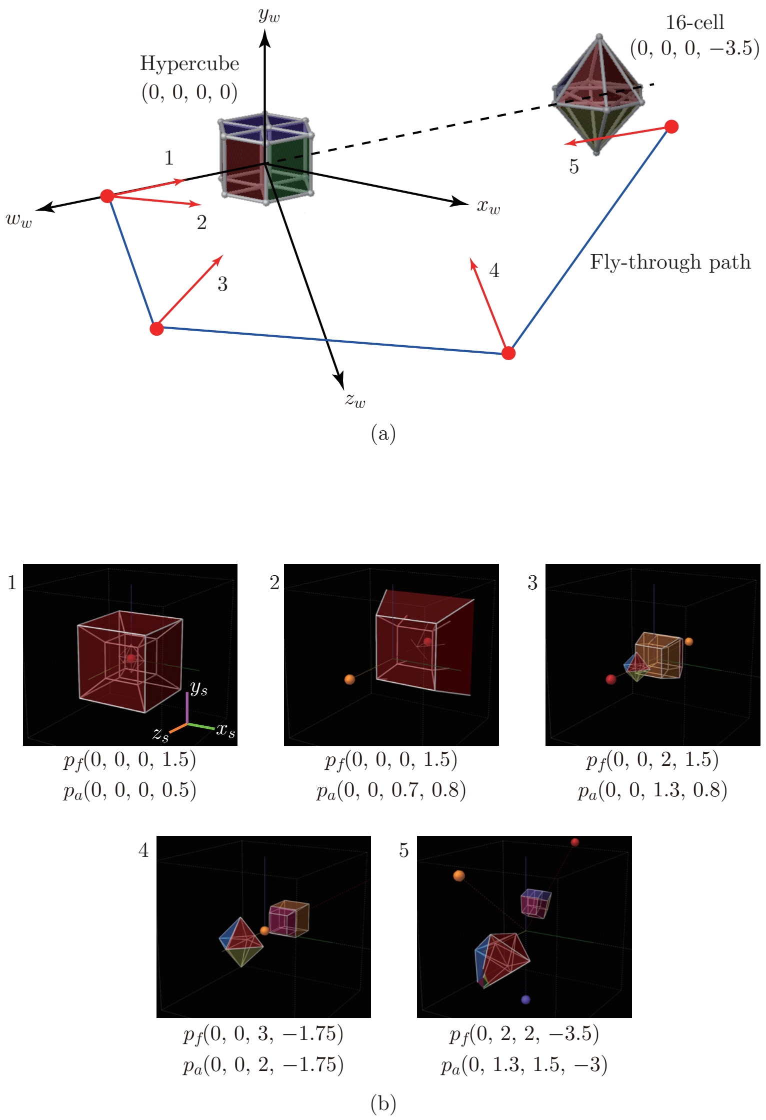

Figure 4.6. Visualization of the 4-D scene by 4-D fly-through actions. (a) Layout of the 4-D solids and fly-through path. (b) Image sequence obtained by the 4-D fly-through actions. The numbers of the pictures correspond to the numbers of the 4-D viewing direction in (a).

4.4 Exploration of 4-D Maze Using 4-D Fly-through Actions

As shown in Section 4.3, the 4-D viewing direction control and 4-D fly-through actions enable us to interactively look around and move in 4-D space to observe a 4-D solid scene. Although the 4-D solid scenes demonstrated above are simple, the proposed system can visualize any 4-D scene, even if they have an intricate structure in 4-D space. Thus, it becomes possible for users to explore intricate 4-D scenes and have a new 4-D experience with entertaining properties. In this section, as an example application of 4-D fly-through actions, we demonstrate a 4-D maze exploration using the proposed system.

4.4.1 Construction of 4-D Maze

In the following, the full 4-D maze consists of straight-line paths and right-angled corners that run in the x_w-, y_w-, z_w-, and w_w-directions in the 4-D world-coordinate system. The straight-line paths and right-angled corners are constructed by connecting multiple hypercubes such that two neighboring hypercubes share one cell. Each hypercube cell acts as an internal wall of the 4-D maze. To explore the 4-D maze, we move the 4-D eye-point as it passes through the insides of the hypercubes with the 4-D fly-through actions. In the maze, the coordinates of the hypercube vertices are normalized, as the hypercubes are inscribed inside a 4-D sphere of radius 1.0.

4.4.2 Straight-line Paths and Right-angled Corners

Figure 4.7 shows the external appearance of a straight-line path constructed in 4-D space. This straight-line path consists of six hypercubes, which align in the positive and negative directions on the w_w-axis. Each end hypercube of the straight-line path has a different color.

Figure 4.8 depicts an image sequence obtained from the exploration of this straight-line path. We explore this straight-line path from one end to the other. When the 4-D eye-point is at the end hypercube, we can see a cube that contains two small cubes and edges that converge towards the principal vanishing point vp_w (image 1 in Figure 4.8(b)). These two small cubes and edges represent two hypercubes next to the end hypercube. On the other hand, when the 4-D eye-point arrives at the other end hypercube, we no longer see such small nested cubes and edges, because there are no more hypercubes in front of the 4-D eye-point (image 4 in Figure 4.8). The number of nested cubes displayed on the 3-D screen depends on the parameter f for the distance from the 4-D eye-point to the 4-D background hyperplane. In this study, we set this parameter to 2.5. Thus, we can see the entirety of the two hypercubes next to the hypercube at which the 4-D eye-point is positioned.

Figure 4.9 shows the external appearances of three L-shaped corridors. Each corridor consists of two straight-line paths and one right-angled corner. The first path consists of three hypercubes, which align in the positive direction on the w_w-axis from the origin of the 4-D world-coordinate system. The second path also consists of three hypercubes, which align respectively in the positive direction on the x_w-, y_w-, or z_w-axes from the origin of the 4-D world-coordinate system. The intersection of two straight-line paths coincides with a right-angled

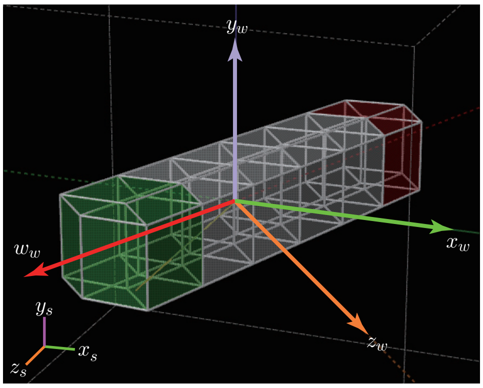

p_f (17, 0, −21, 14) p_a (0, 0, 0, 0)

Figure 4.7. External appearance of the straight-line path. (Parameters (k, h, f) regarding the 4-D viewing field are $(0.1, 1.0, 100)$, respectively.)

1

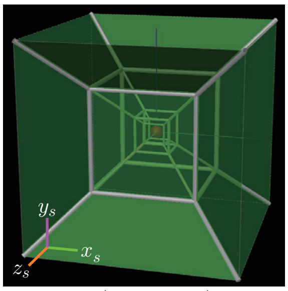

p_f (0, 0, 0, 2.0)
p_a (0, 0, 0, 1.0)

2

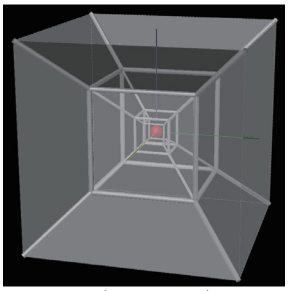

p_f (0, 0, 0, 0.0)
p_a (0, 0, 0, −1.0)

3

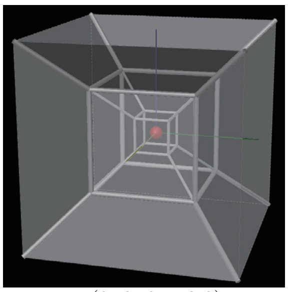

p_f (0, 0, 0, −2.0)
p_a (0, 0, 0, −3.0)

4

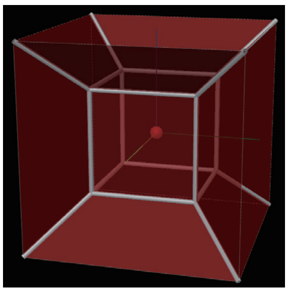

p_f (0, 0, 0, −3.0)
p_a (0, 0, 0, −4.0)

Figure 4.8. Exploration of the straight-line path. (Parameters (k, h, f) regarding the 4-D viewing field are $(0.2, 0.1, 2.5)$, respectively.)

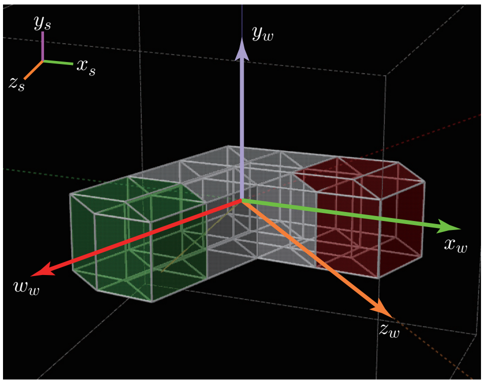

$p_f(17, 0, -17, 11)$ $p_a(0, 0, 0, 0)$

(a)

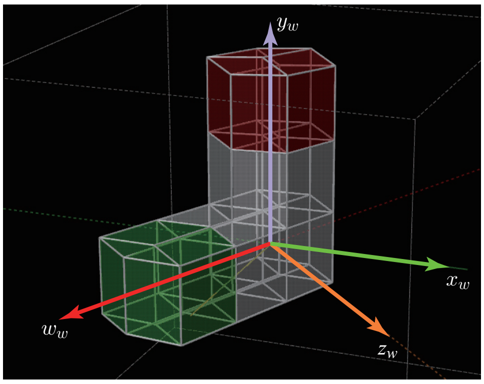

$p_f(17, 0, -17, 11)$ $p_a(0, 0, 0, 0)$

(b)

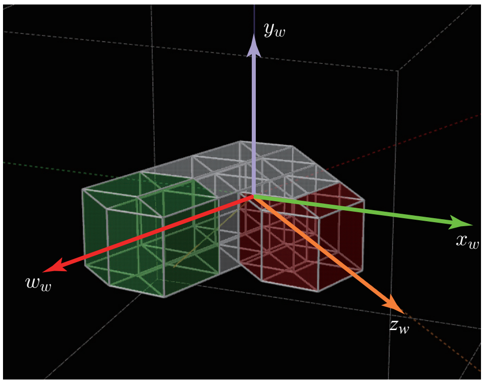

$p_f(17, 0, -17, 11)$ $p_a(0, 0, 0, 0)$

(c)

Figure 4.9. External appearance of the L-shape corners constructed on different coordinate planes. (a) $x_w w_w$-plane. (b) $y_w w_w$-plane. (c) $z_w w_w$-plane. (Parameters (k, h, f) regarding the 4-D viewing field are $(0.1, 1.0, 100)$, respectively.)

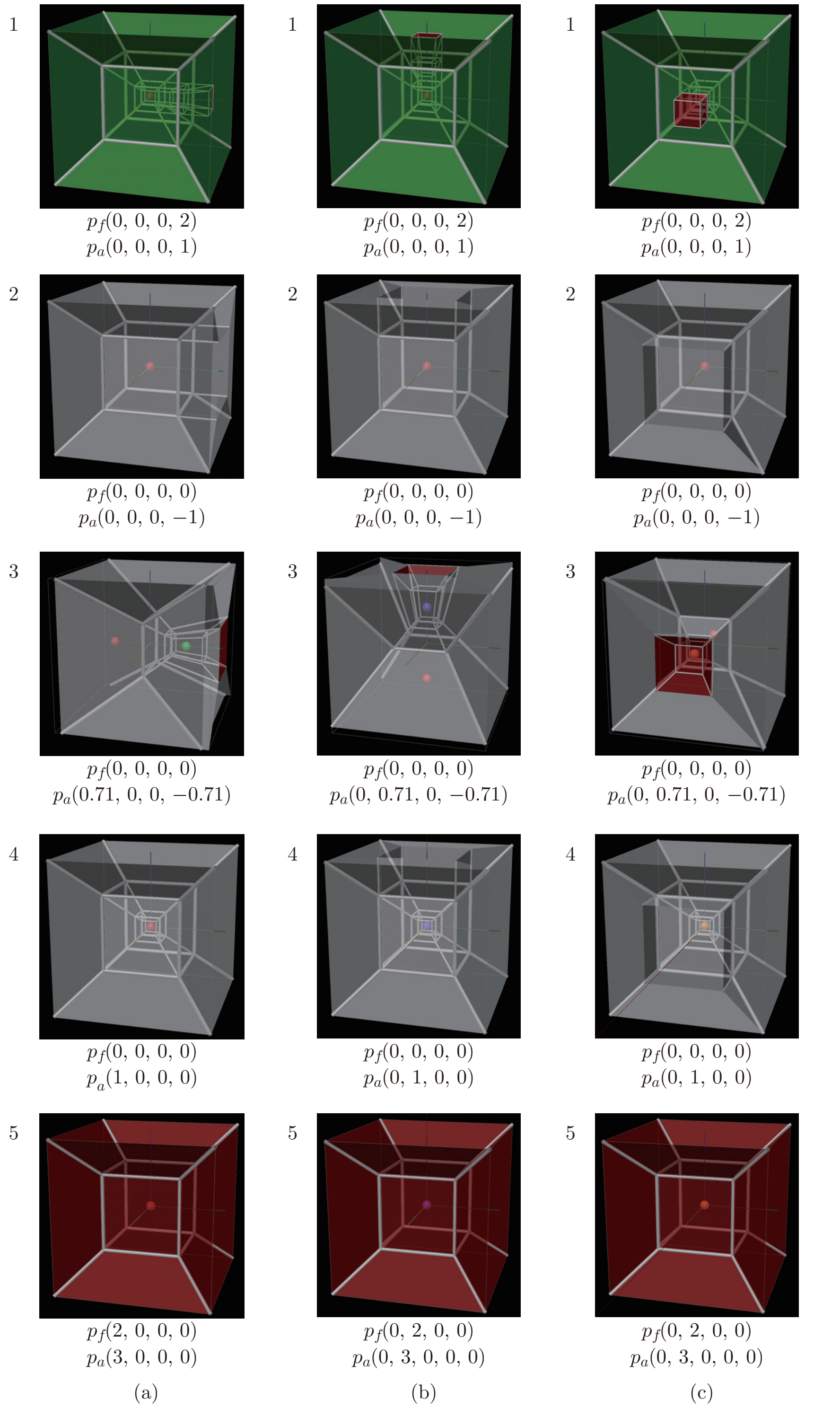

Figure 4.10. Exploration of the L-shape corridors. (a) $x_w w_w$-plane. (b) $y_w w_w$-plane. (c) $z_w w_w$-plane.

corner, and includes one end hypercube in the first and second straight-line paths. Each end hypercube of a corridor is illustrated with a different color.

Figure 4.10 depicts image sequences obtained from the exploration of these corridors. Here, we focus on the image sequence shown in Figure 4.10(a), because the three corridors can be explored in almost the same manner. Starting from the end hypercube of the first straight-line path, when we enter the hypercube at the corner, we can see a 3-D cube corresponding to the dead end wall of the first straight-line path, and edges extending parallel to the x_s-direction (images 1 and 2 in Figure 4.10). Then, when we move the principal vanishing points vp_w and vp_x sequentially to the positive direction of the x_w-axis to turn the 4-D viewing direction, we find that these edges are converged towards the principal vanishing point vp_x (image 3 in Figure 4.10). After we turn the 4-D viewing direction, we see the small nested 3-D cubes representing the second straight-line path running in the x_w-direction (image 4 of Figure 4.10). At this stage, we can move ahead, and finally arrive at the end of the corridor (Picture 5 of Figure 4.10). In this manner, the principal vanishing points help us understand the orientation of the path, because they indicate orthogonality and parallelism in 4-D space.

4.4.3 Practical 4-D Maze

Here, we demonstrate a more practical example. We explored a 4-D maze that consists of multiple straight-line paths and corners. Figure 4.11 shows the external appearance of the 4-D maze. To explain the structure of the maze, we provide a graph representation of the 4-D maze in Figure 4.12. This graph explains the connection relation between the hypercubes. Each node represents a hypercube, and a link between two nodes indicates that the two hypercubes are connected. To indicate the direction of the path constructed by two adjacent hypercubes, we assigned one of four different colors (red, green, orange, or purple) to each of the links. As shown in Figure 4.12, this 4-D maze consists of seven straight-line paths, one corner, two three-way intersections with two corners, and a four-way intersection with four corners. One of the six end hypercubes is colored green, another is red, and the others are orange.

Figure 4.13 presents an image sequence obtained from the exploration of the 4-D maze. We explore the 4-D maze from the green end hypercube to the red end hypercube, along the movement path represented by black arrows in Figure 4.12. In this exploration, we move along the first straight-line path (images 1 through 3 of Figure 4.13), and turn to the positive direction of the x_w-axis at the three-way intersection (images 4 and 5 of Figure 4.13). Then, we come to another three-way intersection at the end of the second straight-line path (images 6 and 7 of Figure 4.13). We operate the principal vanishing points vp_x, vp_w, and vp_z sequentially, to turn the 4-D viewing direction to the negative direction of the z_w-axis (images 8 through 11 of Figure 4.13). Next, we move ahead again, and pass through a corner (images 12 through 16 of Figure 4.13). Finally, we arrive at the red hypercube of the destination (image 17 of Figure 4.13).

The proposed system enables us to explore an intricate 4-D solid scene constructed in 4-D space, and provides various 4-D experiences from the first-person perspective. In this manner, the proposed system improves the latitude of a 4-D space visualization and 4-D space interaction. The framework of the 4-D fly-

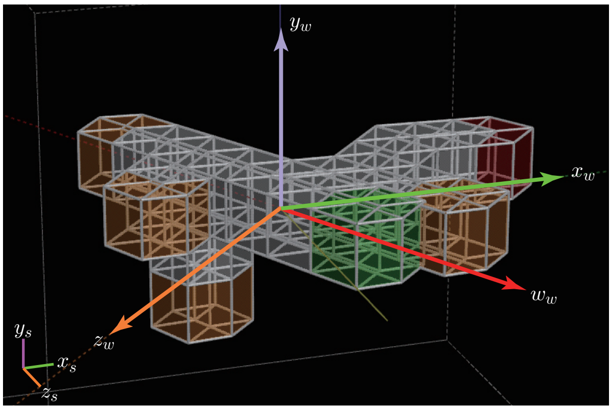

$p_f(-33, 0, -27, 20)$ $p_a(0, 0, 0, 0)$

Figure 4.11. The external appearance of the 4-D maze. (Parameters (k, h, f) regarding the 4-D viewing field are $(0.1, 1.0, 100)$, respectively.)

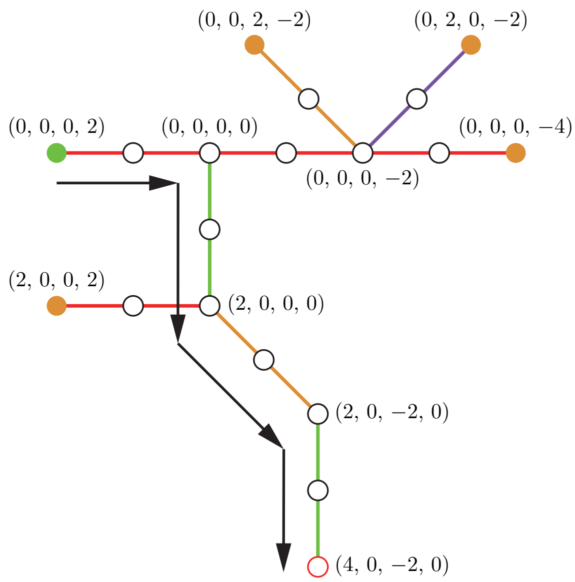

Figure 4.12. The graph representations of the 4-D maze.

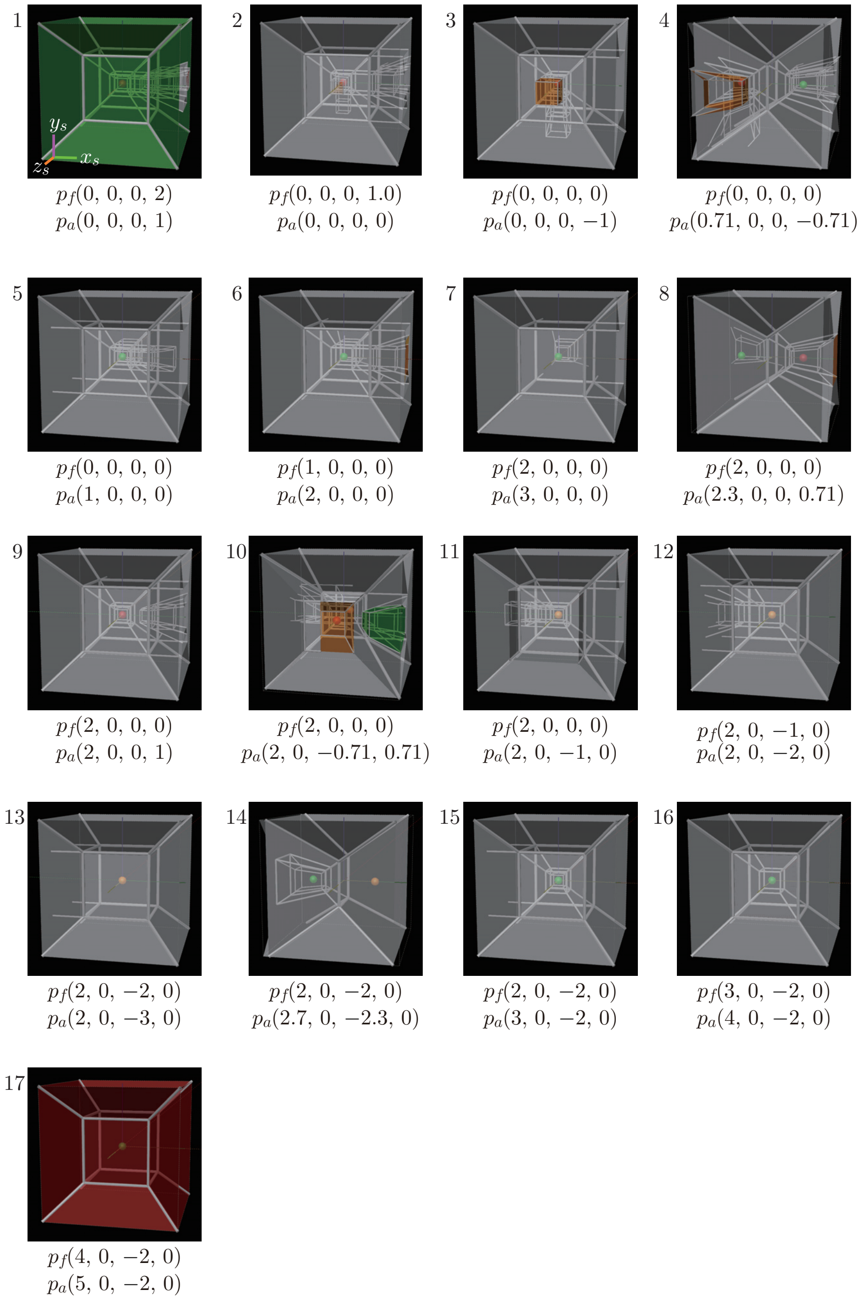

Figure 4.13. Exploration of the 4-D maze from the green end hypercube to the red end hypercube. (Parameters (k, h, f) regarding the 4-D viewing field are $(0.2, 0.1, 2.5)$, respectively.)

through actions will be effective for not only entertainment use, but also as a test bed of cognitive science research. In the near future, by using this framework we will attempt to examine 4-D spatial cognition performed in a large 4-D mazelike environment.

4.5 Usability of the 4-D Viewing Direction Control

To evaluate the usability of the proposed 4-D viewing direction control technique, we ran a user test with an interactive system. In the experiment, participants were told to spot a target object in 4-D space by controlling the 4-D viewing direction. If participants could reduce their response times and show a positive impression about the proposed system, we could conclude that the proposed system has sufficient usability to control the 4-D viewing direction.

4.5.1 Method

We first introduce the participants, apparatus, and stimuli of the experiment.

Participants

Eleven male participants and one female participant were tested. They were students or graduate students who majored in science and engineering at Waseda University. Their mean age was 21.4 years. Seven of the male participants had some experience in observing 4-D solids with our 4-D eye-point control system described in Chapter 2, and thus they had some previous knowledge of 4-D space and objects. However, they had never experienced the 4-D viewing direction control, and did not know the design of the user test. The other four male and one female participants had no knowledge or experience of 4-D space and objects. In addition, they had no experience in the 3-D virtual space displayed on the head mounted display.

We divided the twelve participants into two groups based on their previous knowledge. Thus, group A had seven experienced male participants of mean age 21.6 years, and group B had five beginner participants of mean age 21.0 years. Both groups undertook the same task.

Apparatus

We implemented the proposed 4-D viewing direction control technique into the interactive system in the same manner as described in Chapter3. The proposed system consisted of a personal computer (Intel Core i7 3.90GHz, NVIDIA GeForce GTX 680, 8GB RAM) with Windows 8 installed, a motion sensor (ASUS Xtion Pro Live), a head mounted display with a built-in 6-DoF Sensor (Vuzix Wrap 1200 VR), and a five-button wireless mouse (ELECOM M-GE3DL). The 3-D perspective drawing of 4-D data, principal vanishing points, and 3-D screen were displayed as a side-by-side stereoscopic image on the head mounted display. The participants carried out the experimental tasks with pick-and-move operations of the principal vanishing points performed with the five-button wireless mouse. The 3-D screen, sized at 300 mm $\times$ 300 mm $\times$ 300 mm, was placed 1.5 m off the ground according to the participants' request, and 1.8 m away from the motion sensor. This configuration provided sufficient spatial resolution to track the participants' head and hand positions. The system guaranteed a real-time performance (60 frames per second) with interactive visualization of the 4-D scene, including 45 or fewer hypercubes.

Stimuli and Tasks

The experimental trials were performed in two stages. In each stage, the participants first undertook 20 trials, and then a three-minute break was followed by a repeat of the same 20 trials. Thus, the participants undertook a total of 80 trials in the experiment.

The participants performs the experimental tasks in a 4-D scene that included one target hypercube. This hypercube was normalized, as the vertices were inscribed inside a 4-D spherical surface of radius 1, and were assigned one of eight different colors on each cell. The position of the target hypercube was randomly determined, as the hypercube was placed at distance 2 from the origin of the 4-D world-coordinate system. In addition, in the first stage we restricted the hypercube position such that at least one vertex of the target hypercube was included in the 4-D viewing field when the trial started. In order to perform 20 trials, we randomly chose 20 target positions in 4-D space with this restriction. The mean angle between the initial 4-D viewing direction, which coincided with the negative direction of the w_w-axis, and the target direction, which coincided with the direction from the origin of the 4-D world-coordinate system to the center of the target hypercube, was 42.4 degrees.

Similarly, for the second stage we randomly chose 20 positions in 4-D space, as the target hypercube was located at a distance 2 from the origin of the 4-D world-coordinate system posterior to the 4-D eye-point. In other words, the participants could not see the target when they started the trial in the second stage. The mean angle between the initial 4-D viewing direction and the target direction was 116.8 degrees.

In each trial, the participants were told to spot the target hypercube in the center of the 3-D screen. Starting from the negative direction of the w_w-axis, the participants changed the 4-D viewing direction to the target hypercube in 4-D space. During the experiment, the 4-D eye-point was fixed at the origin of the 4-D world-coordinate system. The participants were allowed to check at will whether they had completed the task. When the participants checked their answer, the system calculated the angular difference between the 4-D viewing direction and the target direction. If the angular difference was under a threshold, then the participants proceeded to the next trial. Otherwise, the participants had to continue the current trial until they faced the target hypercube. In the present experiment, we determined a threshold of 15 degrees, based on the results of our preliminary experiment.

Procedure

Each participant received a brief lecture on 4-D space and objects, and the visualization model, principal vanishing points, and interactive system. This took approximately 10 to 15 minutes. First, the participants studied the definition of 4-D space and the structure of the hypercube. Next, they studied the 4-D visualization model based on an analogy with the human visual system in 3-D space. Then, they studied the principal vanishing points and how to use the interactive system.

Then, the participants practiced using the system for five minutes with a sample 4-D scene. This sample scene included a hypercube placed at $(0, 0, 0, -2)$ in the 4-D world-coordinate system. The 4-D eye-point and initial 4-D viewing direction were the same as those of the actual trials. The participants observed the hypercube moving in and out of the 4-D viewing field, and became accustomed to the 4-D viewing direction control based on the principal vanishing point operations. Note that we adjusted the stereoscopic parallax to display a 3-D image on the head-mounted display in this practice phase.

After the practice phase, the participants took a three-minute break, and proceeded to the first stage of the test. Then, they took another three-minute break, followed by the second stage of the test. The test took approximately 45 to 60 minutes. Although every participant faced the same trials, we presented the trials in a random order in order to avoid any order effects. We recorded their response times, accuracy (the final angular difference between the 4-D viewing direction and the target direction), and action histories for the 4-D viewing direction control in each trial. These results were used to evaluate the usability and learning effect of the proposed system.

To determine the participants' subjective impressions of the proposed system, we asked the participants to complete the following questionnaire after the trials.

A. How was the overall impression of the system, positive or negative?
B. Was it easy to understand how the system works?
C. Was it easy to quickly get accustomed to the system?
D. Were you able to control the 4-D viewing direction as desired?
E. Were you able to understand the relationship between your operations and resulting changes on the 3-D screen?
F. Were you able to enhance your sense of direction in 4-D space?
G. Were you able to reduce the mistakes of the 4-D viewing direction control during the trials?

The rating was on a seven-point scale from "minus three" to "plus three." The scores of "plus three," "zero," and "minus three" always indicate most positive, neutral, and most negative impression responses, respectively.

4.5.2 Results

960 trials were run in total with twelve participants. We regarded 945 trials as valid results, because the motion sensor failed to track the participants' head and hand positions in the middle of the trial in 15 cases.

Response Time

First, we describe the results of the 40 first stage trials. Figure 4.14 shows the mean response times of the trials. We first applied a moving window average of size four to the raw data to compensate for the noise in the time data. Then,

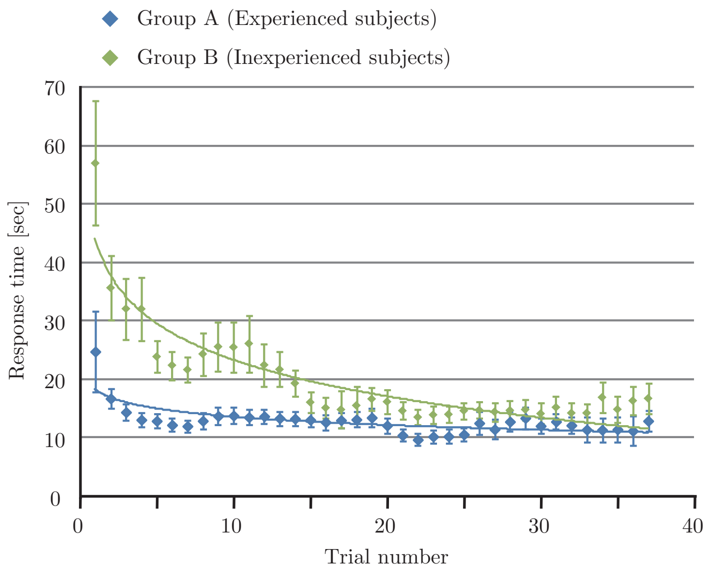

Figure 4.14. Response time to finish a trial in the first stage.

we computed the average response time and standard errors for each trial in each group. Next, we plotted the average response times with standard errors displayed as error bars. Initially, the mean response time of group A was 64.1 s. The participants reduced their response times in the first five trials. Then, their performance stabilized at a mean response time of 12.3 s. Group B showed similar results. Their initial mean response time was 115.8 s. Their response time rapidly dropped in the first five trials. This drop gradually continued in the sixth to the fifteenth trial. Then, their performance stabilized at the mean response time of 15.1 s.

This learning effect was also confirmed in their action histories. Figure 4.15 shows the time histories of the angular difference between the 4-D viewing direction and the target direction. Because the participants exhibited similar trends, we plotted the first, tenth, and twentieth trials of one participant from group B as representative of the results. In the figure, increases in the angular error indicate that the participant turned the 4-D viewing direction in the wrong direction in 4-D space. The results show that as the participants gained experience, the number of incorrect operations decreased. This suggests that the participants were able to understand the relationship between the operations on the principal vanishing points and the resulting changes on the 3-D screen. Thus, the participants learned how to change the 4-D viewing direction to spot a target object in 4-D space, even if they had no previous knowledge of 4-D space and objects.

Next, we describe the results of 40 second stage trials. Figure 4.16 shows the mean response times of the trials. The participants exhibited trends that were similar to the first stage. They reduced their response times in the first ten trials, and then stabilized. The mean response times of the 11th to the 40th trials were 23.2 seconds for group A and 33.7 seconds for group B. These results suggest that the participants were able to search and spot the target hypercube

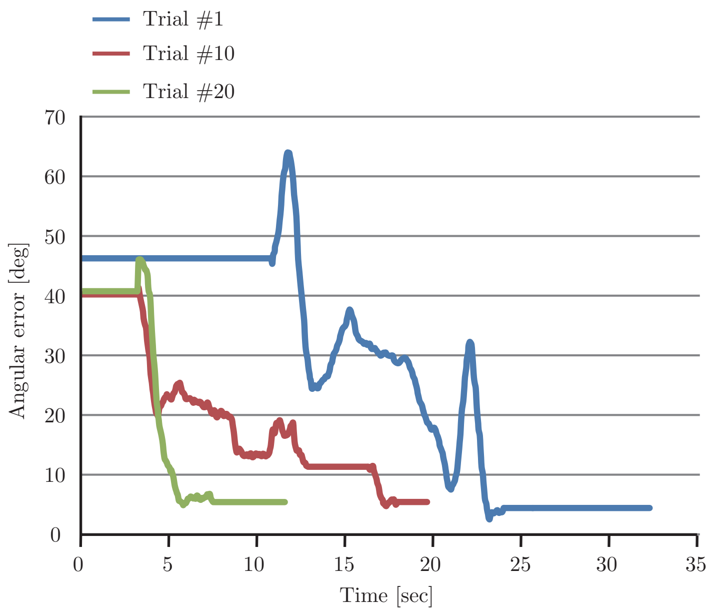

Figure 4.15. Relationship between angular error decreasing and time.

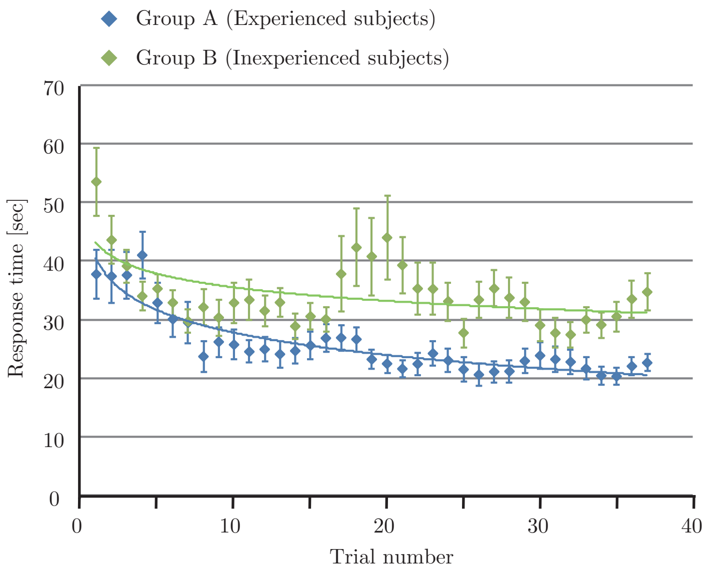

Figure 4.16. Mean response time to finish a trial in the second stage.

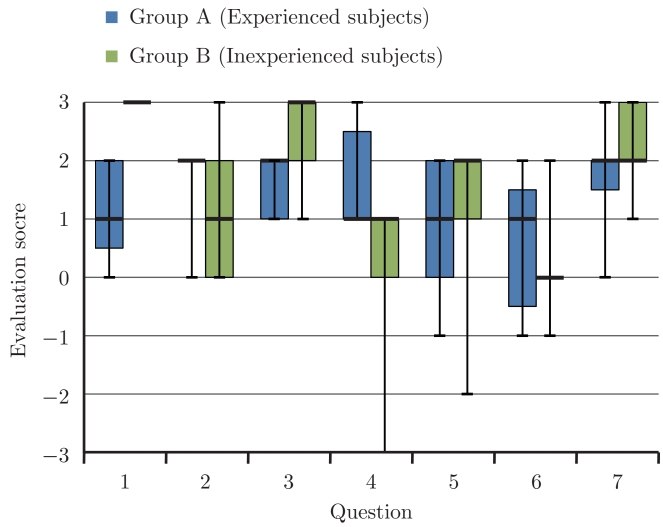

Figure 4.17. Results of the questionnaire about usability and learnability of the developed system.

behind the 4-D eye-point in 4-D space.

Accuracy

We also describe the participants' accuracy in the 4-D viewing direction control, by calculating the mean angular error over 80 trials. The mean angular error of group A was 5.37 degrees. The mean angular error of group B was 6.54 degrees. These angular errors corresponded to the results for when the target hypercube moved approximately 15 millimeters away from the center of the 3-D screen.

Subjective Impression

Figure 4.17 shows a boxplot of the participants' responses to the questionnaire. Question 1 asked for the overall impression. The median responses were a score of "plus two" for group A and the score of "plus three" for group B, respectively. Every participant had a positive impression of the proposed 4-D interaction scheme. Questions 2 and 3 asked about the learnability and usability of the interaction. The median response of group A was a score of "plus two" and "plus two" for the two questions, respectively. Furthermore, the median response of group B was the score of "plus one" and "plus three" for the two questions, respectively. No participant provided a negative response. Questions 4 to 7 asked about the impression of the 4-D viewing direction control. Question 4 asked how easily the participants could change the 4-D viewing direction to the hypercube. The mean responses were a score of "plus one" for both groups. Only participant B3 responded with a negative score. Question 5 asked whether the participants could grasp the relationship between their operations and the resulting 4-D viewing direction changes. The median responses were "plus one" for group A and "plus two" for group B, respectively. Question 6 asked whether they improved their perception of 4-D space. The number of neutral and negative responses were high here compared to the other six questions. We discuss this point in the next section. Question 7 asked whether they felt that they could improve their performance by themselves. Both groups provided a median score of “plus two,” and no participant gave a negative response. In general, from these results it is suggested that the participants found the interactive system easy to learn and use.

4.5.3 Discussion

Ease in Use and Learning

Both groups exhibited a similar trend of results in the first stage. Although the learning speeds were different for each of the participants, they reduced their response times at an early stage of the first 20 trials, and consistently performed smooth 4-D viewing direction control in the latter 20 trials. The interpretation of these performance patterns is that the participants rapidly learned the correspondence between the principal vanishing point operations and the 4-D viewing direction changes within the first five to ten trials. Then, they applied this obtained understanding in the remaining trials. This interpretation is validated by the participants’ positive impressions of the interactive system. According to the participants’ comments, they found the task difficult at the beginning of the experiment. However, once they understood the correspondence between the principal vanishing point operation and its result visualized on the 3-D screen, they found it possible to complete the trials in a shorter time.

In the second stage, the participants had to search for the target while they looked around in 4-D space. Once they located the target hypercube, they captured it in the center of the 3-D screen by using the 4-D viewing direction in a similar manner to the first stage. We found that the participants’ response times were roughly twice as long as for the first stage. Because the target hypercube was located behind the 4-D eye-point, the participants needed to turn the 4-D viewing direction towards the back in 4-D space to find the hypercube. In order to achieve this action, the participants needed to operate at least two principal vanishing points. Moreover, the amount of the operations on the principal vanishing points was approximately twice as much as in the first stage. Considering these conditions, the increase in the response times was reasonable.

In summary, we conclude that the proposed system makes it easy to learn and handle the 4-D viewing direction control, even if the user does not have previous knowledge of 4-D space and objects. The system is suitable for searching and finding 4-D objects in 4-D space.

Evaluation of Accuracy

Based on the results, there were angular error of approximately six degrees when the participants completed the task. This error can be explained as a composite of the following interpretations. First, as the primary cause, it is difficult for users to completely stop their hand in the air. This may create noise, especially when the participants slightly move the principal vanishing points to fine-adjust the 4-D viewing direction. In fact, many participants left feedback comments regarding this point.

Second, there is an approximate 150 millisecond latency in the motion sensor due to the smoothing filter, which reduces the positional noise of head and hand tracking. Although there were no feedback comments regarding the latency, it is possible that this affected the interaction.

Third, the error could be due to the participants confusing the depth of the center of the 3-D screen on the stereoscopic visualization, for example, when the opaque part of the 3-D perspective drawings of the target hypercube occludes the center of the 3-D screen, which is indicated as a cross-point of the x_s-, y_s-, and z_s-axes displayed in 3-D virtual space.

Effects of Previous Knowledge

In both stages, the response time of group A was significantly lower than that of group B ($p = 3.28 \times 10^{-3} < 0.05$ for the first stage, and $p = 1.37 \times 10^{-5} < 0.05$ for the second stage). We also confirm that the performance of group A was more stable across the trials than that of group B. In addition, the scores for Question 4 of the questionnaire for group A were significantly more positive than those of group B ($p = 0.0254 < 0.05$). These results suggest that it was easy for the participants of group A to solve the task compared to those in group B. We speculate that this performance difference occurred due to the difference in the participants' previous knowledge and experience of 4-D space and objects. Because the participants of group A had observed the hypercube by controlling the 4-D eye-point along the 4-D spherical surface via the principal vanishing point operations [25], they might naturally grasp the 4-D viewing direction control in the this experiment. This is proof, at least in part, that humans were able to improve their 4-D spatial cognition through various experiences in the 4-D interactive environment.

Limitations

We have confirmed that the proposed system is easy to learn and provides sufficient usability for handling the 4-D viewing direction. However, some feedback comments highlight the limitations of the system. For example, one participant felt that the viewing field on the head-mounted display was narrow. Some participants were annoyed with the view bobbing that occurred in the 3-D virtual space, especially when their hand occluded their head from the motion sensor. Combined with a discussion about the accuracy, the improvement of the tracking system and stereoscopic display system is one of our future challenges to provide a more comfortable interaction.

As shown by the result of Question 6 in the questionnaire, in the present experiment we cannot confirm whether the participants enhanced their 4-D spatial representations in their mental space. This is because we designed the experiment to primarily assess the usability of the proposed system. In order to evaluate the human 4-D spatial cognition, it will be necessary to plan a cognitive test that examines whether the participants grasp the spatial structure of a 4-D object and 4-D scene. The proposed system could be used as a test bed for such cognitive tests in future work.

4.6 Summary

In Chapter 4, we have proposed a novel 4-D interaction technique that enables us to intuitively control the 4-D viewing direction by operating on the principal vanishing points in 3-D space. Moreover, we applied the proposed technique to realize 4-D fly-through actions. Using the proposed system, we achieved the visualization of various 4-D environments that were difficult to interact with in previous studies, such as the inside of a 4-D solid, a 4-D solid scene consisting of multiple 4-D objects, and a 4-D maze. The results of the user test indicated that the participants easily learned the method of looking around 4-D space and targeting an arbitrary direction in 4-D space, even if they had no previous knowledge and experience of 4-D space and objects. Therefore, the proposed system provided sufficient usability for 4-D viewing direction control. From these results, we are able to conclude that the proposed interaction technique was successful in improving the latitude of 4-D space visualization.

Chapter 5

Acquisition of 4-D Spatial Representations

In Chapter 5, we examine whether humans are capable of formulating 4-D spatial representations through perceptual experience in 4-D space with 4-D objects. Participants learned about 4-D space and hypercubes through the former interactive 4-D space visualization system in Chapter 3, and are then examined on a series of 4-D spatial ability tests. They demonstrated the ability to perform perspective taking, navigation, and mental spatial transformation tasks in 4-D space. The results provide empirical evidence that humans are capable of learning 4-D spatial representations. Moreover, the results support the interpretation that humans form a cognitive coordinate system, consisting of an origin and four directional axes, to understand 4-D space and objects.

5.1 Literature Review of 4-D Spatial Cognition

As discussed in the previous chapters, research has shown that 4-D space and objects can be visualized in 3-D space with the aid of computer graphics and virtual reality. However, it remains to be determined whether humans can acquire mental representations or an intuitive understanding of 4-D space and objects without the aid of mathematical representations.

There are some studies that challenge this possibility. They can be classified into two categories according to how they assess 4-D spatial representations. The first category relies on informal subjective reports that assess the participants' ability to acquire an understanding of 4-D space and objects. For example, Davis et al. [27] reported that mathematicians who interacted with a hypercube visualized by a computer claimed that they suddenly "felt" it. These subjective reports have significant importance as initial evidence of the capability to develop mental representations of 4-D space and objects. Nevertheless, informal subjective reports cannot quantitatively reveal what type of 4-D spatial representations people acquire from the 4-D experience. Thus, studies including objective evaluations are needed to probe the possibility and nature of 4-D spatial representations.

The second category relies on objective evaluation methods that assess performance on cognitive tasks related to 4-D space and objects. As it is assumed that all spatial tasks are solved using internal manipulations of mental images, the ability to solve a certain task within 4-D space can serve as evidence that a person has 4-D spatial representations in their mental space. Aflalo and Graziano [28] used path integration as a test of 4-D navigational skills, because successful path integration requires a mental map of an environment. In the study, participants used a keyboard to navigate from a starting point to an end point in a mazelike environment. They then indicated the direction from the end point back to the starting point by changing the 4-D viewing direction until they were facing the starting point. The results show that the participants learned to indicate the correct direction as they gained 4-D experience over multiple trials. Ambinder et al. [29] used spatial judgment tasks consisting of distance and angle estimation in 4-D space. In their study, participants examined 3-D slices of a 5-cell that were displayed in a CAVE-type virtual reality system. They then formed spatial judgments about the geometric features of the 5-cell, including the distance between two vertices and the angle between two edges. The results indicate a positive correlation between the participant responses and the correct distance and angle, which suggests that participants were able to make judgments about these 4-D properties. A follow-up study [30] in which the visualization method was switched from a slicing approach to orthogonal projection confirmed this finding.

Although people have demonstrated the ability to form certain judgments about 4-D objects, this does not in itself guarantee that their mental representation is actually grounded in four dimensions. People may use a variety of strategies, such as prior intuition, a trial-and-error approach, and mechanical solutions, which are useful for solving the task but not based on 4-D spatial cues. This is always a problem when assessing 4-D spatial ability, and it even often occurs for 3-D imagery [58, 59, 60]. For this reason, when we examine 4-D spatial representations through objective evaluation, it is necessary to design a 4-D spatial ability test such that it can never be solved by such strategies. If it is difficult to design such a task, the solver's strategy can be identified as a 4-D one by behavioral observation, analysis of the experimental results, and post-experiment questionnaires and interviews.

Wang [31] identified this problem and defined the key conditions that 4-D spatial representations should satisfy. According to his assertion, 4-D spatial representations can be defined as perceptual or cognitive representations of 4-D objects or environments that can support judgments about 4-D spatial relations or spatial properties without using definition-based lower-dimensional solutions, algebraic equations, or feedback training. Using these criteria, Wang [32] examined 4-D spatial representations using the hypervolume, which is a geometric property unique to 4-D space, as a test of 4-D object visualization ability. In the study, the task solvers observed the 3-D orthogonal projection of a randomly shaped 5-cell that horizontally rotated to a depth direction in 4-D space. They then provided their answer for the hypervolume of the 5-cell by adjusting the size of a hyperblock to match that of the 5-cell. The results show a positive correlation between the solvers' responses and the correct hypervolume, but not the definition-based, lower-dimensional cues, and Wang concluded that the participants' 4-D spatial representations meet the above mentioned definition of 4-D spatial representations. This suggests that humans are able to form some sort of 4-D spatial representations that help them perform object visualization.

5.2 Condition of the Experiments

Here, we briefly summarize the common points and differences between the previous research and the present study. Considering the characteristics of the previous studies, in this paper, we examine human 4-D spatial representations under the following conditions.

(i) 4-D learning method: As Aflalo and Graziano used extended training [28], we allow participants to practice with 4-D space and objects until they are satisfied with their own understanding. Moreover, unlike Wang, who restricted 4-D rotation to the depth direction [31], we allow participants to observe the 4-D objects from arbitrary 4-D positions and directions. These conditions help the participants to acquire their own 4-D spatial representations and make more complex 4-D judgments than previously shown.

(ii) Experimental tasks: Ambinder et al. [29] and Wang [32] examined participants' understanding of the geometric properties of an object. In contrast, we examine 4-D spatial visualization ability, which corresponds to the ability to process spatial relations, movements, and different perspectives. We therefore use spatial tasks that can be solved by perspective taking, navigational skills, and mental spatial transformations, rather than simple tasks such as distance, angle, and hypervolume estimation. This enables us to verify whether 4-D spatial representations are sufficiently flexible and uniform to perform active cognitive processing, such as predictions of visual changes in 4-D objects, behavioral decisions in 4-D space, and mental creation of a novel 4-D object. Moreover, this helps us develop hypotheses about possible forms of 4-D spatial representations.

(iii) Data analysis: As in conventional studies, we evaluate participants' performance based on individual subject analysis to confirm whether they have solved the experimental tasks with 4-D strategies or mechanical strategies. We evaluate each participant's ability by observing their actions in 4-D space and scoring their performance on the experimental tasks. This enables us to verify whether the participants' mental representations are actually grounded in four dimensions.

5.3 Experiment 1: Perspective Taking

To examine whether humans can form 4-D spatial representations, we conducted two different experiments that assess the ability to perform spatial tasks in 4-D space. In this section, we describe the first experiment, which assesses perspective taking skills and navigational skills in 4-D space.

5.3.1 Methods

We first introduce the participants, apparatus, and stimuli of the experiment.

Participants

Eight male participants and four female participants were tested. Their mean age was 20.5 years. Seven participants were students or graduates in science and engineering courses, and the others were students in arts courses. None of the participants had knowledge or experience of 4-D space and objects, and had no prior knowledge of the design of the experimental tasks.

Apparatus

We used the interactive 4-D visualization system that we have developed in the previous chapters. In the experiment, we used a personal computer (Intel Core i7 3.90 GHz, NVIDIA GeForce GTX 680, 32 GB RAM) installed with Windows 8.1 (Microsoft), a head-mounted display (Oculus Rift DK2), a motion sensor (Microsoft Kinect v2), and a wireless mouse (ELECOM M-GE3DL) to construct the interactive system. The software was implemented in C#, OpenTK, and the SDKs of the system components under Visual Studio (Microsoft). The system guarantees real-time performance (75 frames per second) during the experimental tasks. The participants used the head-mounted display and the five-button wireless mouse to accomplish experimental tasks performed in the interactive system. During the experiment, the 3-D perspective drawing, principal vanishing points, and 3-D screen are displayed in 3-D virtual space as a stereoscopic image. The 3-D screen has a size of 300 mm $\times$ 300 mm $\times$ 300 mm, and is placed 1.5 m off the ground according to the user's request. Although the head-mounted display and motion sensor have a small latency, this did not affect the participants' performance.

Stimuli

We used a hypercube as the observation object (see Appendix B for the definition of a hypercube). In the experiment, the coordinates of the vertices of the hypercube are given as permutations of $(\pm 0.5, \pm 0.5, \pm 0.5, \pm 0.5)$. We assigned a different color (red, pink, green, cyan, purple, white, orange, or yellow) to each cell of the hypercube and placed it at the origin of the 4-D world-coordinate system such that each of the eight cells was located in a different positive or negative position on each axis of the 4-D world-coordinate system, at a distance of 0.5 from the origin. To clearly visualize the edges inside the 3-D perspective drawings of the hypercube, the 3-D perspective drawings were rendered with a semitransparent surface and a reticular stipple pattern. During the experiment, the participants interacted with this hypercube using the interactive system.

5.3.2 Procedure

Each participant took a preliminary test and filled out a self-profiling form at the beginning of the evaluation experiment. This took approximately 30 min. Participants then received a brief lecture on some basic aspects of 4-D space and objects, the 4-D visualization model, and how to use the interactive system based on an analogy with 3-D space. This explanation took approximately 15 min.

After the preliminary test and lecture, the participants underwent a 4-D learning period. We first gave the participants approximately 10 min to practice

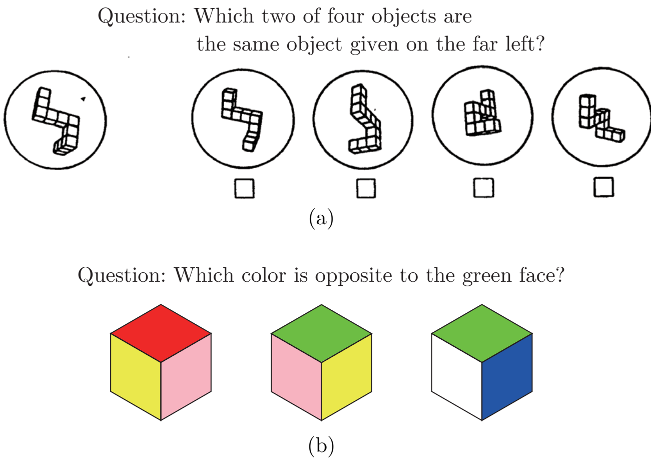

Figure 5.1. Examples of the preliminary test. (a) Mental rotation test. The second and third options from the left are correct. (b) Color cube test. "Red" is the correct answer.

using our system and make personal adjustments. The participants then studied 4-D space and the hypercube to acquire 4-D spatial representations. The length of the learning period varied from 120 to 180 min for each participant. Including breaks, the learning period took approximately 140–210 min in total.

Finally, the participants proceeded to the task period, which took approximately 60 min. The participants were asked to handle the navigational tasks in 4-D space based on their 4-D spatial representations. To check the strategies used by participants for the experimental tasks, we interviewed them after they had finished the test.

Because the total duration of the experiment was too long to run in a single day, we limited the participants' daily operating time to 120 min in consideration of their tiredness. If participants were in the middle of the experimental work when this time limit was reached, they suspended the task and resumed it the next day.

Preliminary tests

As individual differences in 3-D spatial perception could affect the development of 4-D spatial representations, we ran a preliminary test to determine the participants' intrinsic spatial ability. Figure 5.1 shows examples of the preliminary test. We used 20 trials of the redrawn version of the Mental Rotation Test (MRT) [61] and 10 trials of the Color Cube Test (CCT), which we developed ourselves. For both tests, we recorded the number of correct responses and the total response times. The overall score was calculated by dividing the number of correct answers by the total response time; thus, the higher the score, the better the spatial ability. In addition to these two spatial ability tests, we used self-reporting to determine the participants' spatial confidence. We used the Santa Barbara Sense-of-Direction Scale (SBSOD) [62], which consists of 15 questions, and the Visual Imagery Style Questionnaire (VISQ) [63], which consists of 12 questions. For both tests, the participants were asked to respond to each question on a scale of 1–5. The overall score was calculated as the average

Table 5.1. Results of the preliminary tests

	Participant					
Survey items	A	B	C	D	E	F
Spatial ability						
MRT	2.4	5.6	3.6	3.9	2.0	2.4
CCT	1.7	2.7	2.2	2.4	0.7	1.5
Spatial Confidence						
SBSOD	2.5	4.4	2.8	2.7	1.9	1.3
VISQ	2.4	3.1	3.0	2.8	1.6	1.3
Profile						
Age	20	20	20	19	20	19
Sex	Male	Male	Male	Male	Male	Female
Academic background	Science	Art	Science	Science	Art	Art

	Participant					
Survey items	G	H	I	J	K	L
Spatial ability						
MRT	3.1	1.9	3.0	2.7	2.7	1.9
CCT	2.2	1.7	1.9	1.2	2.1	1.3
Spatial Confidence						
SBSOD	1.5	2.3	1.8	2.7	3.1	3.3
VISQ	2.3	2.0	1.6	2.5	2.9	3.5
Profile						
Age	20	19	20	27	22	20
Sex	Female	Female	Female	Male	Male	Male
Academic background	Science	Science	Science	Science	Science	Art

over all responses, where a higher score indicates better spatial confidence.

Table 5.1 presents the results of the preliminary test. The participants exhibited a range of 3-D spatial ability and spatial confidence. We discuss whether these individual variations affected the results of the 4-D spatial ability tests in Section 5.5.

Learning tasks

In the learning task, participants were asked to observe and understand 4-D space and the hypercube. Using the interactive system, each participant observed the hypercube from various positions in 4-D space while moving freely around the hypercube. The participants were allowed to work on the learning task until they were satisfied with their understanding, up to a time limit of 180 min. The participants were allowed a 5-min break every 30 min.

Perspective taking and navigational tasks

In the test, participants were asked to guide themselves to a 4-D checkpoint position. The test consisted of two stages. Each stage had one practice trial followed by ten experimental trials. In the first stage, participants started from a 4-D position on the w_w-axis and moved toward one checkpoint. Thus, the participants visited ten checkpoints in total. The checkpoints were randomly selected from the 4-D positions from which three or four cells of the hypercube could be seen at once. In the second stage, participants again started from a 4-D position on the w_w-axis, and this time traveled through four checkpoints in order. Thus, the participants visited 40 checkpoints in total. The checkpoints were randomly selected from the 4-D positions from which one, two, three, or four cells of the hypercube could be seen at once. For each trial, the target checkpoint was described orally as a set of cell colors that participants would see at the checkpoint, for example, "Go to a position in 4-D space from which you can see red, green, purple, and orange cells simultaneously." To solve this task, participants needed to imagine a point from which they could obtain the desired perspective of the hypercube and identify a reasonable route to the checkpoint in 4-D space, based on their mental representations of 4-D space and the hypercube. If the participants guided themselves to the checkpoints smoothly without losing spatial orientation in 4-D space, they were considered to have successfully acquired 4-D spatial representations.

5.3.3 Results

This experiment was designed around an individual subject analysis based on behavioral observations. The experimental score is the number of target checkpoints that the participants moved to from the starting point or the previous checkpoint without losing track of their position and the direction of the target checkpoint in 4-D space. Considering the tendencies exhibited by the participants in our preliminary research [33], we defined criteria to determine whether the participants had become lost in 4-D space. That is, the participants should not arrive at the checkpoint by a random walk approach, they should not travel back and forth to the same position many times, and they should not move in the wrong direction once they were fairly close to the target checkpoint. For

Table 5.2. Results of Experiment 1

	Participant					
Performance	A	B	C	D	E	F
Learning time [min]	130	180	180	120	180	180
Score						
First stage	9 / 10	8 / 10	7 / 10	7 / 10	5 / 10	—
Second stage	38 / 40	31 / 40	34 / 40	38 / 40	26 / 40	—
Strategy						
Direct flight	◯	×	◯	◯	×	—
Relay-points	◯	◯	◯	◯	◯	—
Trial and error	×	×	×	×	◯	—

	Participant					
Performance	G	H	I	J	K	L
Learning time [min]	150	180	180	180	180	160
Score						
First stage	8 / 10	2 / 10	2 / 10	7 / 10	9 / 10	8 / 10
Second stage	38 / 40	27 / 40	8 / 40	39 / 40	39 / 40	33 / 40
Strategy						
Direct flight	◯	×	×	◯	×	◯
Relay-points	◯	◯	◯	◯	◯	◯
Trial and error	×	◯	◯	×	×	×

each trial, we carefully observed the participants' operations on the principal vanishing points in 3-D space and the moving path of the 4-D eye-point in 4-D space, and judged whether the navigation was a success or failure.

Table 5.2 presents a summary of the learning time, score, and participants' strategy toward the experimental tasks. Overall, eight participants (A, B, C, D, G, J, K, and L) navigated smoothly in both stages, which suggests that they were able to perform perspective taking and acquire navigational skills in 4-D space. Three participants (E, H, and I) exhibited worse performance in the first stage or both stages. Participant F dropped out of the experiment after the learning task, because she was not able to form a mental image of 4-D space and the hypercube.

From our observations of the participants' actions in 3-D and 4-D space, we identified three strategies used in the experiment: the direct flight strategy, the relay-points strategy, and the trial-and-error strategy. Successful participants used the direct flight strategy and the relay-points strategy. The former involves moving directly along the shortest path to the checkpoint, whereas the latter involves creating paths by moving from view to view in a way that will surely lead to the target checkpoint. The participants who used these strategies were able to recover their spatial orientation even if they moved in the wrong direction or made a detour in 4-D space.

A significant difference between the direct flight strategy and the relay-points strategy is the number of operations on the principal vanishing points. Participants who guided themselves in 4-D space with the direct flight strategy performed fewer operations. In most cases, participants needed only one or two steps to accomplish the task. Another distinctive difference is the shape of the 4-D eye-point movement path. When we visualized the trajectory of the 4-D eye-point movement onto the 3-D screen with our interactive system, the trajectory of the direct flight strategy was shorter and had fewer bends than the other strategies. Considering these characteristics, we classified each successful trial manually based on behavioral observations of the participants' operations in 3-D space and visual observations of the trajectory of the 4-D eye-point movement.

We show a typical sample of the operations in Figure 5.2; other results display similar trends. We use trial #26 of the second stage as an example. In this trial, participants moved from the starting point near $(0.75, -0.75, 0.75, 0.75)$ to the checkpoint near $(-0.75, 0.75, -0.75, -0.75)$. In other words, participants moved from the starting point to the other side of the 4-D spherical surface. Figure 5.2 depicts screen shots of a series of principal vanishing point operations. Participant D used the direct flight strategy and accomplished the task in two steps, which was the minimum number of operations required. He simply moved the principal vanishing points vp_y and vp_x parallel to the y_s-axis. In contrast, Participant A required four steps to reach the checkpoint. He moved the principal vanishing points vp_z and vp_w parallel to the z_s-, x_s- and y_s-axis step-by-step using the relay-points strategy. In this strategy, participants create paths by following easy-to-understand views in a way that is sure to reach the target checkpoint.

Figure 5.3 shows the trajectories of the 4-D eye-point movements corresponding to the trial shown in Figure 5.2. Using our interactive system, we draw the trajectory in 4-D space and visualize it on the 3-D screen from the 4-D eye-point $(0, 0, 0, 2.1)$ to the 4-D observed point $(0, 0, 0, 0)$. The parameters (k, h, f) of the 4-D viewing field are $(0.5, 0.5, 100)$. Note that we show the left view of the stereoscopic image displayed on the head-mounted display. Participant D's trajectory generally forms a unique smooth curve that represents the shortest path from the starting point to the checkpoint. Participant D passed through the zenith of the 4-D spherical surface as if it were an aerial passage following the polar route. In contrast, Participant A's trajectory includes three bends. Each bend corresponds to the point at which the participant changed an operation on a vanishing point or changed the direction of movement of the principal vanishing points. Thus, Participant A traveled through some relay points where he could confirm one or two cells included in the target perspective of the hypercube to ensure that he could reach the checkpoint.

According to the post-experiment interviews, all of the successful participants attempted to predict the direction of the target checkpoint. They also reported trying to plan a secure route from the starting point to the checkpoint by predicting the visual changes in the 3-D perspective drawing of the hypercube. For example, Participants A and D reported that they used the direct flight strategy when they were required to move to the other side of the 4-D spherical surface and used the relay-points strategy when they needed to successively operate multiple principal vanishing points to reach a checkpoint. The successful participants had confidence in their strategy and understanding. Therefore, we are probably justified in thinking that the participants developed some sort of mental representations of 4-D space and the hypercube, and performed perspective taking and navigation in 4-D space.

In contrast, the unsuccessful participants relied heavily on the trial-and-error strategy. Figure 5.3(c) visualizes Participant E's trajectory. The zig-zag lines indicate that the participant got lost in 4-D space and moved the principal vanishing points at random in 3-D space. In particular, Participants E and I

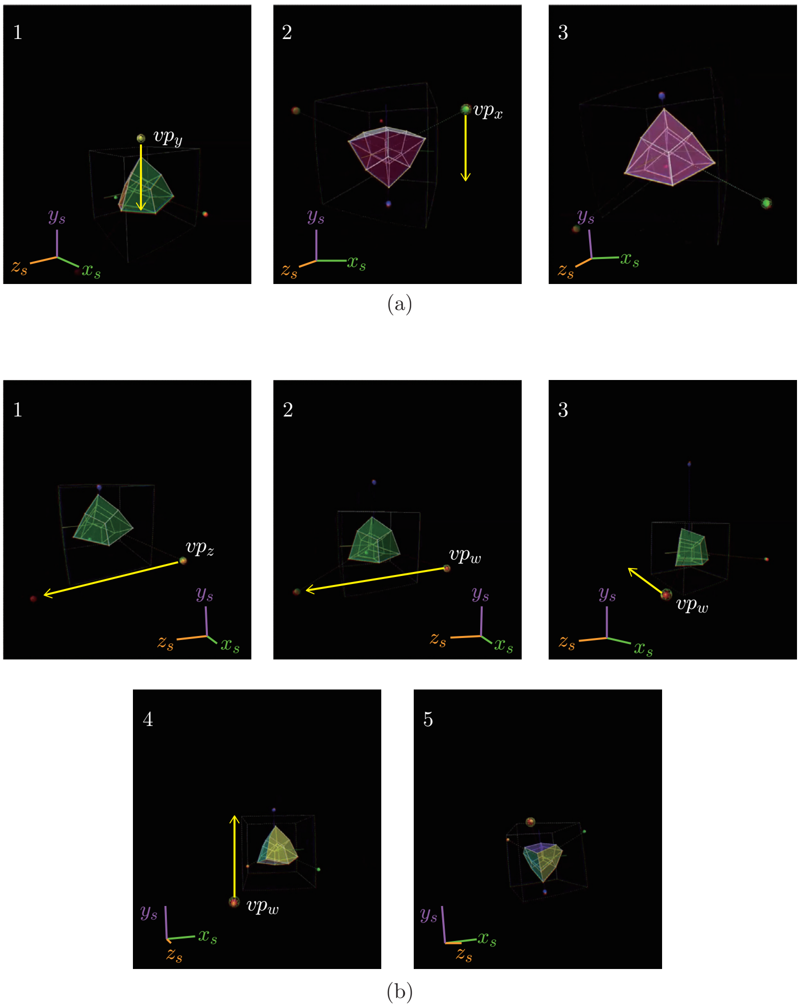

Figure 5.2. Difference in principal vanishing point operations. (a) Direct flight strategy (Participant D). (b) Relay-points strategy (Participant A).

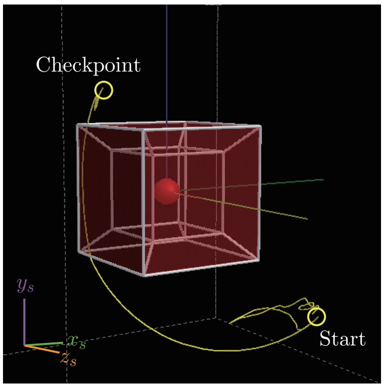

$p_f(0, 0, 0, 2.1)$ $p_a(0, 0, 0, 0)$

(a)

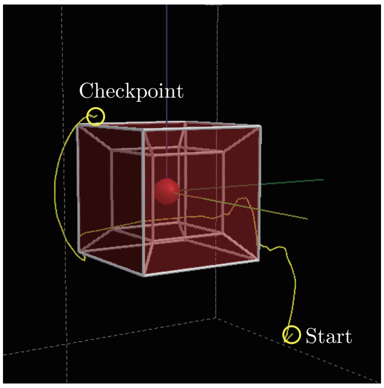

$p_f(0, 0, 0, 2.1)$ $p_a(0, 0, 0, 0)$

(b)

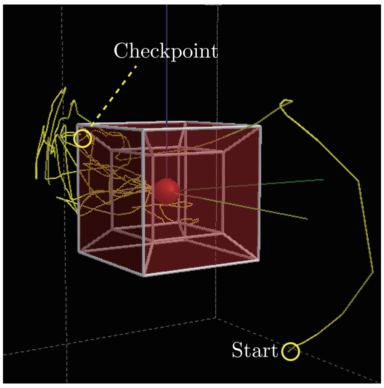

$p_f(0, 0, 0, 2.1)$ $p_a(0, 0, 0, 0)$

(c)

Figure 5.3. Difference in the trajectory of the 4-D eye-point movement. (a) Direct flight strategy (Participant D). (b) Relay-points strategy (Participant A). (c) Trial-and-error strategy (Participant E).

exhibited little skill in operating principal vanishing points vp_z and vp_w in the z_s-direction, and they could not understand the 4-D eye-point movement in the 4-D direction corresponding to that operation. When participants observe a 3-D object from various directions in 3-D space, they need only move their eye-point vertically and horizontally around the object. Thus, the participants might naturally understand the correspondence between the 4-D eye-point movement and the principal vanishing point operations in the x_s- and y_s-directions. However, when the participants attempt to move in 4-D space, this understanding is insufficient. These participants probably saw the 3-D perspective drawing as a 3-D object that changed its appearance according to special transformation rules. As a result, they failed to understand the relationship between the principal vanishing point operations in 3-D space and the eye-point movement in 4-D space. We conclude that these participants failed to acquire 4-D spatial representations and that their understanding was insufficient for perspective taking and navigation in 4-D space.

5.4 Experiment 2: Mental Spatial Transformation

We received a positive insight into the possibility of participants using 4-D spatial representations from the results of Experiment 1. However, because Experiment 1 included some overlap between the learning tasks and the experimental tasks, it remained unclear whether the participants had acquired actual 4-D spatial representations or simply gained route knowledge of operations on the principal vanishing points. Thus, it was necessary to examine whether the participants' representations were universal and flexible enough for a novel 4-D spatial task. In this section, we describe a second experiment that tested the participants' ability to perform mental spatial transformations and manipulations of a 4-D object.

5.4.1 Method

We first introduce the participants, apparatus, and stimuli of the experiment.

Participants

The twelve participants involved in Experiment 1 were invited to join Experiment 2.

Apparatus

We ran the experiment under almost the same conditions as Experiment 1, with the exception that, in this experiment, participants could not use the wireless mouse.

Stimuli

The stimuli were four four-point 3-D perspective drawings of one novel hypercube. Each stimulus was formed by randomly assigning a different color to each cell in the hypercube. The hypercube was then projected from four different

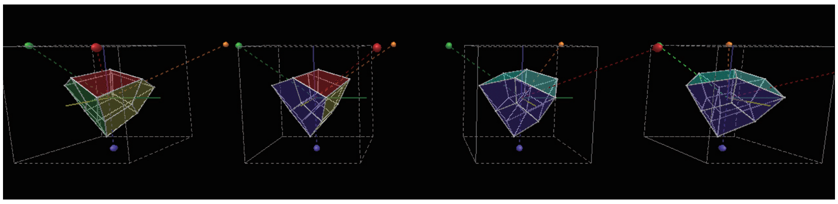

Figure 5.4. Example of the stimuli.

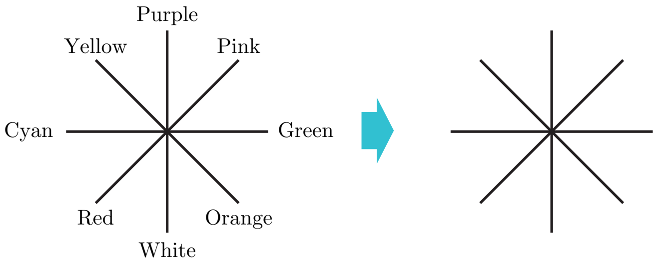

Figure 5.5. Response sheet for the reconstructed coloring pattern.

4-D viewing positions chosen from 16 candidates. As a result, these 3-D perspective drawings had the same exterior shape and different colorings. The four 3-D perspective drawings were arranged in a single line in 3-D virtual space. Using the interactive system, the participants observed the stimuli from various directions in 3-D virtual space to mentally reconstruct the entire image of the hypercube.

Figure 5.4 shows an example of the stimuli. As in Experiment 1, to clearly visualize the inside of the 3-D perspective drawings, we rendered them with semi-transparent surfaces with a reticular stipple pattern. Each of the 3-D screens was sized at 200 mm × 200 mm × 200 mm, and they were positioned 200 mm apart.

5.4.2 Procedure

After completing Experiment 1, the participants proceeded to Experiment 2. Each participant received an explanation of the experimental task before completing one practice trial followed by ten experimental trials. To confirm the participants' strategies toward the task, they were interviewed after finishing all trials.

In each trial, the participants needed to mentally reconstruct a hypercube from the multiple 3-D perspective drawings displayed in 3-D virtual space. They were then asked to complete the response sheet shown in Figure 5.5 to explain the coloring of the hypercube. Thus, this test is the 4-D version of the CCT shown in Figure 5.1(b). Each participant allocated the eight colors to the graph on the right according to the analogy with the sample on the left, which represents the coloring pattern used in Experiment 1. Additionally, the participants rated their self-confidence in each response on a scale of 1–5, where 5 represents the positive end of the spectrum. This task requires the ability to transform and manipulate the 4-D structure of the hypercube from the given 3-D perspective drawings. Therefore, strong performance in this experimental task is an indicator of success in learning 4-D spatial representations.

This experiment was designed around an individual-subject analysis. The experimental score is the number of correct color-pairs, number of correct answers, and mean confidence rating for the ten trials. The number of correct color-pairs corresponds to the number of trials (out of ten) for which the participants correctly identified the four pairs of colors allocated to two cells facing each other in the hypercube. Note that we counted the answers as being correct even if they were rotated in 4-D space.

5.4.3 Results

The participants' performance and confidence ratings are presented in Table 5.3. We summarize the score, mean response time, and participants' strategy. Overall, seven participants (A, C, D, G, J, K, and L) were able to mentally reconstruct the hypercube from its 3-D perspective drawings with a high degree of confidence. Three participants (B, H, and I) exhibited lower performance and confidence levels. Two participants (E and F) dropped out of the test because they could not imagine the structure of the hypercube at all.

As there are 210 possible coloring patterns, the probability of a participant successfully completing the task at random is 1/210. The number of correct answers for participants other than E and F was higher than the random chance level. If the participants were able to find correct color-pairs in some way, they were finally required to decide whether the reconstructed hypercube was the normal object or a mirror object of the correct hypercube. In this case, the chance of correctly guessing at random is ultimately 1/2. Six participants in the high performance group (A, C, D, G, J, and L) performed significantly better than the random chance level, suggesting that they were able to utilize their 4-D mental representations to solve the task. Although Participant K's score only surpassed the level of random chance by a small margin, his performance was distinctive. He was wrong on the first three trials, and then gave the correct answer for seven consecutive trials. According to his comments, after the first three trials, he noticed that his answers were mirror objects due to a misunderstanding of the coloring pattern of the sample hypercube represented on the left side of the response sheet; he then corrected his mental representation. Thus, we consider that Participant K should be included among the successful participants.

According to the post-experiment interviews, the successful participants seemed to solve the hypercube reconstruction test with a two-step approach. First, they found four sets of two cells that face each other in 4-D space. One solution is the elimination method; another is to focus on the principal vanishing points. If the participants understood that two such cells were on the same principal coordinate axis in 4-D space, they were able to determine the four sets by looking for the two cells corresponding to the same principal vanishing point.

The second critical step involves constructing the hypercube by appropriately arranging the four sets of two cells in 4-D space. One solution is to mentally simulate the 4-D eye-point movement to determine the 4-D spatial relationship among the four sets of two cells. For example, Participant C reported that he simulated visual changes in the 3-D perspective drawing of the hypercube, starting from a one-point perspective drawing of each four-point 3-

Table 5.3. Results of Experiment 2

	Participant			
Performance	A	B	C	D
Scores				
Number of correct color-pairs	10 / 10	10 / 10	10 / 10	10 / 10
Number of correct answers	8 / 10	5 / 10	10 / 10	10 / 10
Confidence	5	3.6	4.6	4.3
Mean response time [s]	278 ± 91	564 ± 163	254 ± 248	325 ± 202
Solution				
Mental 4-D eye-point movement	○	×	○	○
Mental 4-D axes simulation	×	×	×	×

	Participant			
Performance	E	F	G	H
Scores				
Number of correct color-pairs	—	—	9 / 10	10 / 10
Number of correct answers	—	—	9 / 10	5 / 10
Confidence	—	—	3.9	2.7
Mean response time [s]	—	—	279 ± 171	375 ± 65
Solution				
Mental 4-D eye-point movement	—	—	○	×
Mental 4-D axes simulation	—	—	×	×

	Participant			
Performance	I	J	K	L
Scores				
Number of correct color-pairs	4 / 10	10 / 10	10 / 10	8 / 10
Number of correct answers	4 / 10	10 / 10	7 / 10	8 / 10
Confidence	3.1	4.7	4.4	3.7
Mean response time [s]	264 ± 73	212 ± 84	578 ± 432	450 ± 279
Solution				
Mental 4-D eye-point movement	×	×	×	○
Mental 4-D axes simulation	×	○	○	×

D perspective drawing, by mentally operating the principal vanishing points. Participants A, D, G, and L reported trying similar solutions. This approach is grounded in 4-D spatial thinking. In addition, the participants' high confidence ratings reflect a successful understanding of 4-D space and objects. Therefore, the results suggest that these participants were able to form mental representations of 4-D spatial structures through 4-D interactions, and that they applied their representations to the novel 4-D task.

Participants J and K used an alternative solution, although they mentioned an awareness of the strategy of mental 4-D eye-point movement. They focused on one 3-D perspective drawing in the stimulus, and used four lines joining each principal vanishing point and the center of the 3-D screen in 3-D space. They assigned each of the four cells appearing in the 3-D perspective drawing to one end of each axis on the response sheet, while remembering the visual change from a one-point 3-D perspective drawing to a four-point 3-D perspective drawing such that these four lines corresponded to the four principal coordinate axes of the response sheet. Then, they simply allocated the remaining four colored cells to the other ends of the 4-D principal coordinate axes. This strategy is more systematic than the first solution. Participants J and K discovered this solution from a deep understanding of the hypercube's structure and principal vanishing points. They mentioned noticing the approach based on 4-D eye-point control simulation, but chose this solution to reduce the mental workload. In particular, Participant K reported that he instantly imagined the entire image of the hypercube while looking at the 3-D perspective drawings and without thinking deeply. Although the exact nature of the structure of their mental representations is not clear, we are probably justified in thinking that Participants J and K were able to acquire 4-D spatial representations.

In contrast to these successful participants, Participants B, H, and I could not reconstruct the hypercube. We consider some possible scenarios for this failure. Firstly, these participants failed to expand their spatial representations from three to four dimensions. The results of Participants B and H fit this scenario, as they reported being able to find the four sets of two cells that faced each other in 4-D space, but could not assemble them correctly because they failed to determine whether the reconstructed coloring pattern was correct or if it was a coloring pattern corresponding to the 4-D mirror image of a stimulus hypercube. It appears that they tried to compare the four 3-D perspective drawings in 3-D space. Secondly, the participants completely failed to acquire 4-D spatial representations. This scenario is consistent with Participant I's result. She reported trying to imagine the 4-D structure of the hypercube, but was unable to. Based on these comments, we conclude that these three participants were unable to apply their experience to the mental simulation and manipulation of 4-D space and objects.

5.5 General Discussion

In this paper, we have investigated whether humans are capable of acquiring 4-D spatial representations. Twelve participants interactively observed and learned about 4-D space and a hypercube with the use of an interactive system that utilizes the principal vanishing points as the interface for 4-D eye-point control. Their performance on two different 4-D spatial ability tests was then examined. Seven participants (A, C, D, G, J, K, and L) demonstrated the ability to imagine themselves at a different perspective in 4-D space with respect to the observation object, to update their understanding of an object while moving in 4-D space, and, having observed the object, to understand the relationship between multiple views of the object. Although the exact nature of the 4-D spatial representations is still not known, the present results suggest, at the very least, that mental representations of 4-D space and objects can be formed from experience and interactions in a 4-D environment.

5.5.1 4-D Spatial Representations vs. Reinforcement Learning

The primary concern about our experimental results is whether the participants' performance can be explained by the use of true 4-D spatial representations or, instead, by other low-level solutions. Although the participants' solutions varied, we can rule out some low-level solutions.

First, the tasks in the experiments cannot be solved with mathematical solutions. The participants were theoretically able to estimate their 4-D position from the principal vanishing points in Experiment 1, as we showed in Section 2.3.2. They were also able to estimate spatial relations of multiple 3-D perspective drawings by calculating the 4-D coordinates of the hypercube vertices based on triangulation, as in Experiment 2. None of the participants reported using this strategy in both experiments. Furthermore, none of the participants had prior knowledge of the geometry of 4-D solids. Even if they did, the relevant calculations would be too difficult to perform in real time during the experiment.

Second, the successful participants did not rely on a trial-and-error approach or chance. The evidence is that, in Experiment 1, the participants' operations on the principal vanishing points and their trajectories in 4-D space show no signs of relying on these approaches. Furthermore, the participants' scores in Experiment 2 cannot be explained by chance.

Third, the performance of the successful participants cannot be explained by the use of low-level solutions akin to reinforcement learning, which does not cover 4-D spatial representations. There is a possibility that the participants remembered the whole sequence of 3-D perspective drawings of the observation object and traced one perspective to the next, which was remembered as being closer to the target checkpoint. Because the participants interacted with the same hypercube in both the learning task and Experiment 1, this explanation could fit the results of Experiment 1 but not those of Experiment 2. As described in Section 5.4, the participants saw only four 3-D perspective drawings of a hypercube, which had a new coloring pattern, in this test. Thus, it would not be possible to rely on the memory of a sequence of 3-D perspective drawings. Rather, the participants were required to interpolate intermediate views of the given 3-D perspective drawings of the hypercube from different perspectives in 4-D space while taking the spatial structure of the hypercube into account. In other words, the experiments did not require the participants to remember all perspectives of the hypercube, but to learn general rules and operations to help them make 4-D judgments on unfamiliar problems. Therefore, combining the results of both experiments, a reasonable interpretation of the present results is that the successful participants developed 4-D spatial representations that help

Table 5.4. Correlation factors between the experimental results and the preliminary tests

Test items	Experiment 1 First stage	Experiment 1 Second stage	Experiment 2
MRT	0.249	−0.017	−0.130
CCT	0.306	0.072	−0.243
SBSOD	0.464	0.290	−0.110
VISQ	0.760	0.520	0.405

in perspective taking, navigational skills, and mental spatial transformations in 4-D space and which go beyond simple reinforcement learning.

5.5.2 Individual variations among the participants

There is some apparent variation among the participants, both in the amount of 4-D experience needed to learn 4-D spatial representations and in their performance level on the 4-D spatial ability tests. We know it is difficult to determine the actual cause for this individual variation because of the small number of participants. However, it is important to study this point for future 4-D spatial cognitive research.

One possible interpretation of the individual variation is that the participants' intrinsic spatial ability, spatial confidence, and focus of attention on the tests varied and affected their 4-D spatial learning. We can verify this interpretation by calculating the correlation factors between the scores on the 4-D spatial ability tests and the scores on the preliminary tests. Table 5.4 presents the correlation factors. Against our expectations, the scores on the 4-D spatial ability tests and the 3-D spatial ability tests are not significantly correlated. In contrast, the hypercube recognition tests and the CCT exhibit a weak negative correlation, even though they differ only in dimension. This suggests that the participants' intrinsic spatial ability has a negligible impact on their development of 4-D spatial representations. Furthermore, this generates the hypothesis that the processing of 4-D visual information and 3-D visual information is related to different mechanisms.

There are positive correlations between the scores on the 4-D spatial ability tests and 3-D spatial confidence. In particular, the correlation between the 4-D spatial ability tests and VISQ is significant. This suggests that self-awareness of good spatial skills encourages the development of 4-D spatial representations. Some recent studies [64, 65] investigating the effect of stereotypical threats on human spatial ability support this suggestion.

There is also a general trend whereby participants from science and engineering courses outperform those from arts courses. Six out of seven participants from science and engineering courses successfully completed the experiments, whereas only one out of five participants from arts courses was able to acquire 4-D spatial representations. Moreover, this arts student had studied science at a high level until fairly recently. As researchers have pointed out, there is some relationship between spatial ability and mathematical aptitude [66, 67]. Thus, it is not unexpected that the participants' intrinsic mathematical knowledge might have positively affected their 4-D learning.

5.5.3 Possible Forms of 4-D Spatial Representations

In Section 2.1, we reviewed several previous studies that examine the possibility of acquiring 4-D spatial representations. Because these only demonstrate that humans can acquire 4-D spatial representations, it is important to discuss possible forms of 4-D spatial representations. Certain explanations are consistent with the participants' strategies in the experimental tasks.

One plausible explanation is that the participants formed a cognitive coordinate system consisting of an origin and four directional axes. This type of representation has been demonstrated in many studies on 3-D spatial cognition. Consequently, it is natural that humans might represent 4-D space and objects within a 4-D coordinate system. In particular, in these experiments, because the participants used principal vanishing points, which represent the points at infinity on the 4-D world-coordinate axes, and because they observed a hypercube that was positioned so that each cell was perpendicular to one corresponding 4-D principal coordinate axis and parallel to the other three 4-D principal coordinate axes, there is a high probability that the participants developed and used this type of 4-D spatial representation. In Experiment 1, if the participants formed a 4-D cognitive coordinate system, they would be able to make a rough estimate of the positional relationship between themselves and a target checkpoint in 4-D space, and to guide themselves to the checkpoint position. This type of spatial representation is consistent with both the direct flight strategy and the relay-points strategy. In Experiment 2, with this coordinate system, they would be able to reconstruct a hypercube by considering its orientation within the 4-D world-coordinate system, which is invariant with respect to the 4-D viewing direction. In particular, the strategy used by Participants J and K supports the validity of this explanation.

Although the 4-D cognitive coordinate system seems appropriate as the hypothetical form of the 4-D spatial representations, it remains to be determined whether the four axes are perpendicular to each other in the participants' mental space. As recent spatial cognitive research has shown that the primary form of human spatial knowledge is a graph structure, rather than an absolute map-like coordinate system [14], it is highly likely that the cognitive 4-D coordinate system of 4-D spatial representations does not have strict orthogonal axes. Therefore, the participants are assumed to have performed the experimental tasks based on static mental representations of 4-D space and objects. The question of the orthogonality of the 4-D cognitive coordinate system will be examined in future work.

Another possible explanation is that the participants perceived the hypercube as a 3-D object that changed its appearance according to special transformation rules. It is possible to solve the perspective taking test by memorizing the rules of shape transformations or the sequence of color changes in the 3-D perspective drawings for all patterns of operations on the principal vanishing points. The unsuccessful participants may have relied on this type of representation. For the successful participants, however, this explanation can be ruled out by their actions in Experiment 1. For example, when the participants were at a 4-D position on the x_w-axis, only principal vanishing point vp_x appeared at the center of the 3-D screen. In this case, the participants could not operate principal vanishing point vp_x in the z_s-direction in 3-D space because of the restriction of the interactive system. In other words, in this situation, the possible movement directions were limited in 4-D space. A similar situation occurred when the participants were at a 4-D position on the y_w-axis, but despite this restriction, some successful participants tried to operate the principal vanishing point in the prohibited direction in 3-D space. If the interactive system were improved to allow the participants to perform such an operation, they could have directly approached the target checkpoint in 4-D space. Because they could not experience such 4-D eye-point movement, conceiving this action required the participants to imagine the 4-D spatial relationship between their own position and the target position. Consequently, the fact that the participants attempted this kind of action indicates the successful acquisition of actual 4-D spatial representations.

5.5.4 Perspective Taking vs. Object Rotations

Although our interaction technique includes the geometric computation of 4-D eye-point movements, it is difficult to distinguish the 3-D perspective drawings from those obtained by object rotation. This may allow the participants to interpret the 4-D experience in two ways: (i) to imagine eye-point movements in relation to the hypercube, or (ii) to imagine rotations of the hypercube about a plane or planes passing through the center of the hypercube. Indeed, according to the comments of the seven successful participants, three (C, K, and L) used the former interpretation and four (A, D, G, and J) used the latter. We consider this difference to underlie the embodiment of spatial cognition. Research has shown that perspective taking is related to transformations of the internal representations of the body [68, 69, 70], whereas object rotations are related to the image of hand motions [71, 72]. In the present experiments, changes in the visual appearance of the hypercube are linked to the participants' hand motion for pick-and-move operations of the principal vanishing points. Although the participants walked around the 3-D virtual space to see the 3-D perspective drawing displayed on the 3-D screen, they stopped at a position from which it was easy to operate the principal vanishing points when moving in 4-D space. Thus, the participants who imagined object rotations may have felt that they were rotating the hypercube by holding and steering a shaft projecting from the side of the hypercube. In contrast, the participants who imagined the 4-D eye-point movements intentionally imagined such actions when they operated the principal vanishing points.

We consider the embodiment to be related to the form of the cognitive coordinate system. Although the present results indicate that the participants acquired 4-D spatial representations in their mental space, the cognitive coordinate system seems to be world-centered or object-centered, as the reference point is located outside the body. A body-centered coordinate system with a reference point inside the body is also necessary to understand 4-D space and objects more intuitively. In particular, when we explore intrinsic 4-D environments such as a 4-D maze, we need to convert these cognitive coordinate systems into one another. An interaction technique that promotes the acquisition of internal representations of the body extended to 4-D space is an interesting topic for future studies of 4-D spatial cognition.

5.5.5 Limitations and Future Work

We offer some notes regarding the limitations of the present study. First, although the results support the possibility of acquiring 4-D spatial representations, our contribution represents one part of the entire scope of 4-D spatial cognition. Using hypercubes and principal vanishing points is too simple to investigate general 4-D spatial representations. The small number of participants made it difficult to interpret the actual cause of the differences among the experimental results. If we were to examine general 4-D spatial representations, we would need more participants to be trained and tested using complex 4-D objects. We consider that the orthogonality and parallelism learned through interaction with a hypercube can form the basis for representations of 4-D space in a cognitive coordinate system. As suggested by the results of the experiments, for some participants, even a hypercube is difficult to understand. General 4-D spatial representations that support 4-D judgments of complex 4-D objects require long-term training after adapting to a simple object.

Second, the scope of the present study was limited to the ability to imagine the visual appearance of an object from different perspectives. Spatial visualization ability in a large-scale 4-D scene was not assessed. In future, a cognitive map of an intricate 4-D environment should be studied, as has been done for 3-D spatial cognition [1, 2, 14]. To acquire knowledge of the environment, people would need to convert their reference spatial representations from the first-person view to the 4-D bird's-eye view. In other words, they would need to convert the cognitive coordinate system from a dynamic one referring to their 4-D position to a static one fixed in 4-D space. To investigate this point, we are currently improving our interactive system to visualize a 4-D scene with accurate expressing of occlusion.

Third, although the 4-D cognitive coordinate system is one possible 4-D spatial representation, other interaction methods may foster different forms of 4-D spatial representations. For instance, a haptic interface would enhance the recognition of the shape of 4-D objects [73, 74]. The present results suggest that 4-D spatial representations can be acquired through interactions with 4-D objects by principal vanishing point operations, whereas the effects of interface design and interaction style on 4-D spatial representations require future research.

5.6 Summary

In Chapter 5, we examined the possibility of human 4-D spatial representations through experiments that assess the ability to perform perspective taking, navigation, and mental spatial transformations of objects in 4-D space. The exact nature of the participants' mental representations is not known, but the results suggest that humans are capable of acquiring 4-D spatial representations and using 4-D spatial skills. We therefore succeeded in providing empirical evidence for 4-D spatial representations.

One important aspect of the present study is that it provides a new perspective for research on 4-D spatial representations. Conventional studies on 4-D spatial cognition focus on scenarios in which humans observe a 4-D object in a static condition. In addition, previous research has only considered the ability to comprehend the geometric properties of 4-D objects. In contrast, the present experiments employed free interaction with a 4-D object and examined the ability to manipulate 4-D imagery, which involves cognitive processing such as prediction, creation, and decision making for spatial visual information. The results suggest that humans are capable of acquiring 4-D spatial representations and that this cognitive processing works properly in 4-D space. This means that human spatial cognition does not have intrinsic dimensionality constraints, even though humans evolved in a 3-D world. Instead, it is thought that human cognitive processing is flexible and can adapt to higher-dimensional space with practice and experience of 4-D space and objects.

Chapter 6

Conclusions

In this dissertation, we have proposed a novel technique for interacting in 4-D space, which employs the principal vanishing points as an interface to observe various 4-D data. We constructed an algorithm that controls movements of the 4-D eye-point in 4-D space through operations on the principal vanishing points in 3-D space. Using this algorithm and virtual reality devices, we constructed a new interactive 4-D space visualization system, which enabled us to gain experience and understanding of 4-D space and objects. Using the proposed interactive system, we can intuitively control the movement of the 4-D eye-point using simple pick-and-move operations on the principal vanishing points, and observe 4-D data from arbitrary positions, directions, and distances in 4-D space. The proposed system can visualize various 4-D data; not only 4-D solids, but also 4-D statistical data, 4-D phase space, and 4-D animations. Therefore, we expect that our 4-D visualization system will be used as a supporting tool for statistical analysis, scientific visualization, and creative activities.

The effectiveness of the proposed interactive system was verified through user experiments. In the experiments, we compared the proposed system with other conventional systems, in both objective and subjective aspects. The results demonstrated that the proposed system was superior to the conventional systems in terms of usability. The experiment participants were able to rapidly learn the corresponding relationship between the principal vanishing point operations and the 4-D eye-point movements. Hence, we were able to conclude that the proposed system provided sufficient usability in observing 4-D data. In addition to these experiments, we investigated the effects of changes in distance and the 4-D viewing field on the system usability. The results suggested that users had difficulty understanding the 4-D data when the 4-D eye-point was positioned closely to the 4-D data, and that the principal vanishing point operations became difficult when we employed a telescopic 4-D viewing field or parallel projection. However, observing both the 4-D data from various distances and the 4-D viewing field itself are helpful for gaining an understanding of the structure of 4-D data. Thus, in future work we will study an interface for interactively controlling the distance and the 4-D viewing field. Such an interface should be an embodied interface.

We extended the proposed 4-D eye-point control algorithm to a method of controlling the 4-D viewing direction. Rather than controlling the 4-D eye-point, we controlled the 4-D observed point using operations on the principal vanishing points. Moreover, we achieved the exploration of a 4-D solid scene through 4-D fly-through actions, by combining changes in the 4-D viewing direction with back and forth movements of the 4-D eye-point and 4-D observed point. In the proposed system, we were allowed to move inward and look around various 4-D scenes, such as the inside of a 4-D solid, 4-D solid scenes constructed of multiple 4-D objects, and a 4-D maze-like environment. The effectiveness of the proposed system was verified by an experiment comprising target-spotting tasks in 4-D space. The results suggested that the proposed system is easy to learn, and has sufficient usability for controlling the 4-D viewing direction, regardless of previous knowledge and experience of 4-D space and objects. We expect that the proposed system will contribute not only to the development of higher-dimensional visualization abilities, but also to spatial cognition research focusing on higher-dimensional space.

Using the proposed interactive 4-D visualization system, we examined the long-established question of whether humans are capable of acquiring mental representations and intuitive understandings of 4-D space and objects through perceptual experience in 4-D space with 4-D objects. In these experiments, the participants observed and learned about 4-D space and objects by using the proposed 4-D space visualization system. After they had studied 4-D space and objects, they undertook the series of the 4-D spatial ability tests. The results suggested that the participants were able to demonstrate perspective taking, navigational skills, and mental spatial transformations in 4-D space. Therefore, it was indicated that humans were able to acquire 4-D spatial representations. Moreover, from the results of the experiments we obtained an interpretation regarding the possible form of 4-D spatial representations. That is, humans form a cognitive coordinate system that consists of four directional axes when they navigate in 4-D space and observe the structure of 4-D objects.

Although it is surmised that there are several forms of cognitive coordinate systems used to understand space in general, the coordinate system that the participants formed in the experiment was expected to be an object-centered or world-centered coordinate system. In order to understand 4-D space and objects, the coordination between different cognitive coordinate systems is important. In particular, the coordination of the eye-centered coordinate system, body-centered coordinate system, and world-centered coordinate system will improve our intuitive understanding of 4-D space and objects. Thus, in future work we will examine whether humans can form such a coordinate system, and investigate which kinds of 4-D experiences help people to form these cognitive coordinate systems. We expect that the experience of exploring maze-like environments through a first-person viewpoint in 4-D space can help people to form an eye-centered or body-centered coordinate system. Furthermore, we will develop a new interactive system to enable people to gain a body-centered coordinate system for understanding 4-D environments. In other words, we will study an interface that enables us to understand 4-D space and objects with reference to our bodies.

Acknowledgment

I would like to express my sincere thanks to Professor Shuji Hashimoto who guided me during doctoral course and taught me the interesting world of science and engineering. My great appreciations for Professor Shigeo Morishima, Professor Hirochika Nakajima and Professor Atsushi Takeuchi for their kindness of providing me with their time and expertise to review this dissertation and helpful comments. I would like to express deep gratitude for Professor Yukihito Sakai who gave me many technical advices, valuable comments and persistent helps during my study and activities in Waseda University. Many thanks for Professor Hideyuki Sawada, Professor Pitoyo Hartono and Professor Shingo Maeda for their valuable helps and encouragement. My special thanks to all members of past and present in Hashimoto Laboratory and the colleagues of Global Robot Academia for their helpful supports. Finally I would like to express my greatest appreciation and gratitude to my family for their endless supports.

This work was supported in part by Global COE Program "Global Robot Academia" from the Ministry of Education, Culture, Sports, Sceince and Technology of Japan and Grants for Excellent Graduate Shools, in part by Grants for Excellent Graduate Schools from the Ministry of Education, Culture, Sports, Science and Technology of Japan, in part by Waseda University Future Robotics Organization, and in part by Waseda University Grant for Special Research Projects (2015S-084).

Takanobu Miwa
July 2017

References

[1] Edward C. Tolman: Cognitive maps in rats and men. Psychological Review 55, 189–208. (July 1948)

[2] Kevin Lynch: THE IMAGE OF THE CITY. MIT Press, Cambridge, Mass. (June 1960)

[3] Jean Piaget, Bärbel Inhelder: The Child's Conception of Space. W. W. Norton & Company, New York. (May 1967)

[4] Roger N. Shepard, Jacqueline Metzler: Mental Rotation of Three-Dimensional Objects. Science 171, 3972, 701–703. (Feb. 1971)

[5] Roland B. Guay: Purdue Spatial Visualization Tests. Purdue Research Foundation, West Lafayette. (1977)

[6] Steven G. Vandenberg, Allan R. Kuse: MENTAL ROTATIONS, A GROUP TEST OF THREE-DIMENSIONAL SPATIAL VISUALIZATION. Perceptual and Motor Skills 47, 2, 599–604. (Nov. 1978)

[7] Marcel Adajm Just, Patricia A. Carpenter: Cognitive coordinate systems: Accounts of mental rotation and individual differences in spatial ability. Psychological Review 92, 2, 137–172. (Apr. 1985)

[8] Theodore J. Branoff: Spatial Visualization Measurement: A Modification of the Purdue Spatial Visualization Test - Visualization of Rotations. Engineering Design Graphics Journal 64, 2, 14–22. (Spring 2000)

[9] Maria Kozhevnikov, Mary Hegarty: A dissociation between object manipulation spatial ability and spatial orientation ability. Memory & Cognition 29, 5, 745–756. (July 2001)

[10] David H. Foster , Stuart J. Gilson: Recognizing novel three-dimensional objects by summing signals from parts and views. Proceedings of The Royal Society of London B Biological Science 269, 1503, 1939–1947. (Aug. 2002)

[11] Mary Hegarty, David Waller: A dissociation between mental rotation and perspective-taking spatial abilities. Intelligence 32, 2, 175–191. (Mar. 2004)

[12] Bernhard E. Riecke, Douglas W. Cunningham, Heinrich H. Bulthoff: Spatial updating in virtual reality: the sufficiency of visual information. Psychological Research 71, 3, 298–313. (May 2007)

[13] Maria Kozhevnikov, Olesya Blazhenkova, Michael Becker: Trade-off in object versus spatial visualization abilities: Restriction in the development of visual-processing resources. Psychonomic Bulletin & Review 17, 1, 29–35. (Feb. 2010)

[14] Elizabeth R. Charstil, William H. Warren: From Cognitive Maps to Cognitive Graphs. PLoS ONE 9, 11, e112544. (Nov. 2014)

[15] Edwin A. Abbott: Flatland: A romance of Many Dimensions. New American Library. (Mar. 1984)

[16] Ludwing Schläfli: Theorie der vielfachen Kontinuität. Birkhäuser Basel. (Jan. 1901) (in German)

[17] Harold Scott MacDonald Coxeter: Regular Polytopes. Dover Books on Mathematics Series. Dover Publications. (June 1973)

[18] Marcel Duchamp: Nu Descendant un Escalier N°2. Philadelphia Museum of Art, Philadelphia. (1912)

[19] Salvador Dali: Crucifixion (Corpus Hypercubus). Metropolitan Museum of Art, New York. (1954)

[20] Christopher Nolan: Interstellar. Warner Bros. Pictures and Paramount Pictures. (2014)

[21] Akira Inoue, Ryouko Itohara, Kuniaki Yajima, Keimei Kaino: CG Image Generation of Four-Dimensional Origami. The Journal of the Society for Art and Science 4, 4, 151–158. (Dec. 2005)

[22] Yukihito Sakai, Shuji Hashimoto: Interactive Four-Dimensional Space Visualization Using Five-Dimensional Homogeneous Processing for Intuitive Understanding. The Journal of the Institute of Image Information and Television Engineers 60, 10, (108)1630–(125)1647. (Oct. 2006)

[23] Yukihito Sakai, Shuji Hashimoto: Four-Dimensional Space Visualization with Four-Dimensional Viewing Field Control. Bulletin of the Society for Science on Form 21, 3, 274–284. (Mar. 2007) (in Japanese)

[24] Takanobu Miwa, Yukihito Sakai, Shuji Hashimoto: Four-dimensional Eyepoint Control by Principal Vanishing Points Operation and Its Evaluation. The Journal of the Society for Art and Science 12, 4, 162–174. (Dec. 2013) (in Japanese)

[25] Takanobu Miwa, Yukihito Sakai, Shuji Hashimoto: Four-dimensional Viewing Direction Control by Principal Vanishing Points Operation and Its Application to Four-dimensional Fly-through Experience. In Proceedings of the 25th Australian Computer-Human Interaction Conference: Augmentation, Application, Innovation, Collaboration, 95–104. (Nov. 2013)

[26] Takanobu Miwa, Yukihito Sakai, Shuji Hashimoto: Interactive Four-dimensional Space Exploration Using Viewing Direction Control Based on Principal Vanishing Points Operation. In Computer-Human Interaction. Cognitive Effects of Spatial Interaction, Learning, and Ability, Lecture Notes in Computer Science 8433, Springer International Publishing, 21–46. (Apr. 2015)

[27] Phillip J. Davis, Reuben Hersh, Elena A. Marchisotto: Four Dimensional Intuition. In The Mathematical Experience, Study Edition, Birkhäuser Boston, 442–447. (Oct. 1995)

[28] Tyson N. Aflalo, Michel S. A. Graziano: Four-Dimensional Spatial Reasoning in Humans. Journal of Experimental Psychology: Human Perception and Performance 34, 5, 1066–1077. (Oct. 2008)

[29] Michael S. Ambinder, Ranxiao Frances Wang, James A Crowell, George K. Francis, Peter Brinkmann: Human four-dimensional spatial intuition in virtual reality. Psychonomic Bulletin & Review 16, 5, 1587–1594. (Nov. 2009)

[30] Ranxiao Frances Wang: A Case Study on Human Learning of Four-Dimensional Objects in Virtual Reality: Passive Exploration and Display Techniques. In Proceedings of the 2009 Fourth International Conference on Frontier of Computer Science and Technology, 519–523. (Dec. 2009)

[31] Ranxiao Frances Wang: Can Humans Form Four-Dimensional Spatial Representations?. In Space in Mind: Concepts for Spatial Learning and Education, MIT Press, Cambridge, Massachusetts, 119–136. (Nov. 2014)

[32] Ranxiao Frances Wang: Human Four-Dimensional Spatial Judgments of Hyper-Volume. Spatial Cognition & Computation: An Interdisciplinary Journal 14, 2, 91–113. (Jan. 2014)

[33] Takanobu Miwa, Yukihito Sakai, Shuji Hashimoto: 4-D Spatial Perception Established through Hypercube Recognition Tasks Using Interactive Visualization System with 3-D Screen. In Proceedings of ACM SIGGRAPH Symposium on Applied Perception 2015, 75–82. (Sept. 2015)

[34] Takanobu Miwa, Yukihito Sakai, Shuji Hashimoto: Learning Four-dimensional Spatial Representations through Perceptual Experience with Hypercubes. IEEE Transactions on Cognitive and Developmental Systems. (in press)

[35] Alfred Inselberg, Bernard Dimsdale: Parallel Coordinates: A Tool for Visualizing Multidimensional Geometry. In Proceedings of the First IEEE Conference on Visualization '90, 361–378. (Oct. 1990)

[36] Alexander K. Dewdney: COMPUTER RECREATIONS: A Program for Rotating Hypercubes Induces Four-Dimensional Dementia. Scientific American, 8–13. (Apr. 1986)

[37] Andrew J. Hanson: Computer Graphics beyond the Third Dimension. Course Notes for SIGGRAPH ' 98, Course 46. (July 1998)

[38] Barbara Hausmann, Hans-Peter Seidel: Visualization of Regular Polytopes in Three and Four Dimensions. Computer Graphics Forum 13, 3, 305–316. (Sept. 1994)

[39] Steven R. Hollasch: Four-Space Visualization of 4D Objects. Master ' s thesis, Arizona State University. (Aug. 1991)

[40] Koji Miyazaki, Keiichi Ishihara: Four-Dimensional Graphics. Asakura-Shoten Publishers, Tokyo. (Sept. 1989) (in Japanese)

[41] Koji Miyazaki, Motonaga Ishii, Satoshi Yamaguchi: Science of Higher-Dimensional Shapes and Symmetry. Kyoto University Press, Kyoto. (Feb. 2005) (in Japanese)

[42] Neophytos Neophytou, Klaus Mueller: Space-Time Points: 4D Splatting on Efficient Grids. In Proceedings of the 2002 IEEE Symposium on Volume Visualization and Graphics, 97–106. (Oct. 2002)

[43] Jonathan Woodring, Chaoli Wang, Han-Wei Shen: High Dimensional Direct Rendering of Time-Varying Volumetric Data. In Proceedings of the 14th IEEE Visualization 2003, 417–424. (Oct. 2003)

[44] Akira Kageyama: A Visualization Method of Four Dimensional Polytopes by Oval Display of Parallel Hyperplane Slices. Journal of Visualization 19, 3, 417–422. (Aug. 2016)

[45] Andrew J. Hanson, Pheng A. Heng: Illuminating the fourth dimension. IEEE Computer Graphics and Applications 12, 4, 54–62. (July 1992)

[46] Alan Chu, Chi-Wing Fu, Andrew J. Hanson, Pheng-Ann Heng: GL4D: A GPU-based Architecture for Interactive 4D Visualization. IEEE Transactions on Visualization and Computer Graphics 15, 6, 1587–1594. (Nov. 2009)

[47] Weiming M. Wang, Xiaoqi Q. Yan, Chi-Wing Fu, Andrew J. Hanson, Pheng Ann Heng: Interactive Exploration of 4D Geometry with Volumetric Halos. In The 21th Pacific Conference on Computer Graphics and Applications - Short Papers, 1–6. (Oct. 2013)

[48] Michael D'Zmura, Philippe Colantoni, Gregory D. Seyranian: Virtual Environments with Four or More Spatial Dimensions. Presence 9, 6, 616–631. (Dec. 2000)

[49] Xiaoqi Yan, Chi-Wing Fu, Andrew J. Hanson: Multitouching the Fourth Dimension. IEEE Computer 45, 9, 80–88. (Sept. 2012)

[50] Akira Kageyama: Keyboard-based Control of Four-dimensional Rotations. Journal of Visualization 19, 2, 319–326. (May 2016)

[51] Julieta C. Aguilera: Virtual Reality and the Unfolding of Higher Dimensions. In Stereoscopic Displays and Virtual Reality Systems XIII, Proceedings of SPIE 6055, 605–612. (Jan. 2006)

[52] Yukihito Sakai, Shuji Hashimoto: Four-dimensional Space-time Visualization for Understanding Three-dimensional Motion. The Journal of the Institute of Image Electronics Engineers of Japan 36, 4, 371–381. (July 2007)

[53] Yukihito Sakai, Shuji Hashimoto: Four-dimensional Mathematical Data Visualization via "Embodied Four-dimensional Space Display System". Forma 26, 1, 11–18. (May 2011)

[54] Yukihito Sakai, Shuji Hashimoto: Four-dimensional geometric element definitions and interferences via five-dimensional homogeneous processing. Journal of Visualization 14, 2, 129–139. (June 2011)

[55] James D. Foley, Andries van Dam, Steven K. Feiner, John F. Hughes: Computer Graphics: Principles and Practice, 2nd edition in C. Addison-Wesley Professional. (Aug. 1995)

[56] Kunio Kondo, Fumihiko Kimura, Taro Tajima: Estimation of a Point of View with Perspective Drawing and the Application. Transactions of Information Processing Society of Japan 29, 7, 686–693. (July 1988)

[57] Robert S. Allison, Laurence R. Harris, Michael Jenkin, Urszula Jasiobedzka, James E. Zacher: Tolerance of Temporal Delay in Virtual Environments. In Proceeding of IEEE Virtual Reality 2001, 247–254. (Mar. 2001)

[58] Mary Hegarty: Mechanical reasoning by mental simulation. TRENDS in Cognitive Science 8, 6, 280–285. (June 2004)

[59] Daniel L. Schwartz, John B. Black: Shuttling Between Depictive Models and Abstract Rules: Induction and Fallback. Cognitive Science 20, 4, 457–497. (Oct. 1996)

[60] Mike Stieff: Mental rotation and diagrammatic reasoning in science. Learning and Instruction 17, 2, 219–234. (Apr. 2007)

[61] Michael Peters, Bruno Laeng, Kerry Latham, Marla Jackson, Raghad Zaiyouna, Chris Richardson: A Redrawn Vandenberg and Kuse Mental Rotations Test: Different Versions and Factors That Affect Performance. Brain and Cognition 28, 1, 39–58. (June 1995)

[62] Mary Hegarty, Anthony E. Richardson, Daniel R. Montello, Kristin Lovelace, Ilavanil Subbiah: Development of a self-report measure of environmental spatial ability. Intelligence 30, 5, 425–447. (Oct. 2002)

[63] Masahiro Kawahara, Kazuo Matsuoka: Development of the Visual Imagery Style Questionnaire. The Japanese Journal of Mental Imagery 7, 1, 19–31. (Dec. 2009) (in Japanese)

[64] Matthew S. McGlone, Joshua Aronson: Stereotype threat, identity salience, and spatial reasoning. Journal of Applied Developmental Psychology 27, 5, 486–493. (Oct. 2006)

[65] Zachary Estes, Sydeny Felker: Confidence Mediates the Sex Difference in Mental Rotation Performance. Archives of Sexual Behavior 41, 3, 557–570. (June 2012)

[66] Jonathan Wai, David Lubinski, Camilla P. Benbow: Spatial Ability for STEM Domains: Aligning Over 50 Years of Cumulative Psychological Knowledge Solidifies Its Importance. Journal of Educational Psychology 101, 4, 817–835. (Nov. 2009)

[67] Yi-Ling Chenga, Kelly S. Mixa: Spatial Training Improves Children's Mathematics Ability. Journal of Cognition and Development 15, 1, 2–11. (Jan. 2014)

[68] Clack C Presson, Daniel R Montello: Updating after rotational and translational body movements: coordinate structure of perspective space. Perception 23, 1447–1455. (Feb. 1994)

[69] Olaf Blanke, Christine Mohr, Christoph M. Michel, Alvaro Pascual-Leone, Peter Brugger, Margitta Seeck, Theodor Landis, Gregor Thut: Linking Out-of-Body Experience and Self Processing to Mental Own-Body Imagery at the Temporoparietal Junction. Journal of Neuroscience 25, 3, 550–557. (Jan. 2005)

[70] Maria Kozhevnikov, Michael A. Motes, Bjoern Rasch, Olessia Blajenkova: Perspective-Taking vs. Mental Rotation Transformations and How They Predict Spatial Navigation Performance. Applied Cognitive Psychology 20, 397–417. (Mar. 2006)

[71] Andreas Wohlschläger, Merideth Gattis, Harold Bekkering: Action generation and action perception in imitation: an instance of the ideomotor principle. Philosophical Transactions of the Royal Society of London B: Biological Sciences 358, 501–515. (Feb. 2003)

[72] Maryjane Wraga, William L. Thompson, Nathaniel M. Alpert, Stephen M. Kosslyn: Implicit transfer of motor strategies in mental rotation. Brain and Cognition 52, 135–143. (July 2003)

[73] Andrew J Hanson, Hui Zhang: Multimodal Exploration of the Fourth Dimension. In Proceedings of IEEE Visualization 2005, 263–270. (Oct. 2005)

[74] Hui Zhang, Andrew J. Hanson: Shadow-Driven 4D Haptic Visualization. IEEE Transactions on Visualization and Computer Graphics 13, 6, 1688–1695. (Nov. 2007)

Appendix

A Equations for Estimation of Principal Vanishing Points

As described in Section 2.3.2, the 4-D eye-point control algorithm is composed of two processing steps. In this appendix, we show the full version of the first processing step.

In order to estimate the parameters regarding the 4-D viewing direction, we first need to estimate the three principal vanishing points from the one principal vanishing point being operated by a user. This estimation was achieved by using the geometric constraints among four principal vanishing points.

Suppose the principal vanishing points vp_{x_b}, vp_{y_b}, vp_{z_b}, and vp_{w_b} are displayed in 3-D space at a 4-D eye-point p_{f_b}. When the principal vanishing point vp_{w_b} moves to $vp_w(x_{vp_w}, y_{vp_w}, z_{vp_w})$ through user operations, from Equation (2.4), the other three vanishing points vp_x, vp_y, and vp_z will be estimated from the principal vanishing point vp_w as follows:

$$\begin{aligned}
vp_x &= (x_{vp_x}, y_{vp_x}, z_{vp_x}) \\
&= \left(-\frac{1}{x_{vp_w}} \left\{ \left(\frac{h}{k} \right)^2 + {y_{vp_w}}^2 \right\}, y_{vp_w}, 0 \right), \\
vp_y &= (x_{vp_y}, y_{vp_y}, z_{vp_y}) \\
&= \left(0, -\frac{1}{y_{vp_w}} \left(\frac{h}{k} \right)^2, 0 \right), \\
vp_z &= (x_{vp_z}, y_{vp_z}, z_{vp_z}) \\
&= \left(x_{vp_w}, y_{vp_w}, -\frac{1}{z_{vp_w}} \left\{ \left(\frac{h}{k} \right)^2 + {x_{vp_w}}^2 + {y_{vp_w}}^2 \right\} \right). \qquad (1)
\end{aligned}$$

Similarly, when the principal vanishing point vp_{z_b} moves to $vp_z(x_{vp_z}, y_{vp_z}, z_{vp_z})$, the other three vanishing points vp_x, vp_y, and vp_w are computed from the principal vanishing point vp_z as follows:

$$\begin{aligned}
vp_x &= (x_{vp_x}, y_{vp_x}, z_{vp_x}) \\
&= \left(-\frac{1}{x_{vp_z}} \left\{ \left(\frac{h}{k} \right)^2 + {y_{vp_z}}^2 \right\}, y_{vp_z}, 0 \right), \\
vp_y &= (x_{vp_y}, y_{vp_y}, z_{vp_y})
\end{aligned}$$

$$
\begin{aligned}
&= \left(0, -\frac{1}{y_{vp_z}}\left(\frac{h}{k}\right)^2, 0\right), \\
vp_w =& (x_{vp_w}, y_{vp_w}, z_{vp_w}) \\
&= \left(x_{vp_z}, y_{vp_z}, -\frac{1}{z_{vp_z}}\left\{\left(\frac{h}{k}\right)^2 + x_{vp_z}{}^2 + y_{vp_z}{}^2\right\}\right).
\end{aligned} \tag{2}
$$

When the principal vanishing point vp_{x_b} moves to $vp_x(x_{vp_x}, y_{vp_x}, z_{vp_x})$, the other three vanishing points vp_y, vp_z, and vp_w is estimated from the principal vanishing point vp_x as follows:

$$
\begin{aligned}
vp_y =& (x_{vp_y}, y_{vp_y}, z_{vp_y}) \\
&= \left(0, -\frac{1}{y_{vp_x}}\left(\frac{h}{k}\right)^2, 0\right), \\
vp_z =& (x_{vp_y}, y_{vp_y}, z_{vp_y}) \\
&= \left(-\frac{1}{x_{pv_x}}\left\{\left(\frac{h}{k}\right)^2 + y_{vp_x}{}^2\right\}, y_{vp_x}, \right. \\
&\qquad \left. -\frac{1}{\tan\alpha}\sqrt{\left(\frac{h}{k}\right)^2\frac{1}{x_{pv_x}{}^2} + \frac{y_{vp_x}{}^2}{x_{vp_x}{}^2} + 1}\sqrt{\left(\frac{h}{k}\right)^2 + y_{vp_x}{}^2}\right), \\
vp_w =& (x_{vp_y}, y_{vp_y}, z_{vp_y}) \\
&= \left(-\frac{1}{x_{pv_x}}\left\{\left(\frac{h}{k}\right)^2 + y_{vp_x}{}^2\right\}, y_{vp_x}, \right. \\
&\qquad \left. \tan\alpha\sqrt{\left(\frac{h}{k}\right)^2\frac{1}{x_{pv_x}{}^2} + \frac{y_{vp_x}{}^2}{x_{vp_x}{}^2} + 1}\sqrt{\left(\frac{h}{k}\right)^2 + y_{vp_x}{}^2}\right),
\end{aligned} \tag{3}
$$

where α is the parameter regarding the 4-D viewing direction. Because the parameter α is invariant to the operations on the principal vanishing points vp_x on the $x_s y_s$-plane in 3-D space, we can use α computed by Equation (2.6) straightforwardly in the principal vanishing points estimation.

Finally, when the principal vanishing point vp_{y_b} moves to $vp_y(x_{vp_y}, y_{vp_y}, z_{vp_y})$, the other three vanishing points vp_x, vp_z, and vp_w is estimated by using the position of the operated principal vanishing point vp_y as follows:

$$
\begin{aligned}
vp_x =& (x_{vp_x}, y_{vp_x}, z_{vp_x}) \\
&= \left(\left(\frac{h}{k}\right)^2\frac{1}{\tan\beta}\sqrt{\left(\frac{k}{h}\right)^2 + \frac{1}{y_{vp_y}{}^2}}, -\frac{1}{y_{vp_y}}\left(\frac{h}{k}\right)^2, 0\right), \\
vp_z =& (x_{vp_z}, y_{vp_z}, z_{vp_z}) \\
&= \left(-\left(\frac{h}{k}\right)^2\tan\beta\sqrt{\left(\frac{k}{h}\right)^2 + \frac{1}{y_{vp_y}{}^2}}, -\frac{1}{y_{vp_y}}\left(\frac{h}{k}\right)^2, \right.
\end{aligned}
$$

$$-\left(\frac{h}{k}\right)^2 \frac{1}{\tan\alpha\cos\beta}\sqrt{\left(\frac{k}{h}\right)^2+\frac{1}{y_{vp_y}{}^2}}\right),$$

$$\begin{aligned} vp_w =&(x_{vp_z}, y_{vp_z}, z_{vp_z}) \\ =&\left(-\left(\frac{h}{k}\right)^2 \tan\beta\sqrt{\left(\frac{k}{h}\right)^2+\frac{1}{y_{vp_y}{}^2}}, -\frac{1}{y_{vp_y}}\left(\frac{h}{k}\right)^2,\right. \\ &\left. -\left(\frac{h}{k}\right)^2 \frac{\tan\alpha}{\cos\beta}\sqrt{\left(\frac{h}{k}\right)^2+\frac{1}{y_{vp_y}{}^2}}\right), \end{aligned} \quad (4)$$

where α and β are the parameters regarding the 4-D viewing direction. Because these parameters are invariant to the operation of the principal vanishing points vp_y along the y_s-axis in 3-D space, we can use them straightforwardly as computed by Equation (2.6).

B Definition of 4-D Solids

A 3-D solid is a geometric object in 3-D space with vertices, edges and surfaces. The 3-D solid is formed as the union of surfaces which arranged in 3-D space so that each edge is shared by two different surfaces and each vertex is shared by at least three different surfaces. There are five regular polyhedrons in 3-D space, known as the Platonic solids. They are the tetrahedron, hexahedron (cube), octahedron, dodecahedron and icosahedron. In a similar manner, a 4-D solid is a geometric object in 4-D space with vertices, edges, surfaces and cells. Cells are three-dimensional analogue of surfaces, and are facets for a 4-D solid. In short, the 4-D solid is formed as the union of cells. Each surface is shared by two different cells, just as each edge of a 3-D solid is shared by two surfaces. There are six regular polytopes (4-D solids) in 4-D space; the 5-cell, the 8-cell (hypercube), the 16-cell, the 24-cell, the 120-cell, and the 600-cell. In the field of geometry, the geometric elements of these 4-D solids are well-defined [16, 17]. Five of them can be thought as analogs of the regular polyhedrons in 3-D space. The 24-cell does not have a analogue in 3-D space. Table B.1 and Table B.2 show the geometric elements and the coordinates of vertices of these 4-D solids, respectively.

Table B.1. Geometric elements of regular polytopes.

Regular polytopes	Vertices	Edges	Surfaces	Cells	Shape of cells	Analogous regular polyhedron
5-cell	5	10	10	5	Tetrahedron	Dodecahedron
8-cell	16	32	24	8	Hexahedron	Hexahedron
16-cell	8	24	32	16	Tetrahedron	Octahedron
24-cell	24	96	96	24	Octahedron	—
120-cell	600	1200	720	120	Dodecahedron	Dodecahedron
600-cell	120	720	1200	600	Tetrahedron	Icosahedron

Table B.2. Coordinates of vertices of regular polytopes.

Regular polytopes	Edge length	Coordinates of vertices
5-cell	$\sqrt{2}$	$(1,0,0,0)$, $(0,1,0,0)$, $(0,0,1,0)$, $(0,0,0,1)$, $(0.5-\tau/2, 0.5-\tau/2, 0.5-\tau/2, 0.5-\tau/2)$.
8-cell	2	The permutations of $(\pm1,\pm1,\pm1,\pm1)$.
16-cell	$\sqrt{2}$	The permutations of $(\pm1,0,0,0)$, $(0,\pm1,0,0)$, $(0,0,\pm1,0)$, $(0,0,0,\pm1)$.
24-cell	2	The permutations of $(\pm1,\pm1,0,0)$, $(\pm1,0,\pm1,0)$, $(\pm1,0,0,\pm1)$, $(0,\pm1,\pm1,0)$, $(0,\pm1,0,\pm1)$, $(0,0,\pm1,\pm1)$.
120-cell	$2/\tau^2$	The permutations of $(\pm2,\pm2,0,0)$, $(\pm\sqrt{5},\pm1,\pm1,\pm1)$, $(\pm\tau,\pm\tau,\pm\tau,\pm\tau^{-2})$, $(\pm\tau^2,\pm\tau^{-1},\pm\tau^{-1},\pm\tau^{-1})$ along with the even permutations of $(\pm\tau^2,\pm\tau^2,\pm1,0)$, $(\pm\sqrt{5},\pm\tau^{-1},\pm\tau,0)$, $(\pm2,\pm1,\pm\tau,\pm\tau^{-1})$.
600-cell	$2/\tau$	The permutations of $(\pm1,\pm1,\pm1,\pm1)$, $(\pm2,0,0,0)$, $(0,\pm2,0,0)$, $(0,0,\pm2,0)$, $(0,0,0,\pm2)$ along with the even permutations of $(\pm\tau,\pm1,\pm\tau^{-1},0)$

($\tau = (\sqrt{5}+1)$ is the Golden Section.)

List of Publications

[Journal Articles]

1. Takanobu Miwa, Yukihito Sakai, Shuji Hashimoto: Learning Four-dimensional Spatial Representations through Perceptual Experience with Hypercubes. IEEE Transactions on Cognitive and Developmental Systems. (in press)

2. Uori Koike, Enriquez Guillermo, Takanobu Miwa, Huei Ee Yap, Madoka Kabasawa, Shuji Hashimoto: Development of an Intraoral Interface for Human-ability Extension Robots. Journal of Robotics and Mechatronics 28, 6, 819–829. (2016)

3. 三輪貴信, 酒井幸仁, 橋本周司: 主消点操作による 4 次元視点制御とその評価. 芸術科学会論文誌 12, 4, 162–174. (2013)

[Book chapter]

1. Takanobu Miwa, Yukihito Sakai, Shuji Hashimoto: Interactive Four-dimensional Space Exploration Using Viewing Direction Control Based on Principal Vanishing Points Operation. Computer-Human Interaction. Cognitive Effects of Spatial Interaction, Learning, and Ability, LNCS 8433, 21–46. Springer, Heidelberg. (2015)

[Peer-reviewed International Conference Papers]

1. Takanobu Miwa, Yukihito Sakai, Shuji Hashimoto: 4-D Spatial Perception Established through Hypercube Recognition Tasks Using Interactive Visualization System with 3-D Screen. In Proceedings of ACM SIGGRAPH Symposium on Applied Perception 2015 (SAP 2015), 75–82. (2015)

2. Takanobu Miwa, Yukihito Sakai, Shuji Hashimoto: Four-dimensional Viewing Direction Control by Principal Vanishing Points Operation and Its Application to Four-dimensional Fly-through Experience. In Proceedings of the 25th Australian Computer-Human Interaction Conference (OzCHI 2013), 95–104. (2013)

[Peer-reviewed Domestic Conference Papers]

1. 三輪貴信, 酒井幸仁, 橋本周司: 主消点操作による 4 次元視点制御. In NICOGRAPH 2012 Autumn, 103–110. (2012)

2. 三輪貴信, 山口友之, 橋本周司: 画像データベースを用いた自己位置推定に関する理論的考察. 第16回画像センシングシンポジウム講演論文集 (SSII2010), IS-13, 1–5. (2010)

[Oral Presentations]

1. 三輪貴信: 主消点操作による4次元インタラクションに関する研究. 第2回次世代ロボット研究機構シンポジウム：ヒューマノイドから始まるロボットテクノロジーの多様化. (2017)
2. 三輪貴信, 橋本周司: 2次元連続DPマッチングによるくずし字認識. 2016電子情報通信学会総合大会　情報・システム講演論文集 2, 75. (2016)
3. 三輪貴信, 酒井幸仁, 橋本周司: 主消点操作の4次元視点移動による4次元立体迷路の探索. 情報処理学会第76回全国大会講演論文集, 4, 3–4. (2014)
4. 三輪貴信, 酒井幸仁, 橋本周司: インタラクティブな4次元スライス操作によるマルチパースペクティブ画像生成. 情報処理学会第74回全国大会講演論文集, 4, 169–170. (2012)
5. 三輪貴信, 酒井幸仁, 橋本周司: 光線空間の直感的理解を目指した可視化に関する研究. 第73回情報処理学会全国大会講演論文集, 4, 89–90. (2011)
6. 三輪貴信, 山口友之, 橋本周司: 自己位置推定のための環境画像データベースの構築. 情報処理学会第72回全国大会講演論文集, 1, 841–842. (2010)

[Poster and Demonstrative Presentations]

1. 上条孝二, エンリケズ ギエルモ, 三輪貴信, 橋本周司: 定トルクぜんまいを用いたモーター出力の増強. ロボティクス・メカトロニクス講演会2016講演論文集, 2A1-05a7. (2016)
2. Takanobu Miwa, Yukihito Sakai and Shuji Hashimoto: Four-dimensional Space Interaction Using Principal Vanishing Points Operation. Italy-Japan Workshop 2014. (2014)
3. 三輪貴信, 酒井幸仁, 橋本周司: 主消点の選択・移動操作を用いたインタラクティブな4次元視点制御システム. 情報処理学会インタラクション2013論文集, 329–336. (2013)

[Master's Thesis]

1. 三輪貴信: 4次元光線空間の探索とスライス操作によるマルチパースペクティブ画像生成. 早稲田大学. (2012)

[Bachelor's Thesis]

1. 三輪貴信: 画像データベースを用いた自己位置推定の理論的考察. 早稲田大学. (2010)

[Other Papers]

1. 下村駿平, エンリケズ ギエルモ, 三輪貴信, 橋本周司: レーザポインタを用いたジェスチャによる家電操作システム. 電子情報通信学会2017年総合大会 基礎・境界/NOLTA講演論文集, 260. (2017)

2. 森貴大, エンリケズ ギエルモ, ヤップ フェイ イー, 三輪貴信, 橋本周司: Control Moment Gyroscopeを用いたパッティングのスイング矯正. 電子情報通信学会 2017 年総合大会 基礎・境界/NOLTA 講演論文集, 237. (2017)

3. 山元亮典, 三輪貴信, エンリケズ ギエルモ, ヤップ フェイ イー, 橋本周司: リズム解析に基づくタップダンスの習熟度評価法. 情報処理学会 第 79 回全国大会講演論文集, 4, 193–194. (2017)

4. 田中宏和, 三輪貴信, 橋本周司: 円筒形タッチスクリーンの同時利用に関するユーザー調査. 情報処理学会 第 79 回全国大会講演論文集, 4, 269–270. (2017)

5. 相澤朋希, 北山 慎太郎, 三輪 貴信, 橋本 周司: ユーザの好みのリズムに基づく自動作曲システム. 情報処理学会 第 79 回全国大会講演論文集, 2, 89–90. (2017)

6. 田中宏和, 三輪貴信, 橋本周司: 円筒形タッチスクリーンを使用したデジタルサイネージの研究. ヒューマンインタフェースシンポジウム 2016 論文集, 19–22. (2016)

7. 下村駿平, エンリケズ ギエルモ, 三輪貴信, 橋本周司: 可視光ビームによる飛行ロボットの操作インタフェース. ロボティクス・メカトロニクス講演会 2016 講演論文集, 1A2-18a5. (2016)

8. 宇高大記, エンリケズ ギエルモ, 三輪貴信, 橋本周司: 逃亡者を追い込むロボットの制御アルゴリズム. ロボティクス・メカトロニクス講演会 2016 講演論文集, 1A2-03b1. (2016)

9. 佐々木貴裕, エンリケズ ギエルモ, 三輪貴信, 橋本周司: 自動掃除ロボットのための汚れ分布を考慮に入れた経路計画. ロボティクス・メカトロニクス講演会 2016 講演論文集, 1A1-13b4. (2016)

10. 小池宇織, エンリケズ ギエルモ, ヤップ フェイ イー, 三輪貴信, 橋本周司: ヘッドセット型口腔内インタフェースの開発. 2016 電子情報通信学会総合大会　基礎・境界講演論文集, 289. (2016)

11. 山元亮典, 三輪貴信, エンリケズ ギエルモ, ヤップ フェイ イー, 橋本周司: タップダンサーの技術向上のためのリズム計測タップシューズの開発. 情報処理学会第 78 回全国大会講演論文集, 4, 255–256. (2016)

12. 北山慎太郎, 三輪貴信, 橋本周司: ユーザの感性を楽曲の好みから抽出する自動作曲システム. 情報処理学会 第 78 回全国大会講演論文集, 2, 455–456. (2016)

13. 小池宇織, エンリケズ ギエルモ, ヤップ フェイ イー, 三輪貴信, 橋本周司: 姿勢センサと大気圧センサを用いた口腔内インタフェースの開発と評価. ロボティクス・メカトロニクス講演会 2015, 1A1-K06. (2015)

14. 座間味卓臣, エンリケズ・ギエルモ, 三輪貴信, 橋本周司: 特徴空間によるロボットのタスク達成可能性の判定. 電子情報通信学会総合大会講演論文集, 2015 年 情報・システム 2, 112. (2015)

15. 松尾祥, 三輪貴信, エンリケズ・ギエルモ, 橋本周司: インプラントデバイスのための超音波経皮エネルギー伝送システムの開発. 電子情報通信学会総合大会講演論文集, 2015 年 通信 2, 31. (2015)

16. 山元亮典, 三輪貴信, エンリケズ・ギエルモ, ヤップ フェイ イー, 橋本周司: タップダンスのリズム解析のためのインソールセンサの開発. 電子情報通信学会総合大会講演論文集, 2015 年 情報システム 2, 103. (2015)
17. 田中宏和, 三輪貴信, 橋本 周司: 双曲面ミラーを用いた全周囲映像の撮影と投影. 電子情報通信学会総合大会講演論文集, 2015 年 情報システム 2, 31. (2015)
18. 野網俊介, 三輪貴信, 橋本周司: 類似画像検索を用いた画像の自動配列による映像生成. 電子情報通信学会総合大会講演論文集, 2015 年 情報システム 2, 1. (2015)
19. 座間味卓臣, 三輪貴信, エンリケズ・ギエルモ, 橋本周司: ロボットのタスク達成可能性評価. ロボティクス・メカトロニクス講演会 2014, 2A1-W02. (2014)
20. 小池宇織, エンリケズ・ギエルモ, フェイ・イー・ヤップ, 山口友之, 三輪貴信, 橋本周司: 9 軸姿勢センサを用いた口腔内インタフェースの開発と評価. ロボティクス・メカトロニクス講演会 2014, 2A2-K04. (2014)
21. 小池宇織, ヤップ フェイ・イー, ギエルモ エンリケズ, 三輪貴信, 山口友之, 橋本周司: 9 軸姿勢センサを用いた口腔内インタフェース. 電子情報通信学会総合大会講演論文集, 2014 年 基礎・境界, 174. (2014)
22. 野網俊介, 三輪貴信, 橋本周司: 類似画像検索を用いた映像生成. 電子情報通信学会総合大会講演論文集, 2013 年 情報・システム 2, 241. (2013)